농학박사학위논문

자일로스 환원효소의 동질효소 시스템을 이용한 효모의 자일로스 대사능 증대

Development of xylose reductase isozyme system for enhancing xylose metabolism in *Saccharomyces cerevisiae*

2017 년 8 월

서울대학교 대학원

농생명공학부 식품생명공학전공

조 정 현

A DISSERTATION FOR THE DEGREE OF DOCTOR OF PHILOSOPHY

Development of xylose reductase isozyme system for enhancing xylose metabolism in *Saccharomyces cerevisiae*

자일로스 환원효소의 동질효소 시스템을 이용한 효모의 자일로스 대사능 증대

August 2017

Jung-Hyun Jo

MAJOR IN FOOD BIOTECHNOLOGY

DEPARTMENT OF AGRICULTURAL BIOTECHNOLOGY

GRADUATE SCHOOL

SEOUL NATIONAL UNIVERSITY

Development of xylose reductase isozyme system for enhancing xylose metabolism in *Saccharomyces cerevisiae*

Advisor: Professor Jin-Ho Seo

A dissertation submitted in partial fulfillment of

The requirements for the degree of

DOCTOR OF PHILOSOPHY

to the Faculty of Department of Agricultural Biotechnology

at

SEOUL NATIONAL UNIVERSITY

by

Jung-Hyun Jo

August 2017

농학박사학위논문

Development of xylose reductase isozyme system for enhancing xylose metabolism in *Saccharomyces cerevisiae*

자일로스 환원효소의 동질효소 시스템을 이용한
효모의 자일로스 대사능 증대

지도교수 서 진 호

이 논문을 농학박사학위논문으로 제출함
2017 년 6 월

서울대학교 농생명공학부 식품생명공학전공
조 정 현

조정현의 농학박사학위논문을 인준함

2017 년 6 월

위 원 장 장 판 식 (인/서명)

부위원장 서 진 호 (인/서명)

위 원 하 남 출 (인/서명)

위 원 김 경 헌 (인/서명)

위 원 박 용 철 (인/서명)

ABSTRACT

Biological production of fuels and chemicals from lignocellulosic biomass is a sustainable and ecofriendly process. Glucose and xylose are the major constituents of lignocellulosic hydrolysates. Although the engineered *Saccharomyces cerevisiae* can use xylose, its fermentative capacity on xylose has been known to be much lower than that on glucose. Therefore, the efficient consumption of xylose is one of the key steps for economically feasible production of biofuels and chemicals. The overall goal of this thesis is to develop metabolically engineered *S. cerevisiae* able to ferment xylose efficiently.

In this thesis, *S. cerevisiae* D452-2 was used as a host strain for production of xylitol and bioethanol, and has been chosen in metabolic and evolutionary engineering studies of other chemicals production from xylose. Many *S. cerevisiae* strains were sequenced, providing additional information of unexplored differences between *S. cerevisiae* strains. On the other hand, the D452-2 strain was not sequenced yet and its underlying beneficial genetic polymorphisms remain unknown. The whole genome sequencing of the D452-2 strain was performed by PacBio sequencing. Its assembled genome sequence was nearly identical to that of S288c which is a reference strain and was sequenced completely. As a result of comparative analysis, the genome of D452-2

was rearranged by transposon elements and small indels, and had nineteen ORFs that were absent in S288c. Compared to the S288c genome, 6,948 of SNPs were detected to change properties of 313 metabolic enzymes. These genetic variations of the D452-2 strain provide the basis for a forward genetic approach for developing xylose-fermenting yeast strains with enhanced performance.

The *XYL1*, *XYL2* and *XYL3* genes involved in the xylose assimilation pathway from *Scheffersomyces stipitis* and a native xylose-fermenting yeast had been introduced into *S. cerevisiae* D452-2 to assimilate xylose. However, the resulting *S. cerevisiae* strains often exhibited undesirable phenotypes. The cofactor imbalance generated from different cofactor requirement between NADPH-dependent xylose reductase (XR) and NAD^+-dependent xylitol dehydrogenase (XDH) inceased xylitol accumultation. To alleviate cofactor imbalance, a XR mutant with NADH preferency was constructed by protein engineering. The adoption of this XR mutant reduced xylitol accumulation but led to slow xylose consumption rate. The availability and balance of cofactors might be limiting factors for xylose fermentation by engineered *S. cerevisiae*. In this thesis, a synthetic isozyme system of XRs was designed to overcome the above mentioned problems. To construct this system, NADH-dependent mutant XR was expressed in the *S. cerevisiae* D452-2 strain expressing NADPH-dependent wild-type XR,

XDH and xylulose kinase (XK). While the strains having only one type of XR exhibited XR acvitities which were highly specific for NADPH or NADH, the *S. cerevisiae* strain having the XR-based isozyme system showed similar XR activities toward NADPH and NADH. The engineered strain exhibited low xylitol accumulation and fast xylose consumption compared to the control strains expressing one type of XR. The xylose fermenting performance was confirmed by fermentations in various conditions. In a batch fermentation using silver grass hydrolysates, the engineered strain produced 50.7 g/L ethanol with 0.43 g/g ethanol yield.

Besides ethanol production, the XR-based synthetic isozyme system was applied to improving the production of value-added products such as xylitol. The engineered *S. cerevisiae* strain having both XRs exhibited higher xylitol productivity than the control strains in both batch and glucose-limited fed-batch fermentations. To supply NADPH and NADH sufficiently, cofactor regeneration enzymes were co-expressed additionally. The coexpression of glucose-6-phosphate dehydrogenase encoded by the *ZWF1* gene and acetyl-CoA synthetase by the *ACS1* gene increased intracellular concentrations of NADPH and NADH, and improved xylitol productivity. In order to extend the period for the highest xylitol productivity and hence elevate final xylitol concentration, fed-batch fermentation strategies were optimized.

Finally, the optimized fed-batch fermentation of the engineered strain resulted in 196.2 g/L xylitol concentration, 4.27 g/L-h productivity and almost the theoretical yield. The synthetic isozym system of XR is a promising strategy to meet the industrial demands for production of ethanol and xylitol.

Key words: *Saccharomyces cerevisiae*, lignocellulosic biomass, xylose, bioethanol, xylitol, synthetic isozyme system, NADH-dependent xylose reductase, cofactor regeneration, mixed sugar fermentation, comparative genomic analysis

Student ID: 2010-21262

CONTENTS

LIST OF TABLES

LIST OF FIGURES

Chapter 1

Literature review

1.1. Lignocellulosic biomass

In the twentieth century, petroleum is used to produce multiple products such as fuels, chemicals and pharmaceuticals. But, the use of petroleum-based fuels increases the level of CO_2 in the atmosphere to cause global warming and aggravates environmental pollution. The petrolueum reserves are declining (Demirbas, 2006). Petroleum is not regarded as sustainable due to these drawbacks. There has been a worldwide interest in biomass as alternative sources. Since biomass such as plant and agricultural wastes can be generated in a few years and capture CO_2 by photosynthesis, it has a short carbon cycle and mitigates grobal warming (Naik et al., 2010) (Fig. 1.1). Biofuels and biochemicals produced from the renewable resourses could help to reduce world's dependence on oil and CO_2 emission.

The first-generation bioethanol uses sugarcane and corn that are more than often edible. C_6 sugars (mostly glucose) extracted from this biomass is fermented by classical or GMO yeast strains such as *Saccharomyces cerevisiae.* Sugarcane is a common feedstock for biofuel production in Brazil. The sugar extraction process from sugarcane is rather simple. Corn is the other major feedstock for production of bioethanol in U.S.A.. This stock requires a preliminary hydrolysis of starch and the enzymes generally used for hydrolysis of

starch are inexpensive. First-generation biofuels are well implemented around the world due to the simple and economic process. But, these had certain restrictions such as utilization of arable lands and the fuel versus food debate (Fig. 1.2). The increased corn demand for bioethanol impacted on food prices (Martin, 2010). Therefore, altenative biomass that did not compete with food is required to produce bioethanol.

Lignocellulosic biomass is a promising resource for producing fuels and chemicals. It can be categorized as follows: agricultural residues such as sugarcane bagasse, corn cob, corn stover, wheat and rice straw; forest residues such as wood; municipal solid wastes such as waste wood from a construction site; industrial residues such as pulp and paper precessing waste; energy crops such as switch grass. Lignocellulosic biomass is a heterogeneous complex of carbohydrate polymers and lignin, a complex polymer of phenylpropanoid units. The carbohydrate complex comprises cellulose which is a polymer of glucose and hemicellulose which is a branced polymer of glucose or xylose (Mosier et al., 2005). The percent dry weight composition of lignocellulosic feedstocks is different from biomass (Table. 1.1). Typically, lignocellulosic biomass contains 55-75% carbohydrates by dry weight.

The process for production of ethanol from lignocellulosic biomass consists of four unit operations: pretreatment, hydrolysis, fermentation and product purification (Fig 1.3). Since lignin impedes enzymatic hydrolysis of the carbohydrates, it should be treated by various physicochemical pretreatment processes such as dilute acid, alkali, steam explosion and hydro-thermal methods (Agbor et al., 2011). In these precesses, a substantial amount of fermentation inhibitors such as furan derivatives, 5-hydroxymethyl-2-furfural, carboxylic acids and phenolic compounds are generated (Almeida et al., 2007) (Fig.1.4).

After pretreatment, cellulose and hemicellulose can be broken down into various hexoses and pentoses either enzymatically or chemically. Regardress of hydrolysis methods, the major sugars of these hydrolysates are glucose and xylose. Typically, cellulosic hydrolysates consist of 60-70% glucose and 30-40% xylose. Many natural organisms can readily ferment glucose to ethanol, but xylose is fermented to ethanol by few native strains and usually at relatively low yields. Therefore, microorganisms which are able to ferment both glucose and xylose are required for producing biofuels and chemicals from lignocellulosic biomass sustainably and economically (Hahn-Hagerdal et al., 2006).

Table 1.1. Percent dry weight composition of lignocellulosic feedstocks (Mosier et al., 2005)

Feedstock	Glucan (cellulose)	Xylan (hemicellulose)	Lignin
Corn strover	37.5	22.4	17.6
Corn fiber	14.3	26.8	8.4
Pine wood	46.4	8.8	29.4
Popular	49.9	17.4	18.1
Wheat straw	38.2	21.2	23.4
Switch grass	31.0	20.4	17.6
Office paper	68.6	12.4	11.3

(scale : % (g/g))

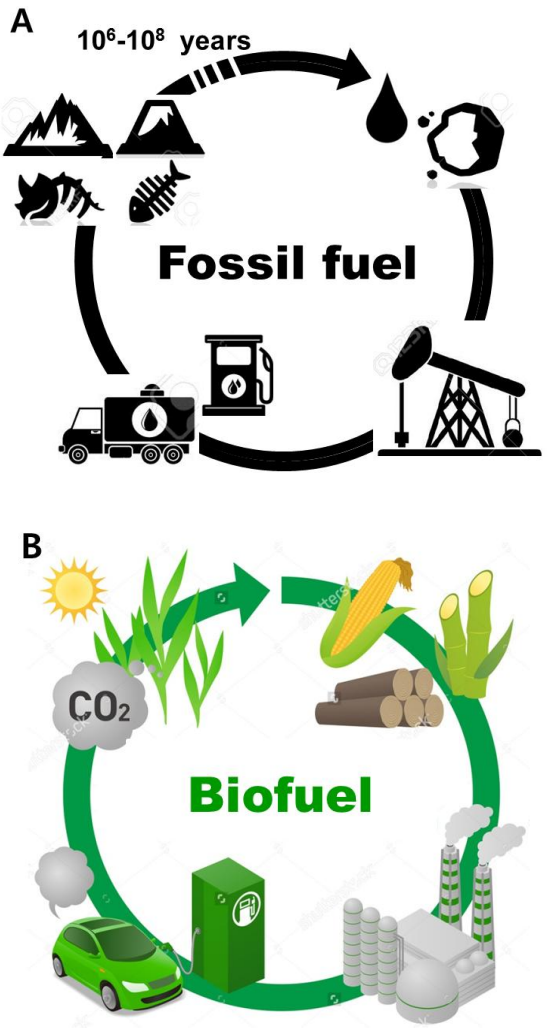

Fig. 1.1. Comparison between fossil fuel and biomass-based fuel focusing on carbon cycle. (A) Petroleum carbon cycle (long-term), (B) Biomass-based carbon cycle (short-term).

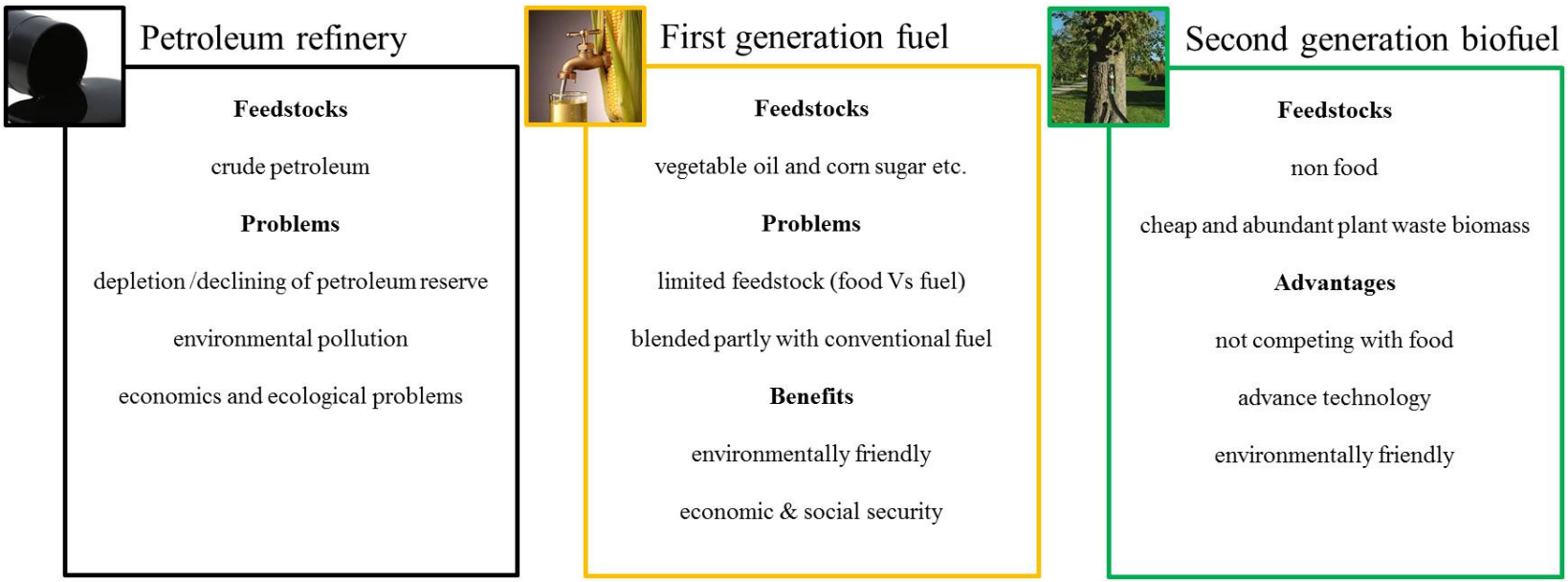

Fig. 1.2. Comparison of first, second generation biofuel and petroleum fuel.

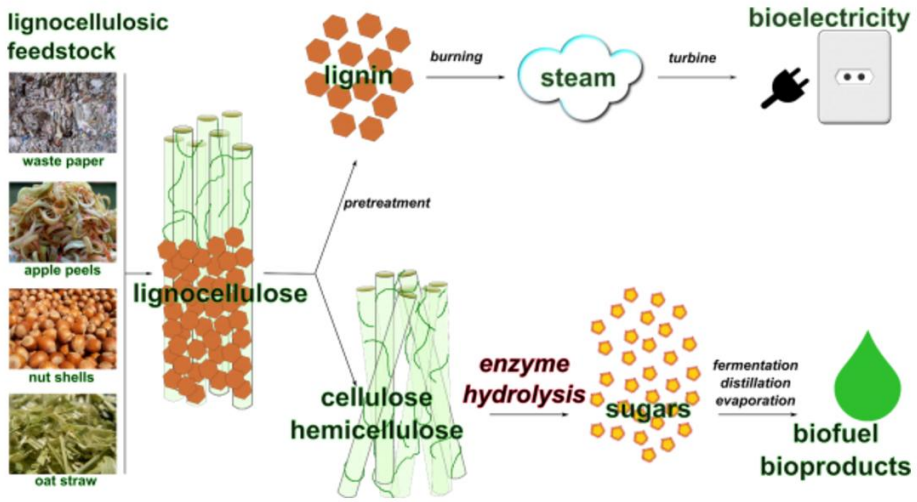

Fig. 1.3. Second generation biofuel production

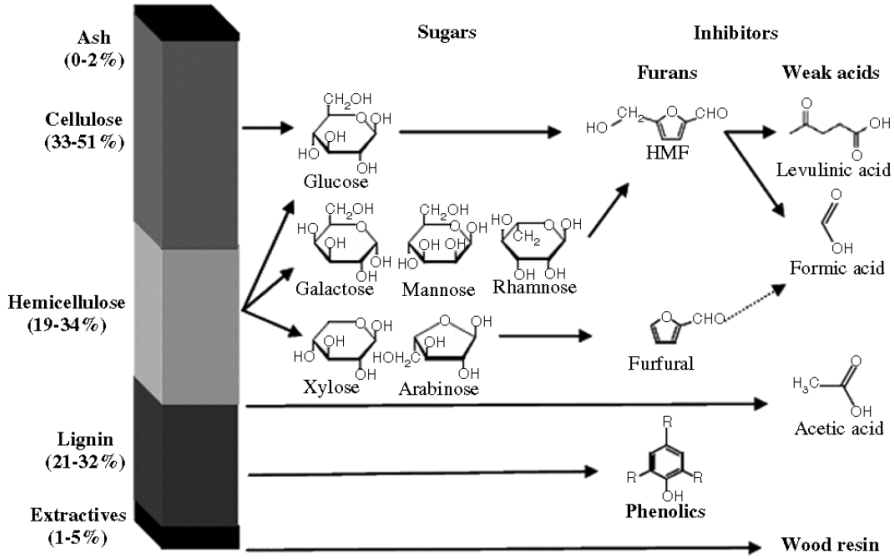

Fig. 1.4. Average composition of lignocellulosic biomass and fermentation inhibitors (Almeida et al., 2007).

1.2. *Saccharomyces cerevisiae* as a bioethanol and biochemical producer

There are various xylose-fermenting microorganisms in nature including *Scheffersomyces stipitis*. However, they cannot ferment sugars from lignocellulosic biomass well under industrial-scale conditions such as high osmotic stress, low pH, strict anaerobic conditions and fermentation inhibitors (Almeida et al., 2011). A traditional glucose fermenting yeast *Saccharomyces cerevisiae* is very attractive for production of bioethanol and chemicals from lignocellulosic biomass. Since *S. cerevisiae* is considered as Generally Recognized As Safe (GRAS), it is safe to manufacturer and applicable to production of food-related chemicals (Ostergaard et al., 2000). And *S. cerevisiae* as a Crabtree positive yeast accumulates ethanol even in the presence of oxygen and has high tolerance to acids, ethanol and inhibitors. These merits make *S. cerevisiae* a desirable host for ethanol production, actually, *S. cerevisiae* has been used in large-scale fermentations of first-generation biomass for ethanol production and value-added chemicals (Kuyper et al., 2005). In addition, abundant genetic and genomic tools have been developed for *S. cerevisiae* so that genetic modifications can be performed for desire purposes (Forsburg, 2001).

While *S. cereivisiae* ferments glucose to ethanol with nearly theoretical yield, it cannot ferment xylose, the second abundant sugar in lignocellulosic biomass, due to the lack of a functional xylose-assimilating pathway. *S. cerevisiae* has been engineered to use it as a host strain for fermentation of lignocellulosic biomass. A common strategy is to express heterologous genes coding for xylose reductase (XR) and xylitol dehydrogenase (XDH) from *Sch. stipitis* (Richard et al., 2006). Second, the *xylA* gene coding for xylose isomerase (XI) from anaerobic fungi or bacteria have been expressed in *S. cerevisiae* to enable xylose assimilation (van Maris et al., 2007) (Fig. 1.5). Xylulose converted by the above two pathways enters main metabolisms via the pentose phosphate pathway and is converted to ethanol by glycolysis.

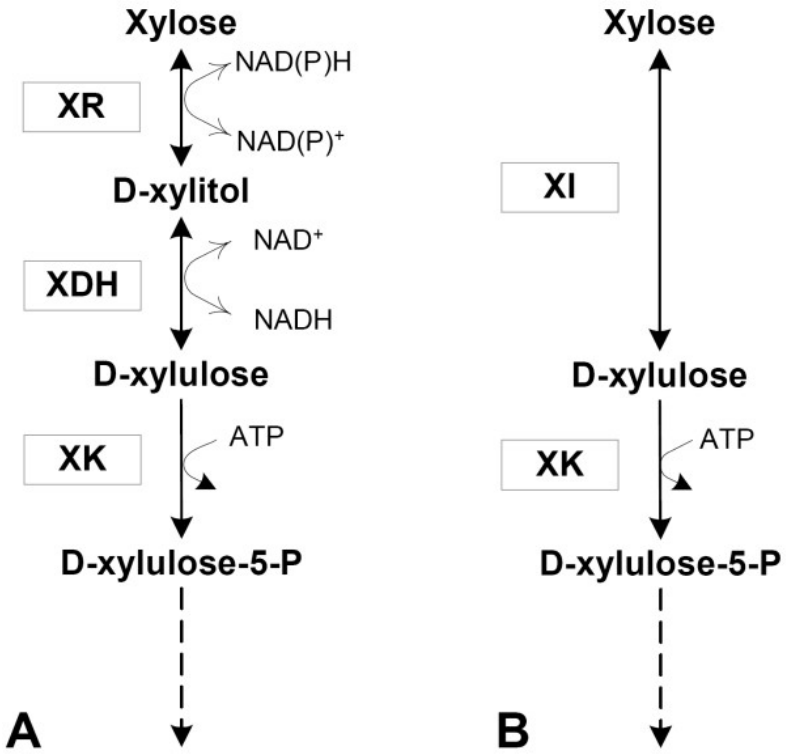

Fig. 1.5. Metabolic pathways for xylose utilization. (A) The XR-XDH pathway, (B) The XI pathway (Karhumaa et al., 2007).

1.3. Challenges in glucose and xylose fermentation

Although the engineered *S. cerevisiae* can assimilate xylose via the expression of heterologous genes, there are several challenges in glucose and xylose fermentation. Typically, a glucose consumption rate is 3-10 fold higher than that of xylose in engineered *S. cerevisiae*. In addition, xylose metabolism is delayed in the presence of glucose (Casey et al., 2010; Lee et al., 2000; Matsushika & Sawayama, 2010). This sequential utilization of sugars results in low overall ethanol productivity (Fig 1.6. 1,2). To solve these drawbacks, mutants of the yeast hexose transporters Hxt7 and Gal2 were expressed. The engineered strains consumed xylose without any inhibition by glucose (Farwick et al., 2014). In addition, the engineered strain expressing the mutant xylose-specific transporter such as *Candida intermedia GXS1* metabolized xylose specifically (Young et al., 2014). Simultaneous co-utilization of cellobiose (a dimer of glucose) and xylose could bypass the inhibition of xylose uptake by glucose. Cellobiose that is an intermediate product of cellulose hydrolysis does not repress xylose fermentation. Because *S. cerevisiae* cannot consume cellobiose, metabolic enzymes for utilization of cellobiose need to be introduced. First, β-glucosidase expressed by a surface display hydrolyzed cellobiose to glucose extracellularly. This glucose did not inhibit the

xylose uptake in the engineered *S. cerevisiae* (Nakamura et al., 2008). Second, the engineered strain containing the genes encoding a cellodextrin transporter and intracellular β-glucosidase from *Neurospora crassa* consumed cellobiose and xylose simultaneously (Ha et al., 2011a).

Two heterologous xylose-fermenting pathways are currently being used to engineer xylose-fermenting *S. cerevisiae*. Xylose isomerase genes from bacteria such as *Bacteroides stercoris* or anaerobic fungi such as *Piromyces* sp. E2 have been expressed in *S. cerevisiae* (Ha et al., 2011b; Karhumaa et al., 2007). But their functional expression in *S. cerevisiae* was not successful. For the successful expression of xylose isomerase in *S. cerevisiae*, screeing for a novel xylose isomerase and codon-optimizing of xylose isomerase had been attempted.

The other xylose-fermenting pathway consists of XR and XDH. A lot of studies had used *XYL1* and *XYL2* genes derived from *Scheffersomyces stipitis*. The difference in the cofactor preference of XR and XDH generates cofactor imbalance, resulting in significant xylitol accumulation and low yield of ethanol (Fig. 1.6. 3, 4). Although the XR/XDH pathway has this intrinsic defect, it exhibited faster xylose assimilation and ethanol production compared to the XI pathway (Karhumaa et al., 2007). To bypass the cofactor imbalance problem,

protein engineering was attempted to modify cofactor preference of XR and XDH. The cofactor preference of XR or XDH was successfully altered by protein engineering such as site-directed mutation of cofactor-binding sites (Petschacher & Nidetzky, 2005; Watanabe et al., 2005). Many studies demonstrated that expresstion of the NADH-dependent XR mutant with the wild type NAD^+- dependent XDH improved ethanol yield and productivity while decreasing xylitol accumulation (Watanabe et al., 2007b). Engineered strains expressing the wild type NADPH-dependent XR and the mutant XDH specific for $NADP^+$ also exhibited lower xylitol and higher ethanol yield than an engineered strain expressing the wild types of XR and XDH (Lee et al., 2012; Matsushika et al., 2008; Watanabe et al., 2007a).

Although *S. cerevisiae* has endogeneous xylulose kinase activity, it is not sufficient to convert xylulose to xylose-5-phosphate. Therefore, XK activity should be reinforced by overexpression of the endogenous *S. cerevisiae* XK gene (*XKS1*) or the introduction of the heterologous XK gene (*XYL3* from *Sch. Stipitis*) (Jin et al., 2005; Matsushika & Sawayama, 2011; Toivari et al., 2001; Wahlbom et al., 2003). However, too strong expression of the XK gene could cause growth inhibition on xylose or reduction in a xylose consumption rate (Jin et al., 2003; Johansson et al., 2001). This negative effect of the XK gene overexpression might be explained by “substrate-accelerated death” as

described previously (Teusink et al., 1998). ATP is invested in order to get substrates into cells. The investment of ATP is subsequently regenerated by glycolysis which has an elaborate reglulatory mechanism (Fig. 1.7). Because a heterologous xylose-assimilating pathway is not controlled by feedback inhibition, an increased demand of ATP by XK overexpression can exceed a supply of ATP, resulting in ATP depletion. On the other hand, two studies suggested that high expression of the XK gene decreased xylitol accumulation (Matsushika & Sawayama, 2011; Parachin et al., 2011). Therefore, the expression ratio of the XR/XDH/XK might be more important than activities of individual enzymes to minimize xylitol accumulation and to improve ethanol yield.

The intracellular metabolites in an engineered *S. cerevisiae* strain expressing XR and XDH in xylose fermentation were measured. The sedoheptulose-7-phosphate, an intermidiate of non-oxidative pentose phosphate, accumulated. This result suggested the insufficient pentose phosphate pathway might be a limiting step in xylose metabolism of engineered *S. cerevisiae* (Kotter & Ciriacy, 1993) (Fig. 1.6. 5). Although the effect of transketolase (*TKL1*) overexpression, the second enzyme in the pentose phosphate pathway, was quiet controversial, the overexpression of transaldolase (*TAL1*), the third enzyme, improved the xylose consumption rate (Lee et al., 2012; Matsushika et al., 2012). The

simultaneous overexpression of all enzymes (*XKS1, RKI1, RPE1, TKL1* and *TAL1*) which are included in the non-oxidative pentose phosphate pathway improved the growth of engineered *S. cerevisiae* strains expressing XI gene (Karhumaa et al., 2005; Kuyper et al., 2005). On the other hand, the same strategy was not effective in the engineered strain expressing XR and XDH moderately and overpressing XK (Bera et al., 2011; Johansson & Hahn-Hägerdal, 2002). Since the oxidative pentose phosphate pathway is a main route for NADPH generation but produces CO_2 to decrease ethanol yield, some studies attempted to decrease carbon flux to the oxidative pentose phosphate pathway. As a result, CO_2 production was decreased and ethanol yield was improved (Fig. 1.8). By deleting *ZWF1* coding for glucose-6-phosphate dehydrogenase and/or *GND1* for 6-phosphogluconate dehydrogenase, the engineered strains expressing XR and XDH showed a higher ehanol yield as expected. However, a xylose consumption rate was decreased due to reduction of the NADPH-dependent XR reaction (Jeppsson et al., 2002; Verho et al., 2003).

Acetic acid, a byproduct in the xylose metabolism and one of the fermentation inhibitors in lignocellulosic hydrolysates, inhibits cell growth and has negative effects on sugar fermentation (Palmqvist & Hahn-Hägerdal, 2000). The undissociated form of acetic acid can enter cells by passive diffusion and dissociates immediately due to higher

intracellular pH in the cytosol (Ullah et al., 2012), resulting in reduction of intracellular pH. To maintain the intracellular pH, cell pumps out the excess protons using ATP. Consequently, undissociated form of acetic acid causes ATP depletion and growth inhibition (Pampulha & Loureiro-Dias, 2000) (Fig. 1.6. 7). Lastly, the deletion of *ALD6* coding for aldehyde dehyrogenase gene reduced accumulation of acetate to improve xylose fermentation (Kim et al., 2013b; Lee et al., 2012).

To explore unknown targets that cannot be captured by the above rational approaches, adaptive evolutionary engineering has been used to develop strains with improved xylose utilization (Kim et al., 2013b; Lee et al., 2014; Qi et al., 2015; Zeng et al., 2017). In general, evolutionary engineering was carried out by cultivating in xylose media, and by transferring the culture to fresh media when the cells reached a certain OD_{600}. During these continuous cultivations, spontaneous mutations which affect cell growth in xylose media occur and the mutant strains with a desired phenotype will be isolated. The evolved strains were analyzed though genome sequencing, transcriptome analysis and metabolomics analysis to identify candidate genes involved in the enhanced xylose fermentation.

The mutations in *pho13* from the evolved xylose utilization strain was

identified though genome sequencing (Kim et al., 2013b). This gene was related to the regulation of the pentose phosphate pathway and NADPH-producing enzymes mediated by the transcription factor Stb5 (Kim et al., 2015b). Aside from genome sequencing, transcriptome analysis is also used to identify changes in evolved strains. The adaptive evolved strain in xylose media exhibited the upregulation of biosynthesis of vitamin B1 and sulfur-containing amino acids and the downregulation of glucose signal pathway regulators Rgs2 and Sip4 (Zeng et al., 2017). Recently, genome sequencing, proteomic profiling and metabolomics analysis were combined to characterize the responsible mutations in the evolved strains (Sato et al., 2016).

Lignocellulosic hyhdrolysates contains various inhibitors such as furan derivatives, carboxylic acids and phenolic compounds (Almeida et al., 2007). The presense of these inhibitos aggravates both growth and fermentation capabilities of yeast. Thus, many studies have attempted to enhance tolerance to inhibitors. Deletion of *PHO13* and overexpression of *MSN2*, *ZWF1*, *ALD6*, *TAL1* and *ADH1* genes led to an improvement in both growth and the ability to ferment xylose in the presence of furan derivatives (Fujitomi et al., 2012; Gorsich et al., 2006; Park et al., 2011; Sasano et al., 2012). In terms of tolerance to acetic acid, the overexpression of *HAA1*, the acetic acid-responsive transcriptional activator, improved cell growth and ethanol production

from xylose in the presence of acetic acid (Sakihama et al., 2015). While these gene manipulations have focused on the tolerance to specific inhibitors, exogenously added spermidine or adequate modulation of spermidine contents in *S. cerevisaie* improved the tolerance to multiple inhibitors (Kim et al., 2015a).

The industrial strains showed much better growth in corn stover hydrolysate compared to that of a laboratory strain, suggesting the need to engineer the industrial strains for lignocellulosic fermentation (Li et al., 2015). However, their genetic manipulation is challenging, as they are usually diploid or polyploid and a lack of available auxotrophic markers. Recently, the CRISPR-Cas9 system was developed and has been applied to genome editing of industrial *S. cerevisiae* (Stovicek et al., 2015; Zhang et al., 2014). The industrial polyploidy *S. cerevisiae* JHS200 was engineered to assimilate xylose through Cas9-based genome editing and the resulting strain exhibited higher ethanol productivity from cellulosic hydrolysates than those of other engineered haploid strains (Lee et al., 2017).

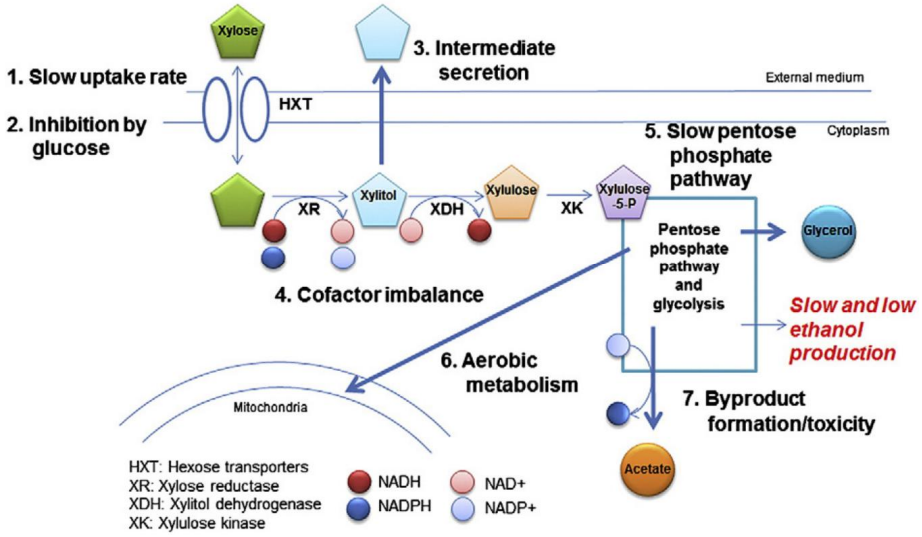

Fig. 1.6. Major limitations in xylose metabolism by engineered *S. cerevisiae* expressing a heterologous xylose-fermenting pathway consisting of XR, XDH and XK (Kim et al., 2013a).

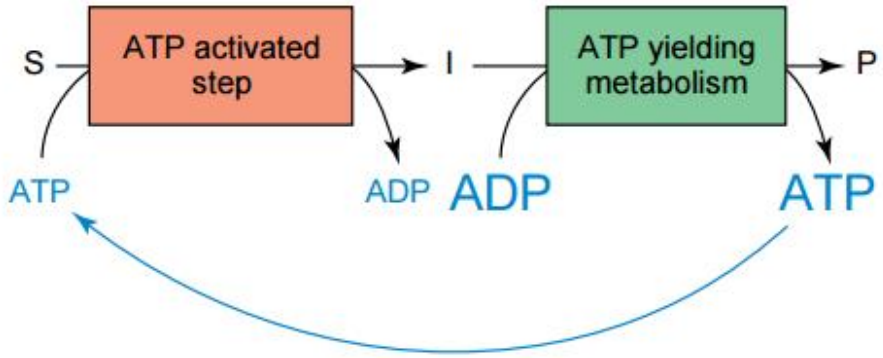

Fig. 1.7. General scheme for a catabolic pathway in which the first step involves coupling of ATP hydrolysis to activation of a substrate (Teusink et al., 1998).

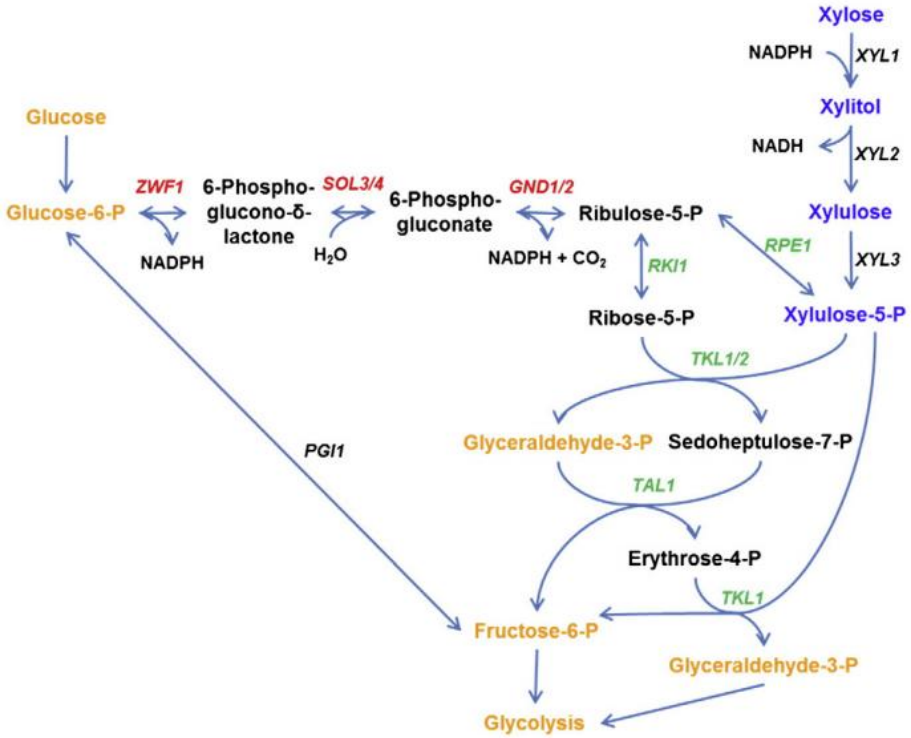

Fig. 1.8. Gene coding for the enzymes engaged in the oxidative (red) and non-oxidative (green) pentose phosphate pathway. Heterologous xylose-assimilating pathway is marked in blue. Metabolic intermediates of glycolysis are marked in orange (Kim et al., 2013a).

1.4. Effects of cofactor regeneration on xylose fermentation

Cofactors such as NAD(P)H and $NAD(P)^+$ provide redox carriers for biosynthetic and catabolic reactions and act as important agents in transfer of energy for the cell (Wang et al., 2013). The $NADPH/NADP^+$ and $NADH/NAD^+$ cofactor pairs are related in numerous biochemical reactions and interact with various enzymes of microorganisms. In addition, they have a series of physiological functions such as regulating energy metabolism, adjusting the intracellular redox state, controlling carbon flux and improving the function and activity of the mitochondrion (Chen et al., 2014). And they serve as electron acceptors in the breakdown of catabolic substrates and the reducing power needed in energy-conserving redox reations to the cell (De Graef et al., 1999). Therefore, maintaining the cellular redox balance is a prerequisite for microbial production of biofuels and chemicals. In order to achieve this aim, various strategies have been attempted: culture conditions or additive alterations, genetic modification of host pathways for increased availability of a desired cofactor, change in enzyme cofactor specificity and introduction of novel redox partners for biochemical processes (Wang et al., 2013).

Cofactors play an important role for the engineering of xylose-

fermenting pathways in *S. cerevisiae*. The cofactor imbalance generated from the difference in the cofactor preferences of XR and XDH leads to NAD^+ and NADPH deficiency, resulting in significant xylitol accumulation and reduction of ethanol yield (Kim et al., 2013a). In order to maintain the cellular redox balance in the engineered *S. cerevisiae* expessing XR and XDH, various strategies have been attempted. As decribed in Chapter 1.3, alteration of cofactor preferences of XR and XDH was genenally used. Second, heterologous expression of a fungal $NADP^+$-dependent glyceraldehyde-3-phosphate dehydrogenase (GAPDH) gene with *ZWF1* deletion improved ethanol yields from xylose (Verho et al., 2003). Third, the engineered strain with the deletion of *GDH1* (NADPH-dependent glutamate dehydrogenase gene) and the overexpression of *GDH2* (NADH-dependent glutamate dehydrogenase gene) in the ammonia assimilation pathway exhibited low xylitol accumulation and high ethanol production in a mixture of glucose and xylose (Roca et al., 2003). Fourth, the *Lactococcus lactis noxE* gene coding for a water-forming NADH oxidase was expressed in the xylose-fermenting *S. cerevisiae* strain, resulting in a reduction of xylitol accumulation (Zhang et al., 2012). Fifth, acetylating acetaldehyde dehydrogenase (*AADH*) from *E. coli* was expessed in the engineered *S. cerevisiae* strain having the XR/XDH pathway to construct the NADH-consuming acetate

consumtion pathway. The surplus NADH genereated from xylose metabolism could be oxidized by acetate reduction to alleviate the redox cofactor imbalance resulting from the xylose fermentation (Wei et al., 2013).

1.5. Effects of genetic backgrounds of xylose-fermenting yeasts

Industrial strains were often compared with laboratory strains in terms of sugar utilization efficiency and stress tolerance (Garay-Arroyo et al., 2004; Hector et al., 2011; Matsushika et al., 2009b). Three industrial and two laboratory *S. cerevisiae* strains having the same xylose-assimilation pathway were used to compare xylose-fermenting capability. Among these engineered strains, industrial strains consumed higher amount of xylose and produced higher amount of ethanol than the laboratory strains. In other study, an engineered laboratory strain having the xylose-assimilation pathway showed a similar xylose consumption rate compared with six industrial strains expressing the same genes (Hector et al., 2011). These results suggested that the genetic background strongly influenced the xylose consumption, ethanol yield and xylitol yield when fermenting xylose or glucose/xylose mixtures. As genome sequencing technologies have advanced, a genome-wide level analysis has increased to understand direct genotype to phenotype relationships. Since the genome of *S. cerevisiae* strain S288c was sequenced completely (Goffeau et al., 1996), the genomes of several other yeasts strains have been sequenced (Akao et al., 2011; Borneman et al., 2011; Jeffries et al., 2007;

McIlwain et al., 2016; Otero et al., 2010; Wohlbach et al., 2011), providing important molecular information regarding the evolutaionary and ecological diversity of this key model organism (Babrzadeh et al., 2012). Specially, whole genone sequencing and comparative genomics have been applied to identifying and understranding the molecular basis of efficient xylose utilization. Expression of the *Cantida tenuis* aldo/keto reductase improved xylose consumption by playing a role as $NADP^+$-dependent glycerol dehydrogenase in *S. cerevisiae* (Wohlbach et al., 2011).

1.6. Objectives of the dissertation

This dissertation focuses on production of value-added products from lignocellulosic biomass by engineered *S. cerevisiae*. The specific objectives of this research are listed:

1) Comprehensive genomic analysis of *S. cerevisiae* D452-2 for identification of genes related to xylose fermentation,

2) Construction of efficient xylose-fermenting *S. cerevisiae* for production of ethanol through a synthetic isozyme system of xylose reductase from *Scheffersomyces stipitis*,

3) Improvement of xylitol production through dual utilization of NADPH and NADH cofactors in engineered *S. cerevisiae*.

Chapter 2

Genome sequencing and comparative analysis of *Saccharomyces cerevisiae* D452-2

2.1. Summary

S. cerevisiae D452-2, a laboratory strain for xylose fermentation has been used as a host strain for production of biofuels and chemicals. The genomic background of a specific strain is also an important factor for efficient fermentation. But, the genome of the D452-2 strain was not completed yet and its benefical genetic polymorphisms remain unknown for xylose fermentation. To understand the associations between the genetic background and the desired phenotypes, the whole genome of D452-2 was sequenced and compared with that of the reference strain S288c. A total of 6,948 SNPs and a 172,733 length of gaps were detected to result in a different gene expression pattern. The *GPD2*, *GAL2*, *ACS1*, *ALD4* genes and glycogen metabolic genes were selected as a candidate gene for enhanced xylose fermentation. Additionally, the DXS strain having unexpected higher XR activity in Chapter 3 was sequenced to identify genetic perturbations. The XR expression cassett was amplified by homologous recombination. This genome information of D452-2 could be used for developing an enhanced xylose-fermenting yeast strain.

2.2. Introduction

As petroleum-based fuels hold disadvantages, such as depletion of sources, causing global warming and aggravating environmental pollution, bioethanol production from sustainable resources has received considerable attention. First, stratchy biomass such as sugargane and corn as raw material was used to produce ethanol. But this resource had competition for its use as both food and fuel (Martin, 2010). Due to this competition, production of bioethanol from lignocellulosic biomass has been eagerly researched worldwide. Lignocellulic biomass such as woods and agricultural residues is a promising feedstock for bioethanol production and the second most common fermentable sugar in hydrolysates is xylose. So its efficient fermentation is essential for the economic conversion of lignocellulose to ethanol (Weber et al., 2010). By using metabolically engineered *Saccharomyces cerevisiae*, bioethanol production from xylose has been extensively attemped. Although several approaches have successfully engineered the strain to metabolize xylose, these approaches are insufficient for industrial bioprocesses mainly due to the low fermentation rate of xylose in comparison with that of glucose (Matsushika et al., 2009a).

The microbes with desired traits had been obtained though directed

evolution and random mutagenesis. But, these approach provided little to mechanistic understanding of which specific genetic perturbations lead to improved strains. The genetic basis of the phenotype needs to be elucidated by genome sequencing (Warner et al., 2009). Genome sequencing of *S. cerevisiae* S288c as the reference genome for the *Saccharomyces* Genome Database (SGD) strain was completed, that provided a framework for gene annotation through functional genomics (Otero et al., 2010). Owing to the development of a genome sequencing technique, genome sequencing technologies have been applied to the engineered *S. cerevisiae* to better understand these phenomena observed in the engineered *S. cerevisiae* and identify a new target gene for efficient xylose fermentation. For example, *Scheffersomyces stipitis* (known as *Pichia stipitis*), a native xylose-fermenting yeast, was sequenced and assembled. The sequence data have revealed unusual aspects of numerous genes for bioconversion and regulation of the central metabolic pathway and provides insights into how *Sch. stipitis* regulates its redox balance when fermenting xylose in microaerobic coditions. Genome characteristics obtained from the genome sequence of *Sch. stipitis* may serve as important guides for further development of engineered *S. cerevisiae* (Jeffries et al., 2007). In addition, the rapid-developing genome-sequencing technologies make adaptive evolution popular these days for identifying gene targets. Through genome

sequencing the evolved xylose-fermenting strains, the genetic basis for the altered phenotype can be identified and used as potential engineering targets for rational design (Kim et al., 2013b). There have been several attempts to characterize the genomes of industrial *S. cerevisiae* strains which have uncovered differences that include single nucleotide polymorphisms (SNPs), strain-specific ORFs and localized variations in genomic copy number (Argueso et al., 2009; Novo et al., 2009; Wei et al., 2007).

The *S. cerevisiae* D452-2 strain, a preferred laboratory strain for xylose fermentation, has been applied to metabolic and evolutionary engineering studies (Kim et al., 2013b; Lee et al., 2012; Watanabe et al., 2007a). Other *S. cerevisiae* strains have been sequenced and compared with the S288c strain, while the D452-2 strain was not sequenced yet (Nijkamp et al., 2012). The goal of this Chapter is to make the high-quality assembled and annotated reference genome of *S. cerevsiae* D452-2 sequence available to the academic and industrial research for xylose fermentation. The genome of D452-2 was sequenced and compared to that of the S288c strain to idenfity their underlying beneficial genetic polymorphisms. To this end, single nucleotieds variations, transposons, strain-specific sequences and ORFs were analyzed. Additionally, the engineered *S. cerevisaie* DXS strain having

the unexprected xylose reductase activity in Chapter 3 was sequenced in order to capture genetic changes.

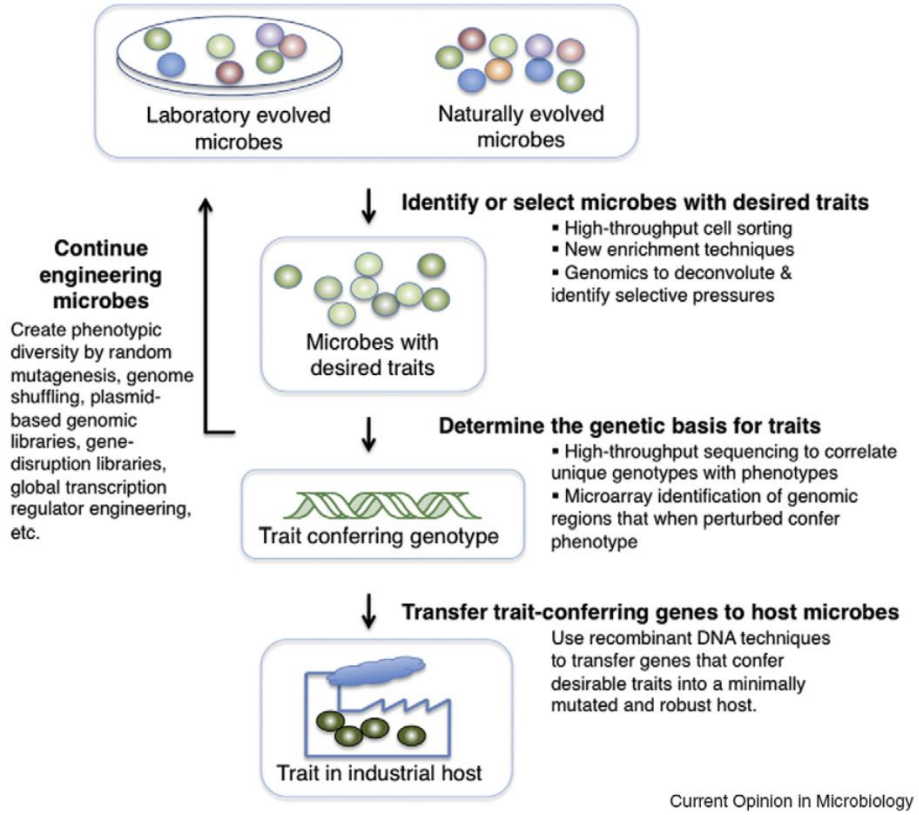

Fig. 2.1. Genomics tools applied to inverse metabolic engineering (Warner et al., 2009).

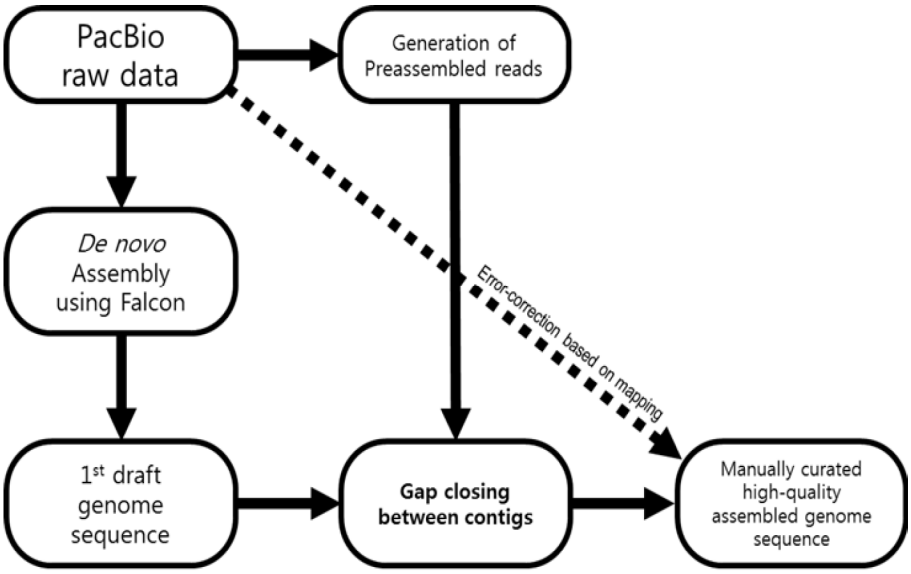

Fig. 2.2. Work flow of whole genome assembly.

2.3. Materials and methods

2.3.1. Isolation of genomic DNA

A single colony of D452-2 was cultured in 5 mL 10 g/L yeast extract, 20 g/L peptone and 20 g/L glucose (YPD) media at 30°C overnight. Cells were centrifuged at 13200 rpm for 2 min. The resulting cell pellet was washed with DDW and centrifuged. The washed cell pellet was then resuspended in 200 μL lysis buffer. Lysis buffer consisted of 0.1 M Tris pH 8.0, 1 mM NA_2EDTA, 2% triton X-100 and 1% SDS final concentration. The lysis buffer suspension was transferred to a 2 mL screw cap tube, to which 200 μL PCI solution (phenol, chloroform, isoamyl alcohol) and 0.3 g glass beads (0.5 mm) was added. After vortexing for 4 min, 200 μL TE buffer (10 mM Tris, 0.5 mM EDTA and pH 8.0) was added. The resulting cell suspension was centrifuged for 5 min, and the resulting clear liquid, approximately 350 μL, avoiding white cell debris and beads, was aspirated with a pipette and transferred to 1.5 mL eppen tubes. 1 mL absolute ethanol was added to each tube and mixed by inversion. The resulting suspension was centrifuged for 2 min. The DNA pellet was dissolved in 100 μL TE buffer and incubated with 10 mg/mL RNase A at 37°C for 1hr.

2.3.2. PacBio library preparation and sequencing

The isolated genomic DNA was sent to National Instrumentation Center for Environmental Management (NICEM, Seoul National University, Seoul, Korea) for library construction and Pacbio sequencing. Initial quantification was preformed using a Qubit® dsDNA BR assay Kit (Thermo Fisher Scientific, Waltham, MA, USA). About 10 μg of intact genomic DNA was sheared to 10 kbp using Covaris gTube (Covaris, Woburn, MA, USA). The sheared gDNA was purified and concentrated with a 0.45x washed Ampure bead (Pacific Bioscience, Menlo Park, CA, USA). A PacBio sequencing library was constructed using the SMRTbell™ Template Kit 1.0. P5 Polymerase was coupled with the resulting SMRTbell™ library. For sequencing, the library was bound to MagBeads by incubating for 4 hr at 30°C. The final library was run over 8 SMRT cells on the PacBio RS II using a C4 chemistry sequencing kit.

2.3.3. Whole genome assembly and sequence anlaysis

The genome of strain was *de novo* assembled using the hierarchical genome-assemble process (HGAP) pipeline of the SMRT Analysis v2.3.0 (Chin et al., 2013) and Falcon assembler v0.3.0, respectively. In order to correct sequencing errors that can occur at contigs, the SMRT

resequencing protocol was performed. The sequence analysis was performed using CLC genomics workbench (CLC Bio, Rarhus, Denmark).

2.3.4. Gene prediction

Open reading frames were initially predicted by GeneMark (http://genemark.biology.gatech.edu/GeneMark/). This program predicted ORFs though the algorithm that computes for a given DNA fragment posterior probabilities of either being "protein-coding" (carrying genetic code) in each of six possible reading frames (including three frames in complementary DNA strand) or being "non-coding" (Besemer & Borodovsky, 2005). Even though the ORFs of S288c strain were already detected and available in web, ORFs of this strain were predicted newly to analyze with the same conditions. ORFs were predicted from the sequences of S288c (Accession numbers : NC001133-NC001148) and D452-2. Those predicted ORFs were analyzed to determine their homology to proteins of known function using the BlastP (http://seqsim.ncgr.org/newBlast.html) and were clustered with a sequence-idendity cutoff of 90% with BlastClust (Altschul et al., 1997). The functional categories of genes were classified by COGs (http://ncbi.nlm.nih.gov/COG) (Tatusov et al., 2000).

2.3.5. Genome rearrangement analysis

The D452-2 genomes, along with the reference strain S288C, were aligned and oriented with the software MAUVE version 2.4.0 using the pregressive algorithm (http://darlinglab.org/mauve/mauve.html) (Darling et al., 2004). This tool provides a simple comparative picture of genome organization including inversion, gene gain, loss, and duplication. The gaps generated from transposon, rearrangement of genes and unique sequence were exported and filtered by subtraction of fragments less than 10 bp and telomere sequence. The filtered fragments were further analyzed to search genes involved in gap sequence using BlastALL program with a cutoff E-value of 10^{-5}.

2.4. Results and discussion

2.4.1. Comparison of xylose fermentation by 288c and D452-2

The fermentation performance of the D452-2 strain was compared with that of the BY4741 strain. The BY4741 strain was based on *S. cerevisiae* S288c in which commonly used selectable marker genes are deleted (Brachmann et al., 1998). The *XYL1*, *XYL2*, and *XYL3* genes from *Sch. stipitis* were introduced into the D452-2 and S288c strains in previous studies (Fujitomi et al., 2012; Kim et al., 2013b). The resulting strain DX123 was cultivated in similar condition to that of previous fermentation in order to compare with the fermentation performance of BY4741X. Fermentation was carried out in YP medium containing 80 g/L xylose at 30°C and 80 rpm. The initial cell concentration was adjusted to 50 g wet cells/L. The DX123 strain showed 10% and 36% higher ethanol yield and productivity than those of the BY4741X, respectively (Table 2.1). These results suggested that the genetic background of the D452-2 is more suitable for the xylose fermentation than that of the S288c strain.

Table 2.1. Yields and productivities of ethanol from xylose

Strain	Maximum yield (g ehtnaol / g xylose)	Maximum productivity (g/L-h)	Reference
BY4741X	0.279	0.826	(Fujitomi et al., 2012)
DX123	0.307	1.12	This study

These parameters were calculated from the change in ethanol and xylose with respect to time from 3 to 9 h.

2.4.2. Genome sequencing and assembly

Genome sequencing of D452-2 was performed using PacBio RS II single-molecule real-time (SMRT) sequencing technology. Standard PacBio libraries with an average of 20 kb inserts from D452-2 was prepared and sequenced, yielding >107.94x average genome coverages. The genome of D452-2 was *de novo* assembled from the 192,893 reads with 8,063 nucleotides on the average (1,555,393,883 bp in total) using the hierarchical genome-assembly process (HGAP) pipeline. The contigs were combined with the HGAP2 output and Falcon assembler output. Gap and low quality regions were closed with pre-assembled reads. Sequencing errors occurring at contigs were corrected though the SMRT resequencing protocol. Finally, 17 contigs were assembled and corresponded to the set of S288c chromosomes and mitochondrial DNA, yielding nealy the complete genome sequence of D452-2. The whole genome size of D452-2 was 12.26 Mb with 38.19% of GC content and 5350 genes were predicted. Genome characteristrics of the D452-2 strain are similar to S288c for genome parameters including total size and GC content. Table 2.2 summarizes Pacbio genome sequencing and annotation results.

Table 2.2. Genome sequencing and annotation results

Sequencing parameter	S288c	D452-2
Total size (Mb)	12.16	12.26
GC content (%)	38.15	38.19
ORFs	5332	5350

2.4.3. Comparative genome analysis

Since strains belonging to the same species had a similar genome synteny, whole genome sequence data were verified by comparing genome synteny with the reference genome. In addition, a genome could be changed by small/large indels, small-/large-scale rearrangements, duplications and SNPs. Comparative analysis of the complete genomes can provide a comprehensive view of genes and genomic regions which are responsible for the desired property. Knowing the precise sequence at regions of rearrangement gives an insight into underlying molecular mechanisms (Eichler & Sankoff, 2003; Minkin et al., 2013). To confirm the genome assembly of D452-2, the whole genome of D452-2 was aligned to S288c using MAUVE software (Fig. 2.3). The result was very similar to that of S288c, indicating that the assembled D452-2 genome has good quality.

Altough the overall genome structure of D452-2 resembled that of S288c, gaps were detected when observing each chromosome in detail. These gaps were a result of considerable heterozygosity between the two homologous chromosomes due to in-del and retrotransposon (Fig. 2.4). The retrotransposons are ubiquitous components of eukaryotic genomes and have played an important role in genome evolution. *S. cerevisiae* has five retrotransposon types (Ty1-Ty5) (Kim et al., 1998).

As a result of gaps detection though MAUVE software, the total length of gaps presented in D452-2 and S288c are 109,259 bp and 63,474 bp, respectively. After extraction of the gaps, BlastALL was performed to detect the genes involved in gap sequences and the alteration of gene locations was checked using CLC genomics workbench. The genome of D452-2 contained 10 Ty elements with a length of about 6 kbp each and S288c had 6 transposons. The chromosomal insertion of these Ty fragments resulted in loss of genes. For example, a region *SRD1* and YCR108C-A was replaced by Ty in the D452-2 chromosome III (Fig. 2.4). In chromosome IV, a gene duplication event was detected (Fig. 2.5 A). While S288c had 3 copies of the *ENA* gene that encode plasma membrane sodium-pumping ATPase, five copies of the *ENA* genes was detected in D452-2. Other *S. cerevisiae* strains had one to five *ENA* genes tandemly arraged. (Akao et al., 2011). Since these genes correlated with detoxificaton to sodium and lithium ions, D452-2 might be more tolerant than S288c (Ruiz & Ariño, 2007). In addition, other genetic modifications occurred in chromosome VIII (Fig. 2.5 B). YHR054C of S288c was deleted by homolous recombination generated from similar sequence genes (RUF5-1, 2). Small indels could cause frame shifts to block expression of genes or to change properties of proteins (Fig 2.5 C). The 38 genes mutated by Ty replacement, homolous recombination and small indel are listed in Table 2.3 and

were categorized by MIPS functional catalogue. The major portion was glycogen biosynthesis containing *HKR1*, *IMA3*, *GSY2*, *HPF1* and YIL169C genes. Glycogen, a branched polymer of glucose, plays a role serving as a storage factor during carbon starvation and providing quickly a higher carbon and ATP flux when the growth is recovered (Silljé et al., 1999). In a privous study, the xylose fermentation ability of an engineered strain containing XI was significantly improved though evolution strategy. The strain showed downregulated expression of trehalose and glycogen synthetic genes (Shen et al., 2012). These results suggested that the gene related to glycogen might affect xylose fermentation.

To search for differentially present genes between D452-2 and S288c, ORF comparative analysis was performed. ORFs of the genome of strains were predicted using GeneMark. Predicted ORFs were clustered with a sequence-identity cutoff of 90% with BlastClust. ORFs having similar amino acid sequences formed group and remanent ORFs were extracted. The extracted ORF were analyzed to determine their function using the BlastP. As a result, 19 genes were predicted as present in only D452-2 and 16 genes were predicted as present in only S288c (Table 2.4, 2.5).

Table 2.3. List of genes mutated by gap

Gene	Chr	Derstription	Mutation method
RRN6	2	Component of the core factor (CF) rDNA transcription factor complex	Ty replacement
FMT1	2	Methionyl-tRNA formyltransferase	Ty replacement
SRD1	3	Protein involved in the processing of pre-rRNA to mature rRNA	Ty replacement
YDR544C	4	Dubious open reading frame	ORF breakage by indel
HKR1	4	Mucin family member that functions as an osmosensor in the HOG pathway	changed property by indel
ENA1	4	P-type ATPase sodium pump	homolous recombination
ENA2	4	P-type ATPase sodium pump	homolous recombination
ENA5	4	Protein with similarity to P-type ATPase sodium pumps	homolous recombination
YER135C	5	Putative protein of unknown function	Ty replacement
GDI1	5	GDP dissociation inhibitor	Ty replacement
YER137C	5	Putative protein of unknown function	Ty replacement
MTL1	7	Putative plasma membrane sensor	ORF breakage by indel
YHR145C	8	Dubious open reading frame	ORF breakage by indel
CRP1	8	Protein that binds to cruciform DNA structures	ORF breakage by indel
YHR054C	8	Putative protein of unknown function	ORF breakage by indel
DSE2	8	Daughter cell-specific secreted protein with similarity to glucanases	changed property by indel
YHR054C	8	Putative protein of unknown function	homolous recombination
YIL169C	9	Protein of unknown function	ORF breakage by indel

IMA3	9	Alpha-glucosidase	ORF breakage by indel
VTH1	9	Putative membrane glycoprotein	ORF breakage by indel
PAU14	9	Protein of unknown function	ORF breakage by indel
YIL014C-A	9	Putative protein of unknown function	Ty replacement
TOR1	10	PIK-related protein kinase and rapamycin target	ORF breakage by indel
DAN4	10	Cell wall mannoprotein	ORF breakage by indel
YJR030C	10	Putative protein of unknown function	Ty replacement
SPA2	12	Component of the polarisome	ORF breakage by indel
LCB5	12	Minor sphingoid long-chain base kinase	ORF breakage by indel
GSY2	12	Glycogen synthase	ORF breakage by indel
HSP60	12	Tetradecameric mitochondrial chaperonin	ORF breakage by indel
RPS30A	12	Protein component of the small (40S) ribosomal subunit	changed property by indel
YMR317W	13	Putative protein of unknown function	ORF breakage by indel
YNL179C	14	Dubious open reading frame	changed property by indel
YOL013W-B	15	Dubious open reading frame	ORF breakage by indel
HPF1	15	Haze-protective mannoprotein	changed property by indel
PLB3	15	Phospholipase B (lysophospholipase) involved in lipid metabolism	changed property by indel
YPR203W	16	Putative protein of unknown function	ORF breakage by indel
YPR204W	16	DNA helicase encoded within the telomeric Y' element	ORF breakage by indel
YPL229W	16	Putative protein of unknown function	changed property by indel

Table 2.4. D452-2 genes absent in S288c

Gene	Chr	Description
PHO11	1	One of three repressible acid phosphatases
PFF1	2	Multi-spanning vacuolar membrane protease
LYS2	2	Alpha aminoadipate reductase
SPR28	4	Sporulation-specific homolog of the CDC3/10/11/12 family of genes
PEP7	4	Adaptor protein involved in vesicle-mediated vacuolar protein sorting
NAT1	4	Subunit of protein N-terminal acetyltransferase NatA
YEA4	5	Uridine diphosphate-N-acetylglucosamine (UDP-GlcNAc) transporter
SPF1	5	P-type ATPase, ion transporter of the ER membrane
RTR1	5	CTD phosphatase
DSD1	7	D-serine dehydratase (aka D-serine ammonia-lyase)
LSO1	10	Protein with a potential role in response to iron deprivation
HRD3	12	ER membrane protein that plays a central role in ERAD
ASP3	12	Cell-wall L-asparaginase II involved in asparagine catabolism
MCM1	13	Transcription factor
TOP2	14	Topoisomerase II
PRM1	14	Pheromone-regulated multispanning membrane protein
BIL1	15	Protein that binds Bud6p and has a role in actin cable assembly
YPL109C	16	UbiB family protein
DPM1	16	Dolichol phosphate mannose (Dol-P-Man) synthase of ER membrane

Table 2.5. S288c genes absent in D452-2

Gene	Chr	Description
HIM1	4	Protein of unknown function involved in DNA repair
FIN1	4	Spindle pole body-related intermediate filament protein
GIM4	5	Subunit of the heterohexameric cochaperone prefoldin complex
SMD1	7	Core Sm protein Sm D1
RSC30	8	Component of the RSC chromatin remodeling complex
YIL165C	9	Putative protein of unknown function
FAF1	9	Protein required for pre-rRNA processing
CSS1	9	Protein of unknown function
TRK1	10	Component of the Trk1p-Trk2p potassium transport system
YJR030C	10	Putative protein of unknown function
SEG1	13	Component of eisosome required for proper eisosome assembly
YMR317W	13	Putative protein of unknown function
YOR012W	15	Putative protein of unknown function
IZH4	15	Membrane protein involved in zinc ion homeostasis
WHI2	15	Protein required for full activation of the general stress response
GDE1	16	Glycerophosphocholine (GroPCho) phosphodiesterase

(be continued)

Fig. 2.3. A mauve alignment of D452-2 to S288c. Colored blocks [Locally Collinear Blocks (LCB)] indicate matches between the two genomes.

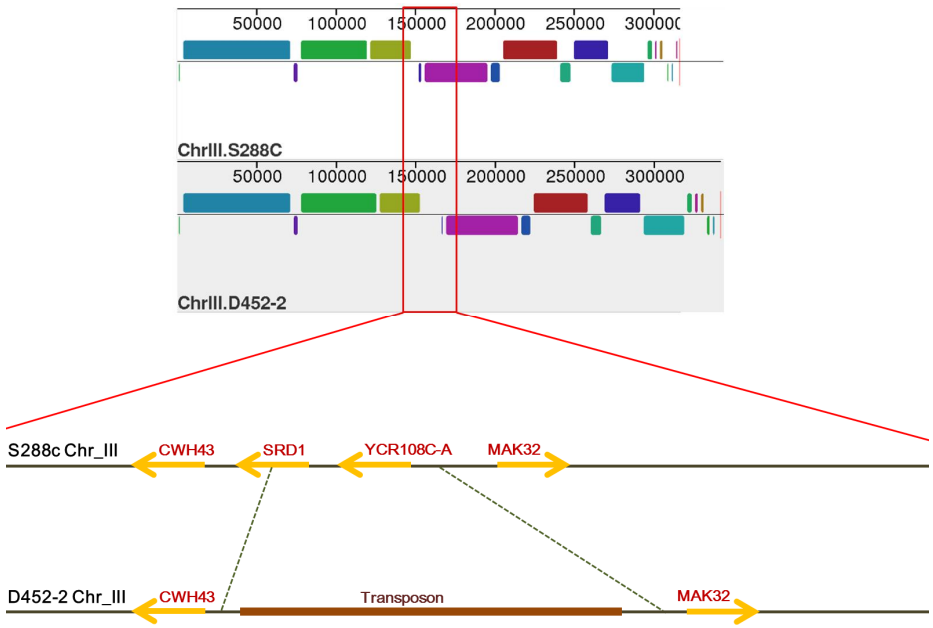

Fig. 2.4. Loss of genomic regions by Ty1 replacement in the D452-2 genome.

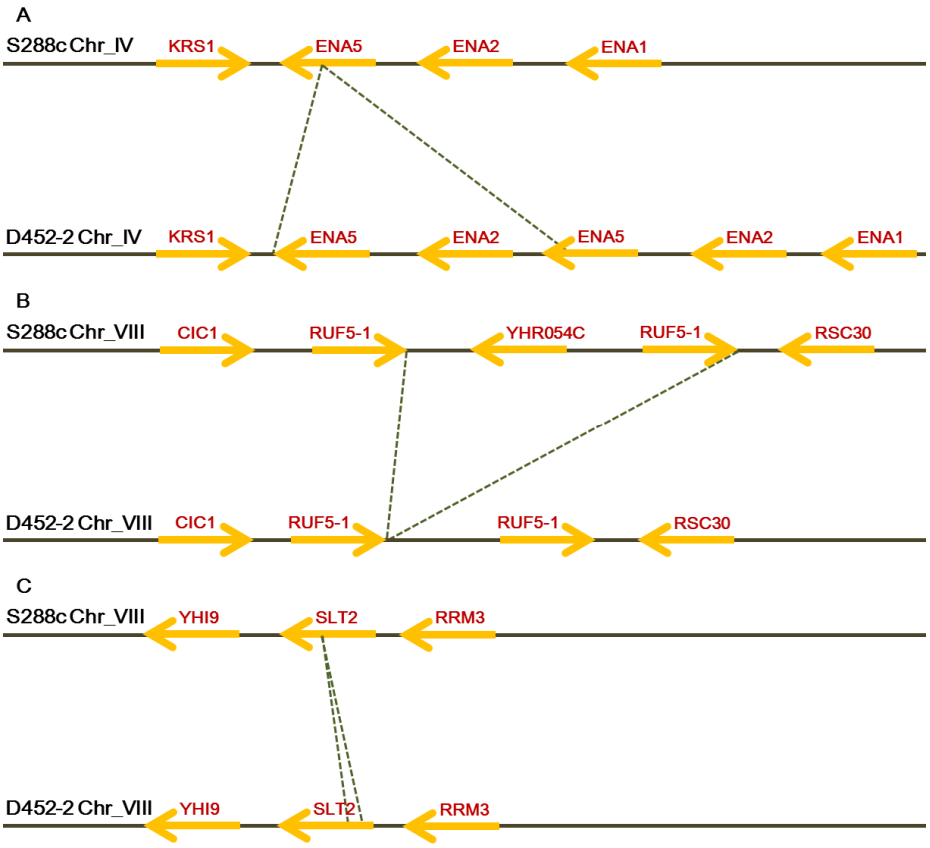

Fig. 2.5. Chromosomal modification methods. A. duplication, B. pop-out, C. small indel.

2.4.4. Single nucleotide polymorphisms (SNPs) identification

Single nucleotide polymorphisms (SNPs) analysis was performed by alignment of the D452-2 assembly and the reference sequence of S288c using CLC genomics workbench. This progrom can visulalize genome sequences, annotated genes, and SNPs of D452-2. This analysis identified a total of 6948 SNPs, which were located in 685 open reading frames. 482 ORFs of mutated genes were defined as metabolic genes by SGD (*Sacchromyces* Genome Database, http://www.yeastgenome.org). Since nucleotide mutation did not always lead to substitution of amino acids, ORFs that had changed property by SNP were detected using BlastP. A total of 313 metabolic genes of D452-2 (65%) were affected and might be candidate genes for xylose fermentation. In order to characterize the above mutated genes indentified in D452-2 with biological significance, a COG process was performed. The database of Clusters of Orthologous Groups of proteins (COGs) is a useful tool for functional classification and annotation of proteins (Tatusov et al., 2003). Of 313 genes, 216 genes were classified into 26 COG categories (Table 2.6, Fig. 2.6). The general function prediction (28, 13%) represented the largest group, followed by translation, ribosomal structure and biogenesis (24, 11%), signal transduction mechanisms (20, 9.3%), carbohydrate transport and

metabolism (16, 7.4%) and so on. The detailed data were listed in Appendix 1. This Chapter focused on transport, central metabolism and cofactor related enzymes for xylose fermentation. The selected genes were listed in Table 2.7.

The *GAL2* gene, which encodes galactose permease, is a high-affinity hexose transporter. A strain in which main sugar transporter genes *HXT1-17* and *GAL2* were deleted was unable to grow on xylose. The growth of this strain on xylose could be restored by the reintroduction of the *GAL2* gene (Hamacher et al., 2002). These results suggested that the Gal2 transporter is able to transport hexose as well as xylose. But, the xylose transporter is competively inhibited by glucose, which delayed the fermentation of lignocellulose biomass. Using a growth-based screening system, the Gal2 mutant which was insensive to the presence of glucose was selected (Farwick et al., 2014). Gal2-N376F had the highest affinity for xylose and had completely lost the ability to transport glucose. This study suggested that the conserved asparagine residue was decisive for determining sugar specificity (green square in Fig. 2.7). The D452-2 *GAL2* gene carries a non-synonymous mutation that results in an amino acid substitution (His392Arg). While other transporters aligned had arginine at 392 position, the *GAL2* gene in D452-2 had histidine. To identify that whether this susbtitutions of

amino acid in the *GAL2* gene exhibit an enhanced xylose fermentation, kinetic properties of Gal2 of D452-2 needed to be determined.

Other candidate is the *GPD2* gene encoding NAD-dependent glycerol 3-phosphate dehydrogenase. The Gpd2 mainly played a role as a redox sink. For example, the *GPD2* gene is induced in order to consume NADH produced by the formic acid breakdown reaction (Hasunuma et al., 2011). Deletion of *GPD2* increased ethanol production from glucose due to alteration of carbon flux. But a decrease of glycerol by deletion of *GPD2* increased NADH accumulation in the cell, inhibiting the growth rate (Guo et al., 2009). And expression of *GPD2* is not induced by osmotic stress but by anoxic condition (Ansell et al., 1997). Therefore, *GPD2* is an important gene for efficient xylose fermentation in anaerobic condition. *GPD2* of the D452-2 strain had two amino acid substitutions compared to that of S288c (Ser110Pro, Leu375Thr). To identify the effects of these amino acid alterations on protein structure, secondary structures of two Gpd2 (S288c and D452-2) were predicted using CLC genomics workbench. As shown in Fig 2.8, S288c Gpd2 consisted of β-strand, α-helix and α-helix at position 361-381. On the other hand, D452-2 Gpd2 consisted of β-strand and α-helix. This structural change might influence the gene expression and property.

ALD4 and *ACS1* genes were involved in the central metabolic pathway

and encoded acetyl-CoA synthetase and mitochondrial dehydrogenase, respectively. Ald4 converts acetaldehyde to acetate by utilizing $NADP^+$ and NAD^+ equally and can substitute for cytosolic $NADP^+$-dependent aldehyde dehydrogenase (Mukhopadhyay et al., 2013). The *ACS1* reaction is the main source of acetyl-CoA and the *ACS1* gene was expressed during growth on nonfermentable carbon sources including xylose (Kratzer & Schüller, 1995). As these enzyme reactions were related to cofactor and central metabolites such as acetate and acetyl-CoA, a change of expression level generated from mutated genes might affect xylose fermentation. Besides the genes mentioned above, a lot of ATPases and kinases were mutated as well.

Table 2.6. One-letter abbreviations for the functional categories of COG

#	Description
A	RNA processing and modification
B	Chromatin structure and dynamics
C	Energy production and conversion
D	Cell cycle control, cell division, chromosome partitioning
E	Amino acid transport and metabolism
F	Nucleotide transport and metabolism
G	Carbohydrate transport and metabolism
H	Coenzyme transport and metabolism
I	Lipid transport and metabolism
J	Translation, ribosomal structure and biogenesis
K	Transcription
L	Replication, recombination and repair
M	Cell wall/membrane/envelope biogenesis
N	Cell motility
O	Posttranslational modification, protein turnover, chaperones
P	Inorganic ion transport and metabolism
Q	Secondary metabolites biosynthesis, transport and catabolism

(be continued)

#	Description
R	General function prediction only
S	Function unknown
T	Signal transduction mechanisms
U	Intracellular trafficking, secretion, and vesicular transport
V	Defense mechanisms
W	Extracellular structures
X	Mobilome: prophages, transposons
Y	Nuclear structure
Z	Cytoskeleton

Table 2.7. Candidate genes for enhanced xylose fermentation

D452-2 gene	COG description	BlastP positives
PYC1	Pyruvate carboxylase	1178/1179
ALD4	Acyl-CoA reductase or other NAD-dependent aldehyde dehydrogenase	519/520
GPD2	Glycerol-3-phosphate dehydrogenase	422/424
POS5	NAD kinase	414/415
HXT16	MFS family permease	567/568
GAL2	MFS family permease	574/575
ACS1	Acyl-coenzyme A synthetase/AMP-(fatty) acid ligase	713/714
ENV9	NAD(P)-dependent dehydrogenase, short-chain alcohol dehydrogenase family	330/331
HST1	NAD-dependent protein deacetylase, SIR2 family	491/492

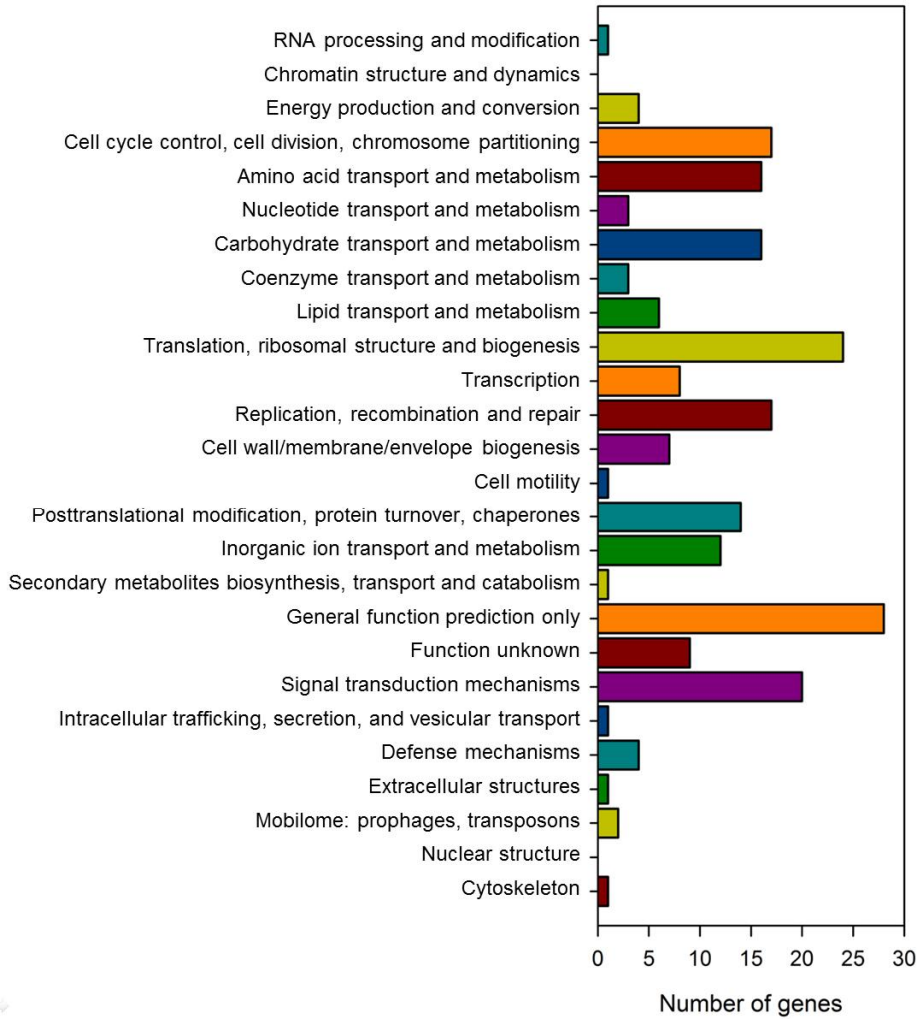

Fig. 2.6. COG function classification of 313 genes.

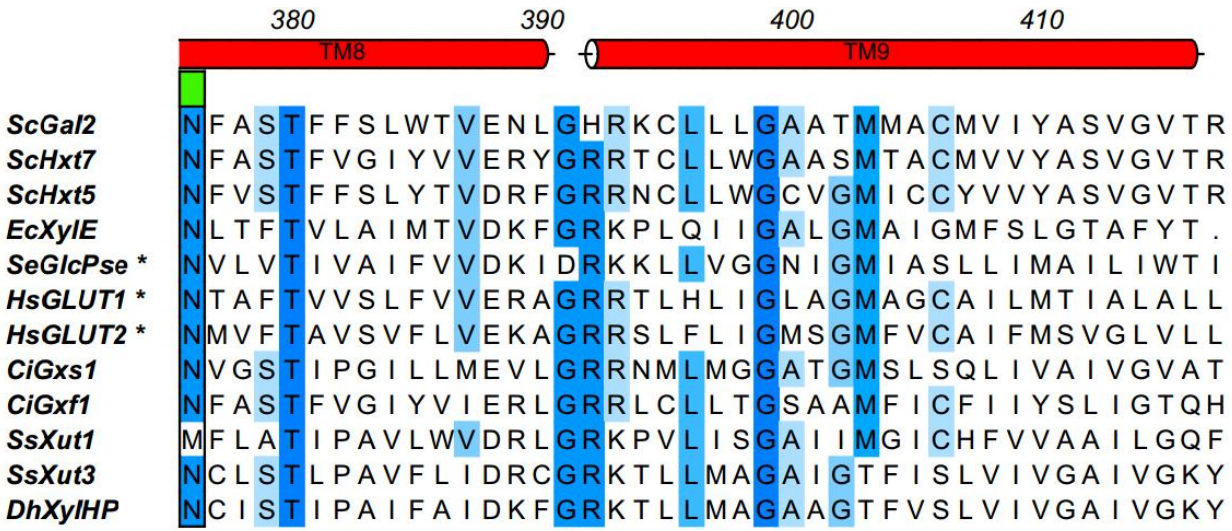

Fig. 2.7. Protein sequence alignment of different sugar transporters. Transporters aligned are *Saccharomyces cerevisiae* Gal2, Hxt7, and Hxt5, *Escherichia coli* XylE, *Staphylococcus epidermidis* $GlcP_{SE}$, *Homo sapiens* GLUT1 and GLUT2, *Candida intermedia* Gxs1 and Gxf1, *Scheffersomyces stipitis* Xut1 and Xut3, and *Debaryomyces hansenii* xylHP (Farwick et al., 2014).

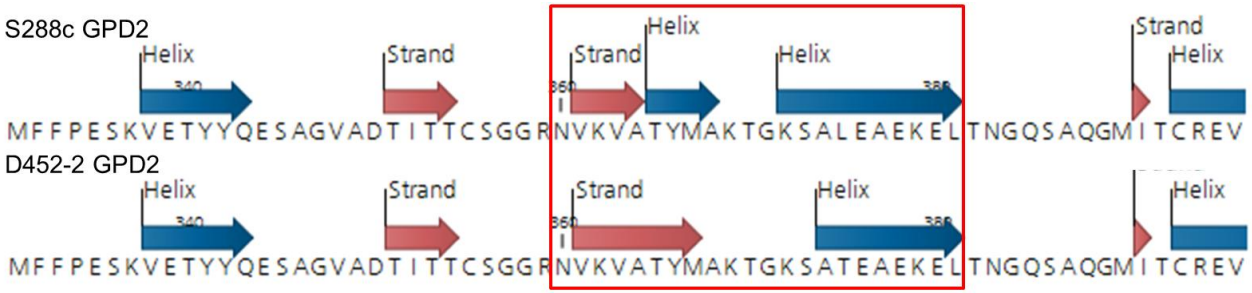

Fig. 2.8. Comparison of secondary structures of S288c Gpd2 and D452-2 Gpd2.

2.4.5. Identification of mutation for enhanced XR activity in the DXS strain

In Chapter 3, the DXS strain having unexpected high XR activity was constructed. To identify the mutations responsible, comparative genome analysis was used. After genome sequencing of the DXS strain, it was compared with that of D452-2. The vector p403_mXR expressing the mutant XR was integrated into the DX123 strain expressing a wild-type XR, XDH and XK though homologous recombination (Fig. 2.9 A). As unexpected, the vector p403_mXR was integrated in twice and the XR expression cassett of p306_X123 was increased by tandem amplication (Fig. 2.9 B). As a result, the DXS strain had 3 copies of wild XR and 2 copies of mutant XR to exhibit higher XR activity. The tandem amplification of the XR genes might be initiated by the unequal crossover of the his3::HIS3 GPDp-mXR-CYC1t or TDHp-XK-TDHt TDHp-wXR-TDHt construct in the genome. This tandem amplification was observed in evolution engineering. In a prior study, the evolved strain harbored higher copy numbers of the cellodextrin transporter gene and β-glucosidase gene in the genome by tandem amplication enhanced cellobiose fermentation (Oh et al., 2016).

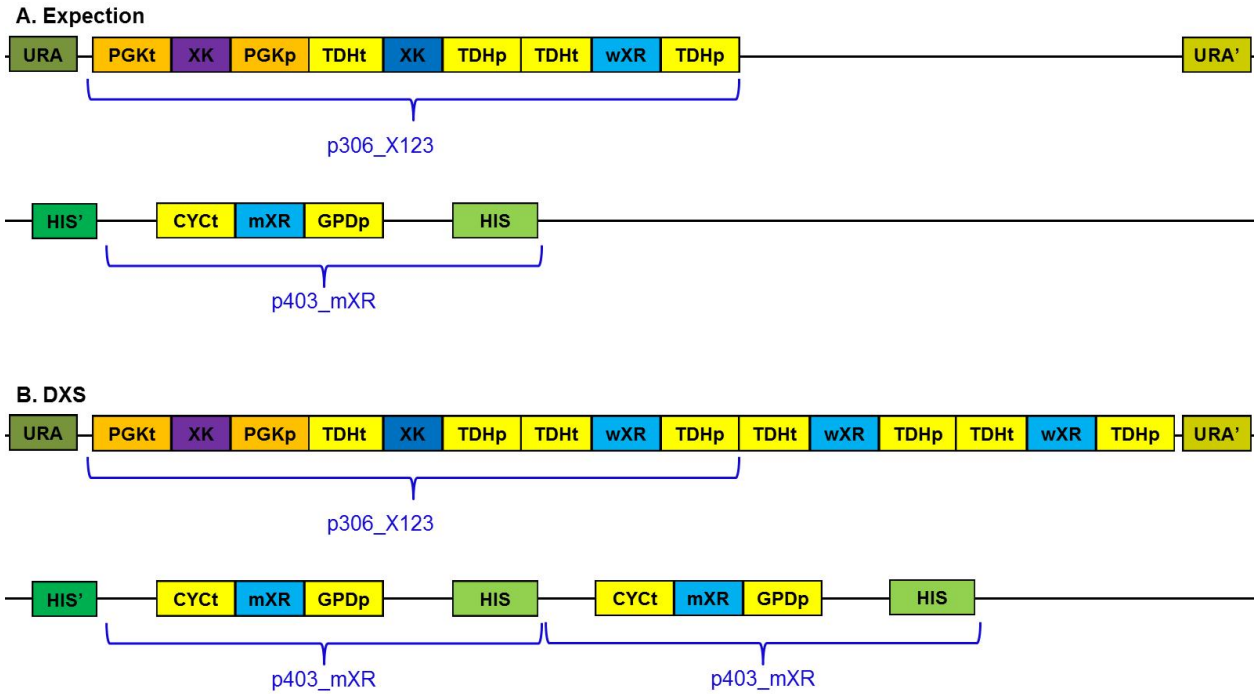

Fig. 2.9. Genome-integration of XR expression cassett by homolous recombination.

Chapter 3

Production of ethanol from cellulosic biomass by engineered *Saccharomyces cerevisiae*

3.1. Summary

Engineered *Saccharomyces cerevisiae* has been used for ethanol production from xylose, the abundant sugar in lignocellulosic hydrolyzates. Development of engineered *S. cerevisiae* able to utilize xylose effectively is crucial for economical and sustainable production of fuels. To this end, the xylose-metabolic genes (*XYL1*, *XYL2* and *XYL3*) from *Scheffersomyces stipitis* have been introduced into *S. cerevisiae*. The resulting engineered *S. cerevisiae* strains, however, often exhibit undesirable phenotypes such as slow xylose assimilation and xylitol accumulation. In this chapter, a synthetic isozyme system of xylose reductase (XR) was developed to construct an improved xylose-fermenting strain. The engineered strain having both wild XR and mutant XR showed low xylitol accumulation and fast xylose consumption compared to the engineered strains expressing only one type of XR, resulting in improved ethanol yield and productivity. These results suggest that the introduction of the XR-based synthetic isozyme system is a promising strategy to develop efficient xylose-fermenting strains.

3.2. Introduction

Petroleum-based fuels hold disadvantages, such as depletion of sources, causing global warming and aggravating environmental pollution. To address these drawbacks, bioethanol has been extensively studied for decades. Lignocellulosic biomass, such as agricultural residues, dedicated energy crops, wood residues and municipal paper waste, are abundant and sustainable feedstocks for bioethanol production. Lignocellulosic materials are composed of cellulose, hemicelluloses, and lignin. After hydrolysis, these materials are decomposed to hexoses, pentoses and inhibitors (Ko et al., 2016). Typically, lignocellulsic hydrolyzates consist of 60~70% glucose and 30~40% xylose (Mosier et al., 2005). Therefore, a microorganism capable of assimilation of mixed sugars is needed for bioethanol production from lignocellulosic biomass (Hahn-Hagerdal et al., 2006). As *Saccharomyces cerevisiae* exhibits high tolerance to ethanol and inhibitors and is Crabtree-positive, the baker's yeast has been used traditionally for ethanol production (Jeffries & Jin, 2004). While *S. cereivisiae* can convert glucose to ethanol with a high yield, *S. cereivisiae* can not ferment xylose (Kim et al., 2013a; Weber et al., 2010). To produce bioethanol from lignocellulosic biomass economically, it is crucial to develop engineered *S. cereiviaiae* capable of co-fermenting glucose and xylose

efficiently by introducing the xylose metabolic pathway into *S. cerevisiae*.

In microbial xylose metabolism, xylose is converted into xylulose by two different xylose-metabolic pathways. Xylulose enters main metabolism via the pentose phosphate pathway, and then ethanol is produced by glycolysis. Numerous prior studies have been attempted to increase flux from xylose to ethanol. First, the xylA gene coding for xylose isomerase (XI) from various bacteria and fungi have been expressed in *S. cerevisiae* to enable xylose assimilation (Ha et al., 2011b; Madhavan et al., 2009; Tanino et al., 2010). Because the XI pathway can convert xylose to xylulose directly and does not require any cofactor, it could lead to high theoretical yields. The other xylose-assimilating pathway consists of xylose reductase (XR, *XYL1*) and xylitol dehydrogenase (XDH, *XYL2*) from *Scheffersomyces stipitis*. XR reduces xylose to xylitol by using NAD(P)H as cofactor and XDH further oxidizes xylitol to xylulose using NAD^+. While the XR-XDH pathway can offer higher metabolic fluxes than the XI pathway, it accumulates xylitol which is produced due to cofactor imbalance caused by different cofactor requirement between XR and XDH (Jin et al., 2004; Richard et al., 2006). To solve this problem, numerous genetic manipulations have been applied to *S. cerevisiae* expressing XR and XDH. First, protein engineering was undertaken to change cofactor

preferences of NAD(P)H-dependent XR and NAD^+-dependent XDH. The strains expressing the engineered XR or XDH with an NADPH- or NADH-balanced xylose assimilating pathway exhibited reduced xylitol accumulation and high ethanol yields (Bengtsson et al., 2009; Runquist et al., 2010; Watanabe et al., 2007a). Second, additional metabolic reactions alleviating redox imbalance have been introduced into the XR/XDH xylose fermenting *S. cerevisiae*. These reactions reoxidized surplus NADH from the xylose metabolism into NAD^+, resulting in mitigating the redox cofactor imbalance (Lee et al., 2012; Suga et al., 2013; Wei et al., 2013). Despite of these efforts, xylose consumption rates and ethanol yields of xylose fermentation by engineered *S. cerevisiae* were lower than those of glucose fermentation. No best strategy to develop efficient xylose fermenting yeast strains has been determined yet.

In this chapter, a synthetic isozyme system was introduced into *S. cerevisiae* to develop an engineered strain fermenting xylose efficiently. An isozyme is defined as different variants of the same enzyme having identical functions and permits the fine-tuning of metabolism (Hunter & Markert, 1956). The engineered strain with the XR based isozyme was constructed by coexpressing both wild-type XR and mutant XR. Effects of the synthetic isozyme system on ethanol production were investigated in batch fermentations using a glucose/xylose mixture.

3.3. Materials and methods

3.3.1. Strains and plasmids

Engineered *S. cerevisiae* DX123 and DX23 strains were constructed by integrating pSR306-X123 and pSR306-X23 into *S. cerevisiae* D452-2 (Kim et al., 2013b; Nikawa et al., 1991). Plasmid pSR306-X123 consists of the *XYL1*, *XYL2*, and *XYL3* genes from *Sch. stipitis* by sub-cloning the three gene cassettes (TDH3p-XYL1-TDH3t, PGK1p-XYL2-PGKt, TDH3p-XYL3-TDH3t). To construct a xylose reductase (XR)-based isozyme system, integrated plasmid pRS403_mXR was transformed to the DX123 strain. The mutant XR used in this thesis was the *XYL1* gene from *Sch. stipitis* and had R276H substitution (Watanabe et al., 2007b). The transformant showing high XR activity was selected and the strain was named as DXS. As a control strain, the SR6 strain expressing wild-type XR only was used (Kim et al., 2013b). Other control strain expressing mutant XR only was constructed by delta-integration of plasmid pITy-3_mXR into the DX23 strain (Jo et al., 2015). The resulting strain was named as MM.

3.3.2. Fermentation conditions

Fermentation experiments were conducted as follows. Engineered strains were pre-grown in 5ml of YP medium containing 20 g/L glucose

at 30°C and 250 rpm for 20 hours. The grown cells were centrifuged and inoculated to 50 ml of an YP medium containing 70 g/L glucose and 40 g/L xylose, 40 g/L glucose and 65 g/L xylose and cellulosic hydrolysates. Cellulosic hydrolysates derived from silver grass obtained from the Bioenergy Crop Research Institute in Muan county, Jeonnam Province were used (Cha et al., 2016). After filtering cellulosic hydrolysates using a 0.45-μm pore-sized membrane Disc filter (Supor R-450, PALL, USA) it was used for a main fermentation. Initial cell density of cultures was adjusted to OD_{600} 1(0.33 g/L) in all culture conditions. Flask fermentations were performed by 50 ml culture in a 250 ml Erlenmeyer flask at 30°C and 80 rpm. Batch fermentations in a bioreactor were carried out using a bench-top fermentor (KobioTech, Korea) with 500 mL of YP medium containing 70 g/L glucose and 40 g/L xylose, adjusted to pH 5.5 by addition of 2N NaOH and set at 200 rpm. All experiments were conducted by triplicate.

3.3.3. Enzymatic activity assay

To prepare crude extract, the engineered cells were harvested, washed, and treated with Y-PER (Pierce, Rochford, IL, USA). The treated cells were incubated for 20 min at room temperature. After centrifugation for 10 min at 4°C and 13,200 rpm, the supernatant containing the protein crude extract was used for the enzyme assay. For XR, crude extract,

NAD(P)H (0.4 mM) and xylose (0.2 M) were added into 50 mM potassium phosphate buffer (pH 6.0) pre-incubated for 10 min at 30°C. Absorbance at 340 nm was monitored with a 96-well microplate reader (Molecular Devices Co., Menl Park, CA, USA) for 30 sec. One unit of enzyme activity is defined as the amount of an enzyme that catalyzes 1 μmol of a substrate per min at 30°C.

3.3.4. Yeast transformations

The vectors for expression of xylose assimilating enzymes were transformed into *S. cerevisiae* by the yeast EZ-Transformation kit (BIO 101, Vista, CA, USA). Transformants were selected on YNB medium (6.7 g/L yeast nitrogen base without amino acids and 1.6 g/L yeast synthetic drop-out medium supplement w/o histidine) or YP medium supplemented with 20 g/L glucose and an appreciate concentration of G418 antibiotic (Calbiochem Co., USA).

3.3.5. Analytical methods

Cell concentration was measured using a spectrometer (Ultrospec 2000, Amersham Phamacia Biotech., Uppsala, Sweden) at 600 nm. Dry cell mass was obtained by multiplication of OD with a pre-determined conversion factor, 0.30 g/L/OD. Concentrations of fermentation products were determined by high performance liquid chromatography

(HPLC, Agilent 1100LC, Santa Clara, CA, USA) equipped with a refractive index detector at 35°C and Rezex ROA-Organic Acid H^+(8%) column (Phenomenex, Torrance, CA, USA). The column was eluted with 0.01N of H_2SO_4 at a flow rate of 0.6 ml/min at 60°C. Protein concentration was measured by a protein assay kit (Bio-rad Laboratories, Hercules, CA, USA). Concentrations of intracellular NAD(P)H and $NAD(P)^+$ were measured using the $NADP^+$/NADPH and NAD^+/NADH assay kits (BioAssay Systems, Hayward, CA, USA). *S. cerevisiae* cells grown in mixed sugar fermentation were harvested at the glucose-consumption phase and xylose-consumption phase and suspended in 125 μl of the $NAD(P)^+$ extraction buffer. The concentration measurement followed the manufacturer's instruction.

3.3.6. Genome sequencing and determining genomic copy numbers of XR

The genomic DNA of the SR6, MM and DXS strains were prepared by the genomic DNA preparation method described in chapter 2. The prepared Genomic DNAs were sent to National Instrumentation Center for Environmental Management (NICEM, Seoul National University, Seoul, Korea) for library construction and Pacbio sequencing. XR copy numbers of the three strains were identified using CLC Genomics workbench (CLC Bio, Rarhus, Denmark).

3.4. Results

3.4.1. Construction of a synthetic isozyme system

The *S. cerevisiae* DX123 strain was previously constructed by genome-integrating the xylose-assimilating genes (*XYL1, XYL2, XYL3*) from *Sch. stipitis* (Kim et al., 2012). The expression levels of *XYL1* and *XYL2* were optimized to achieve high XDH activity for minimizing xylitol accumulation (Kim et al., 2012). Additionally, the expression level of *XYL3* was controlled at a moderate level to minimize the toxicity caused by the accumulation of xylulose-5-P (Jin et al., 2003). In a previous study, an engineered yeast strain containing NADPH-linked XR showed fast xylose assimilation, but produced a high amount of xylitol with a low yield of ethanol. On the other hand, an engineered yeast strain expressing the NADH-preferred mutant XR (R276H) produced less xylitol but exhibited slow xylose assimilation (Kim et al., 2013). Since high levels of $NADP^+$ can inhibit the XR activity using NADH, the xylose metabolism entirely based on NADH-specific XR can be delayed by high levels of $NADP^+$ (Verduyn et al., 1985). As such, restricted availability of cofactor might cause a low yield of ethanol in the engineered yeast with the wild-type XR and lead to slow xylose consumption in the engineered yeast with the NADH-preferred mutant XR. To solve these drawbacks caused by the limited co-factor

dependence, both NADPH-specific and NADH-specific XRs were expressed in the engineered yeast to implement a synthetic isozyme system. Isozymes (also known as isoenzymes) are a set of enzymes that differ in amino acid sequences but catalyze the same chemical reaction (Hunter & Markert, 1956). These enzymes (for example lactate dehydrogenase and glucokinase) are generally used in various microorganisms to manage rapidly changing cellular circumstances. Although isozyme systems hold many advantages in terms of providing flexibility and robustness of metabolism, no attempt has been made to exploit the benefits of isoenzyme systems for metabolic engineering. A synthetic isozyme system was used to improve ethanol fermentation from xylose. The engineered strain having two type of XRs with distinct kinetic properties was constructed through integration of the vector p403_mXR expressing a mutant XR into the DX123 strain expressing a wild-type XR, XDH and XK. The XR activities in the wild-type XR expressing strain (wXR in Fig. 3.1) were 0.24 U/mg-protein for NAPDH and 0.13 U/mg-protein for NADH. The XR activities in the mutant XR expressing strain (mXR in Fig. 3.1) were 0.03 U/mg-protein and 0.32 U/mg-protein. It was expected that the engineered strain expressing both the wild-type and the mutant XRs would show a combined activity of the wild XR and mutant XR activities (wXR+mXR in Fig. 3.1). Interestingly, the engineered strain

(DXS) with two types of XRs showed a much higher XR activity than a simple sum of both wXR and mXR (DXS in Fig. 3.1). To capture genetic changes in the DXS strain, the whole genome of the DXS strain was sequenced. The DXS strain had 5 copies of the XR expression cassette instead of one copy of each wXR and mXR. Specifically, three copies of the wild-type XR expression cassette and two copies of of the mutant XR expression cassette were integrated in the DXS strain. The unexpected high XR activity of the DXS strain might be caused by non-specific integration of the XR genes. As the DXS strain had multiple copies of wild XR and mutant XR, proper control strains harboring multiple copies of either wild XR or mutant XR were constructed (SR6 and MM) for further phenotypic comparison with the DXS. The SR6 and MM strains were constructed through random integration of the wild XR or mutant XR expression cassette at the multiple δ elements of the genome of *S. cerevisiae* D452-2 (Kim et al., 2013b). To check the copy numbers of wild XR and mutant XR genes, the genomic DNA of the SR6 and MM strains were sequenced. The whole genome sequencing results suggested that the SR6 and MM strains had 5 copies of wild *XYL1* and mutant *XYL1* in the each genome, respectively. *In vitro* XR activities of the SR6 and MM strains were shown in Fig. 3.1. The XR activities in the SR6 strain were 1.2 U/mg for NADPH and 0.62 U/mg for NADH. The XR activities in the MM

strain were 0.07 U/mg for NADPH, and 1.64 U/mg for NADH. These XR activity results correlated with the genomic copy numbers and the known cofactor preferences of wild XR and mutant XR. Finally, the three recombinant strains (DXS, SR6, and MM) exhibiting similar levels of XR activity but different cofactor preferences were constructed.

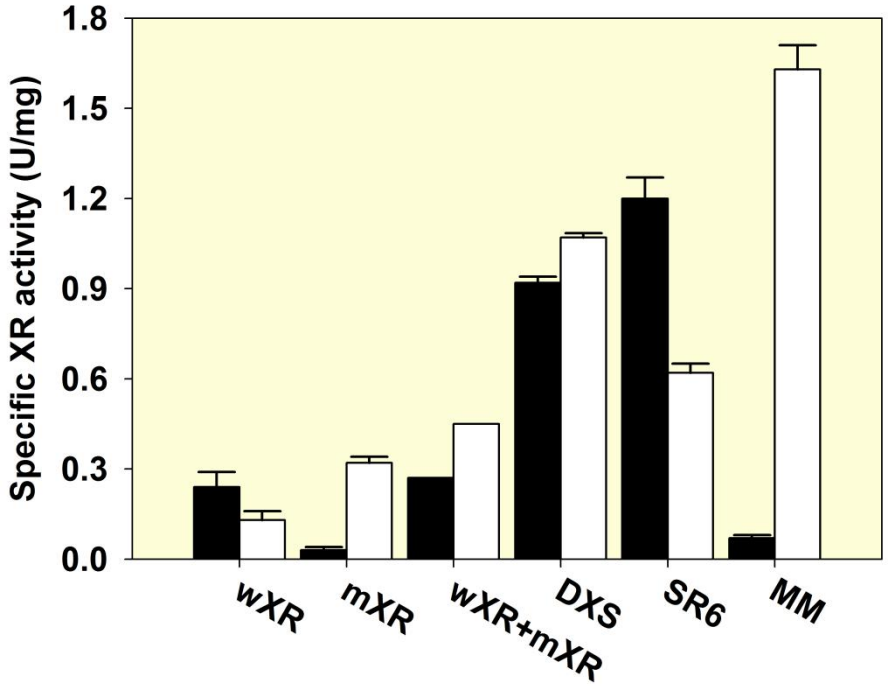

Fig. 3.1. Specific activities of xylose reductase (XR) in engineered *S. cerevisiae* strains SR6, MM and DXS. Results are the means of triplicate experiments and error bars indicate s.d.. Symbols : NADPH dependent XR (filled bar); NADH dependent XR (open bar)

3.4.2. Comparison of fermentation performances by three engineered *S. cerevisiae* expressing wXR, mXR, or wXR/mXR under the 70 g/L glucose and 40 g/L xylose conditions

To examine the influence of XR activities in the three *S. cerevisiae* expressing wXR, mXR, or wXR/mXR on fermentation of mixed sugars, the SR6, MM, DXS strain were cultivated in YP medium containing 70 g/L of glucose and 40 g/L xylose that is a typical composition of lignocellulosic hydrolyzates. (Fig. 3.2) The SR6, MM, DXS strains consumed 70 g/L glucose within 13 hours without utilization of xlyose. After the depletion of glucose, the three engineered strains showed different xylose-fermenting capacities. The SR6 strain having only NADPH-preferred XR produced xylitol with the highest yield among the three strains (0.279 g xylitol/g xylose for SR6 vs. 0.036 g xylitol/g xylose for MM and 0.049 g xylitol/g xylose for DXS) (Table 3.1). Due to high accumulation of xylitol, the SR6 produced only 5 g/L of ethanol from 17 g/L of xylose consumed. On the other hand, the MM strain expressing only NADH-preferred mutant XR showed a low xylitol yield but slow xylose metabolism. The amount of xylose consumed by the MM strain was only 13 g/L as compared to 17 g/L by the SR6 strain and 23 g/L by the DXS strain for 11 hr. These results suggested that redox imbalance caused by the cofactor differences of XR and XDH might be a limiting factor of xylose fermentation by engineered *S.*

cerevisiae expressing wild-type XR and XDH. Also, the recombinant strain (MM) designed to balance the cofactor requirement by expressing the mutant XR showing XR activities with NADH than NADPH did not perform xylose fermentation well. On the other hand, the DXS strain with the XR-based isozyme system (wXR/mXR) capable of using both NADPH and NADH exhibited efficient xylose-fermentation. Compared to the SR6 and MM strains, the DXS strain showed a faster xylose consumption rate (2.02 g xylose/L-h for DXS vs. 1.19 g xylose/L-h for MM) and lower xylitol yield (0.049 g xylitol/g xylose for DXS vs. 0.279 g xylitol/g xylose for SR6) (Table 3.1). Finally, the DXS strain produced 44.5 g/L of ethanol with a high ethanol yield of 0.427 g/g sugars from a mixture of sugar of 70 g/L glucose and 40 g/L xylose within 24 hr. While the total activities of the XR of three engineered strains were similar, the three engineered strains showed different xylose-fermenting capacities. These results suggest that an important factor for efficient xylose fermentation is not the total activity of XR measured from *in vitro* XR activity assay, but the the balanced cofactor availability of the XR-based isozyme system..

The intracellular cofactor concentrations (NAPDH, $NADP^+$, NADH and NAD^+) of the three recombinant strains were measured to investigate the changes of cofactor concentrations during mixed sugar fermentation. In the glucose consumption phase (8 hr), the ratios of

NAPDH to $NADP^+$ and of NADH to NAD^+ of the three strains were similar (Table 3.2). In the xylose fermenting phase, cofactors existed mostly in reduced forms instead of oxidized forms and the cofactor ratios were different in each strain. Because the wild XR converts NAPDH to $NADP^+$, the NADPH/$NADP^+$ ratio in the SR6 strain having only the wild XR was the lowest (1.14 for SR6, 1.39 for MM and 1.25 for DXS) among the three strains. As the mutant XR oxidizes NADH to NAD^+, it was expected that the MM strain expressing only mutant XR showed the lowest NADH/NAD^+ ratio. However, the NADH/NAD^+ ratio of the SR6 strain was the lowest (1.02 for SR6, 1.27 for MM and 1.19 for DXS). Unlike NADPH, the NAD^+ oxidized by the mutant XR might be regenerated by many metabolic reactions in glycolysis, ethanol production and TCA cycle. It was speculated that these reactions might change the NADH/NAD^+ ratio. Even though the NADH/NAD^+ ratios of the three strains were not expected results, the DXS strain showed the moderate NADPH/$NADP^+$ and NADH/NAD^+ ratios. These results suggested that coexpression of the wild-type XR and mutant XR might regulate intracellular cofactor concentrations to enhance xylose fermentation.

Also, batch fermentation was carried out in a 1 L-bench-top bioreactor containing 500 mL of YP medium with 70 g/L glucose and 40g/L xylose to confirm if the DXS strain could ferment xylose efficiently in

an industrial fermentation scheme. As a result, the final ethanol concentration of 45.8 g/L was obtained with 0.431 g/g yield, suggesting the DXS strain had an efficient xylose fermenting capacity.

Table 3.1. Fermentation parameters of engineered *S. cerevisiae* strains in mixed sugar fermentations

Carbon source	Strain	Xylose consumption rate (g/L-h)	Ethanol productivity (g/L-h)	Ethanol concentration (g/L)	Yield (g/g)				
					Ethanol	Xylitol	Glycerol	Acetate	DCW
70 g/L glucose 40 g/L xylose	SR6	1.55	1.63	39.1	0.397	0.279	0.027	0.011	0.093
	MM	1.19	1.60	38.3	0.418	0.036	0.034	0.008	0.111
	DXS	2.02	1.85	44.5	0.427	0.049	0.034	0.006	0.082
40 g/L glucose 65 g/L xylose	SR6	0.98	0.74	30.3	0.363	0.263	0.027	0.020	0.086
	MM	1.03	0.82	33.7	0.415	0.043	0.031	0.012	0.116
	DXS	1.35	0.96	39.3	0.408	0.035	0.039	0.014	0.070

Xylose consumption rates were calculated after glucose depletion

Table 3.2. Intracellular concentrations of cofactors (NADPH, $NADP^+$, NADH and NAD^+) in engineered *S. cerevisiae* strains

Phase	Strain	Concentration (μmol/g cell)		$NADPH/NADP^+$ ratio	Concentration (μmol/g cell)		$NADH/NAD^+$ ratio
		NADPH	$NADP^+$		NADH	NAD^+	
Glucose consumption	SR6	0.37 ± 0.02	0.44 ± 0.02	0.85	1.25 ± 0.18	1.66 ± 0.07	0.75
	MM	0.62 ± 0.01	0.76 ± 0.10	0.82	1.22 ± 0.07	1.68 ± 0.04	0.72
	DXS	0.54 ± 0.05	0.61 ± 0.05	0.88	1.44 ± 0.08	2.02 ± 0.04	0.71
Xylose consumption	SR6	0.48 ± 0.01	0.42 ± 0.01	1.14	1.48 ± 0.07	1.45 ± 0.00	1.02
	MM	0.72 ± 0.00	0.52 ± 0.09	1.39	1.32 ± 0.02	1.04 ± 0.01	1.27
	DXS	0.75 ± 0.01	0.60 ± 0.08	1.25	1.51 ± 0.05	1.27 ± 0.02	1.19

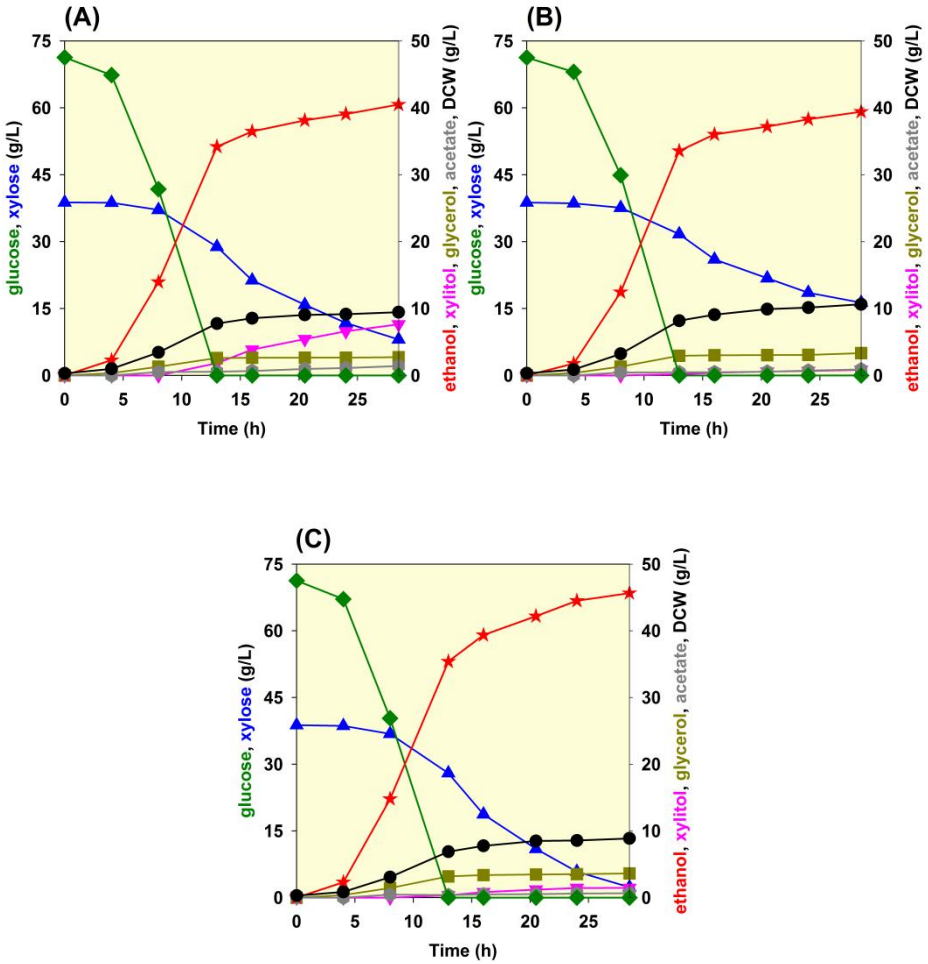

Fig. 3.2. Comparison of glucose and xylose fermentation by *S. cerevisiae* (A) SR6, (B) MM and (C) DXS strains in YP medium containing 70 g/L xylose and 40 g/L of xylose. Symbols : glucose (diamond); xylose (triangle up); xylitol (triangle down); glycerol (square); acetate (open circle), ethanol (filled triangle), DCW (filled circle). Results are the means of triplicate experiments.

3.4.3. Comparison of fermentation performances by three engineered *S. cerevisiae* expressing wXR, mXR, or wXR/mXR under the 40 g/L glucose and 65 g/L xylose conditions

The three engineered strains (SR6, MM, DXS) were cultivated in YP medium containing mixed sugars (40 g/L glucose and 65 g/L xylose) to evaluate the fermentation performances in high xylose condition (Fig. 3.3). While their fermentation characteristics were similar to those in YP medium containing 70 g/L glucose and 40 g/L xylose, their xylose consumption patterns were different. Since *S. cerevisiae* has been known not to possess any xylose-specific transporters, xylose is transported into a cell by diffusion which depends on the gradient of xylose concentration (Jo et al., 2016). It is expected that xylose consumption rates in fermentations with 65 g/L xylose will be higher than those with 40 g/L xylose. In order to exclude the effect of increased dry cell mass due to high glucose concentration, specific xylose consumption rate was measured. The three engineered strains in fermentations with 65 g/L xylose showed 46~71% higher specific xylose consumption rate than those in fermentations with 40 g/L xylose. Among these strains, the DXS strain showed the highest specific xylose consumption rate. In a high glucose conditions (70 g/L of glucose and 40 g/L of xylose), the MM strain showed a 30% lower xylose

consumption rate as compared to the SR6 strain. But the MM strain consumed xylose as fast as the SR6 in a high xylose condition (40 g/L of glucose and 65 g/L of xylose). As mentioned above, the XR activity with NADH might be inhibited by $NADP^+$ at high concentrations. Because the MM strain possessed an NADH-linked XR activity only, xylose consumption might be largely influenced by intracellular concentrations of $NADP^+$. Under the conditions of changing $NADP^+$ concentration, the xylose consumption rate of the DXS strain was the highest (1.35 g xylose/L•h for DXS vs. 0.98 g xylose/L•h for SR6 and 1.03 g xylose/L•h for MM). Among the three strains, the DXS strain could convert xylose to xylitol using NADPH in order to bypass the inhibition of $NADP^+$ on NADH-dependent XR activity. Because the XR-based isozyme system can utilize both NADPH and NADH as cofactor, the DXS strain might be able to handle the status of varying cofactor availability easily.

Different sugar compositions also affected accumulation of acetate. Unlike glucose metabolism, xylose was metabolized by using NADPH and NADH to accumulate byproducts such as xylitol, glycerol and acetate. Among these byproducts, acetate was mainly produced by *ALD6* encoding $NADP^+$-dependent aldehyde dehydrogenase and related to NADPH regeneration. Therefore, acetate yield might be increased when more xylose was used or where NADPH-dependent XR

activity was high. As expected, the acetate yields of the three strains in cultures with 65 g/L xylose were higher than those in fermentations using 40 g/L xylose. The SR6 showed the highest acetate yield and the acetate yields of the MM and DXS strains were similar (0.020 g acetate/g sugar for SR6, 0.012 g acetate/g sugar for MM and 0.014 g acetate/g sugar for DXS) (Table 3.1). It was suggested that the DXS strain regulated xylose conversion by NADPH-dependent XR to reduce accumulation of acetate.

Considering the above results, it was suggested that changes in mixed sugar compositions might impose quite different fermentation circumstances to yeast cells. Nevertheless, the DXS strain showed an efficient and consistent xylose fermentation capacity even in a high xylose condition. The XR-based isozyme system can use both NAPDH and NADH for XR-mediated conversion of xylose to xylitol. It is known that the intracellular pool of NADH is larger than that of NADPH. Because of the above merits of the isozyme system, the DXS could metabolize xylose by using NADPH to avoid $NADP^+$ inhibition and by using NADH to result in a reduction of acetate accumulation. As a result, the DXS strain produced only 1.52 g/L of xylitol as compared to 9.63 g/L of xylitol accumulation by the SR6 strain and the amount of ethanol by the DXS strain was the highest (39.3 g/L for DXS vs. 30.3 g/L for SR6 and 33.7 g/L for MM).

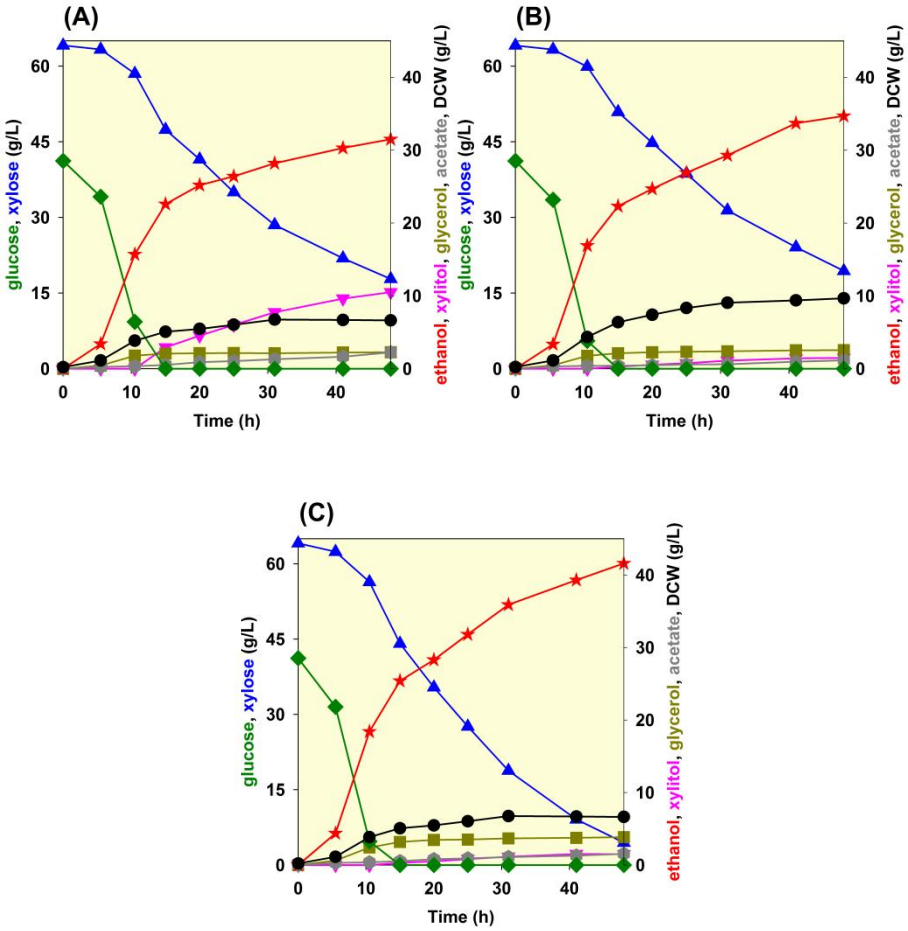

Fig. 3.3. Comparison of glucose and xylose fermentation by *S. cerevisiae* (A) SR6, (B) MM and (C) DXS strains in YP medium containing 40 g/L glucose and 65 g/L of xylose. Symbols : glucose (diamond); xylose (triangle up); xylitol (triangle down); glycerol (square); acetate (open circle), ethanol (filled triangle), DCW (filled circle). Results are the means of triplicate experiments.

3.4.4. Cellulosic hydrolysates fermentation by *S. cerevisiae* having XR based isozyme

Cellulosic hydrolysates contain numerous toxic fermentation inhibitors that influence xylose fermentation. To verify the fermentation performances of the three engineered yeast strains in a real cellulosic hydrolysate, the three engineered strains (SR6, MM, DXS) were cultured in the silver grass hydrolysate containing 92 g/L glucose and 32 g/L xylose. All strains consumed 92 g/L glucose within 13 hr, indicating that glucose consumption did not inhibit by hydrolysate inhibitors. (Fig. 3.4 A) On the other hand, the xylose consumption rate of the SR6, MM, DXS strains were 31%, 33% and 39% lower than those in YP medium. It was confirmed that xylose assimilation was hindered by hydrolysate inhibitors. Nonetheless, the DXS strain showed the best xylose fermentation by consuming 26 g/L xylose as compared to 18.4 g/L by SR6 and 15.1 g/L by MM) (Fig. 3.4 B). The amount of xylitol produced by the SR6 strain was much higher than those by the MM and DXS strain and consumed xylose was not converted to ethanol after 21.5 hr (Fig. 3.4 C). The MM strain accumulated a little of xylitol but assimilated xylose slowly without producing ethanol efficiently. Whereas the SR6 and MM strain did not produce ethanol to the end of fermentation, the DXS strain was able to convert xylose into ethanol up to 36 hr (Fig. 3.4 D). As a result, the

DXS strain produced 2-fold higher ethanol from xylose than those of the SR6 and MM strain (8.7 g/L for DXS vs. 4.5 g/L for SR6 and 4.3 g/L for MM). In the silver grass hydrolysates fermentation, the DXS strain produced 50.7 g/L ethanol with 0.43 g/g ethanol yield. The engineered strain with the XR-based isozyme system (DXS) adapted to harsh condition such as cellulosic hydrolysates and showed efficient xylose fermentation.

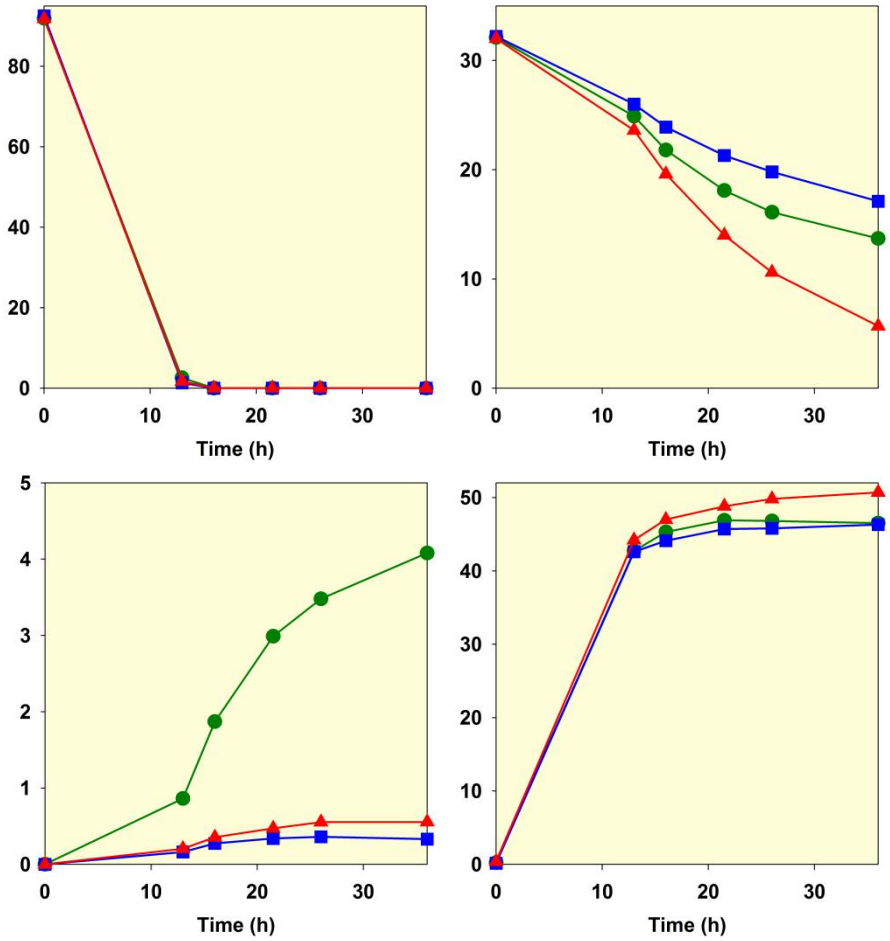

Fig. 3.4. Profiles of metabolites (A) glucose, (B) xylose, (C) xylitol and (D) ethanol of three engineered strains (SR6, MM and DXS) grown in lignocellulosic hydrolysate. Symbols: SR6 (circle); MM (square); DXS (triangle). Results are the means of triplicate experiments.

Chapter 4

Production of xylitol in engineered *Saccharomyces cerevisiae*

4.1. Summary

Xylitol, a natural sweetener, can be produced by hydrogenation of xylose in hemicelluloses. In microbial processes, utilization of only NADPH cofactor limited commercialization of xylitol biosynthesis. To overcome this drawback, *Saccharomyces cerevisiae* D452-2 was engineered to express two types of xylose reductase (XR) with either NADPH-dependence or NADH-preference. Engineered *S. cerevisiae* DWM expressing both the XRs exhibited higher xylitol productivity than the yeast strain expressing NADPH-dependent XR only (DWW) in both batch and glucose-limited fed-batch cultures. Furthermore, the coexpression of *S. cerevisiae ZWF1* and *ACS1* genes in the DWM-ZWF1-ACS1 strain increased intracellular concentrations of NADPH and NADH and improved maximum xylitol productivity by 17%, relative to that for the DWM strain. Finally, the optimized fed-batch fermentation of *S. cerevisiae* DWM-ZWF1-ACS1 resulted in 196.2 g/L xylitol concentration, 4.27 g/L-h productivity and almost the theoretical yield. Expression of the two types of XR utilizing both NADPH and NADH is a promising strategy to meet the industrial demands for microbial xylitol production.

4.2. Introduction

Xylitol is a five-carbon sugar alcohol with a number of advantageous properties. As xylitol is as sweet as sucrose and has a 33% lower calorie, and extreme cooling and caries-preventative effects, xylitol has been commercially used as a sugar substitute in various products such as chewing gums, candies and toothpastes(Mäkinen, 2011). Xylitol was also chosen as one of the top 12 value-added chemicals from biomass and could be used as a platform chemical for polymer synthesis such as xylaric acid and glycols, directly polymerized for production of unsaturated polyester resin (Clark & Deswarte, 2011). Ethylene glycol, an important chemical intermediate, can be produced by ruthenium-mediated hydrogenolysis of xylitol (Yue et al., 2012). Due to these properties, demand of xylitol has increased in food and chemical industries. Currently, the annual xylitol market was estimated to be 125,000 tons of demand and priced at 4.5-5.5 US dollars per kg (de Albuquerque et al., 2014).

Xylitol is chemically synthesized by hydrogenation of xylose, one of major sugars in lignocellulosic biomass, in the presence of a metal catalyst and hydrogen gas at over ambient conditions such as 120°C of temperature and up to 5.5 MPa of pressure (Park, 2015; Yadav et al., 2012). Due to the sustainability issue, especially biological production of xylitol has gained an interest from academia and industries (Pérez-

Bibbins et al., 2015). Instead of metal catalysts, a biocatalyst of xylose reductase can undertake the hydrogenation reaction of xylose with aid of NADPH and NADH cofactors. Because of instability and high cost of xylose reductase and the cofactors, the biological production of xylose should be devised by microbial systems. To date, robust microorganisms have been developed to express xylose reductase highly and to supply the cofactors sufficiently. Among several microorganisms, *Candida* species is well established to produce high concentration of xylitol over 237 g/L with high productivity (Kim & Oh, 2003). *Candida* species is recognized as a good xylitol producer, however, it consumes xylose as an energy source so the xylitol yield does not reach a commercially applicable value over 90% (Kim et al., 2002; Kim & Oh, 2003). *Saccharomyces cerevisiae* is a GRAS (generally recognized as safe) microorganism not only used in food and alcoholic beverage industries but also applicable for production of biochemicals, biofuels and biopharmaceuticals. In spite of its outstanding properties, *S. cerevisiae* is unable to produce xylitol from xylose because it does not have an enzyme, xylose reductase (XR) endogenously. For xylitol biosynthesis in metabolically-engineered *S. cerevisiae*, various research efforts have been made including genetic introduction of the XR gene, supply of the cofactors, control of the pentose phosphate pathway (Bae et al., 2004; Chung et al., 2002; Kwon

et al., 2006; Oh et al., 2007). In addition, xylitol was also produced though the geneticaaly modified industrial strain, co-utilization of cellobiose and xylose and directed conversion of rice straw hydrolysate (Guirimand et al., 2016; Kogje & Ghosalkar, 2017; Oh et al., 2013). Because engineered *S. cerevisiae* expressing XR cannot metabolize xylitol into the central carbon metabolism, it converts xylose to xylitol at almost the theoretical yield (~100%).

Xylose reductase catalyzes the one-step hydrogenation of xylose to xylitol in the presence of NADPH or NADH cofactor (Fig. 4.1). Most XRs in nature depend on NADPH, of which the oxidized form should be reduced again inside cells. Since the NADPH regeneration is done by a few metabolic steps, insufficient supply of NADPH limits rapid production of xylitol. Meanwhile, a NADH-preferring XR mutant was developed by protein engineering and applied to conversion of xylose to ethanol in engineered *S. cerevisiae* (Lee et al., 2012; Watanabe et al., 2007b). An engineered *S. cerevisiae* expressing the mutant XR showed much higher xylose consumption rate than the same yeast harboring the wild-type XR dependent on NADPH. Considering these results, it was hypothesized that utilization of both NADPH and NADH as cofactors would improve xylitol biosynthesis in engineered *S. cerevisiae*. In this chapter, engineered *S. cerevisiae* strains expressing the NADPH-dependent wild XR (wXR) and the NADH-preferring mutant XR

(mXR) originated from *Scheffersomyces stipitis* was constructed. Additionally, glucose-6-phosphate dehydrogenase for NADPH regeneration and acetyl-CoA synthetase for NADPH and NADH regeneration were overexpressed to improve the xylitol production performance further (Fig. 4.1). Finally, fed-batch fermentation strategies were optimized to produce xylitol with a high concentration and productivity.

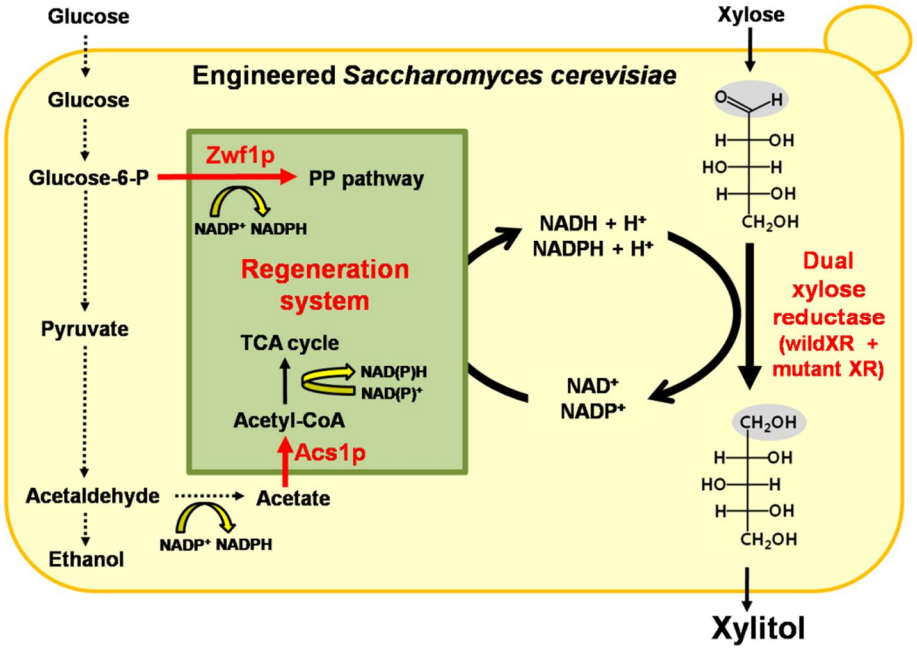

Fig. 4.1. Metabolic pathways for xylitol biosynthesis and regeneration of NADPH and NADH cofactors in engineered *S. cerevisiae*. Zwf1p, glucose-6-phosphate dehydrogenase; Acs1p, acetyl-CoA synthetase; PP pathway, pentose phosphate pathway; TCA cycle, tricarboxylic acid cycle

4.3. Materials and methods

4.3.1. Strains and plasmids

Escherichia coli TOP 10 (Invitrogen, Carlsbad, CA, USA) was used for gene manipulation. LB medium (10 g/L tryptone, 5 g/L yeast extract and 10 g/L NaCl) was used for *E. coli* cultivation. *S. cerevisiae* D452-2 was used as a host strain for xylitol production and a source of the yeast genomic DNA. Plasmids p426GPD and p425GPD with the *GPD* promoter and *CYC1* terminator were used for the expression of the wild (Genbank accession No. 4839234) and mutant genes of *XYL1* encoding *S. stipites* XRs, and the *S. cerevisiae ZWF1* (No. 855480) and *ACS1* (No. 851245) genes coding for glucose-6-phosphate dehydrogenase (Zwf1p) and acetyl-CoA synthetase (Acs1p), respectively. Plasmids pRS403, pRS405 and pITy-3 were used for chromosomal integration of the *XYL1* genes. Yeast strains and plasmids used in this chapter are listed in Table 4.1.

4.3.2. Genetic manipulation

To construct the expression cassettes of the wild XR (wXR) and mutant XR (mXR), the two type of XR genes were amplified by polymerase chain reaction (PCR) from previously constructed vectors of YEpM4-$XR^{WT}$and YEpM4-$XR^{MUT}$with the corresponding PCR primers: F1 and

R1(Table 4.2) (Lee et al., 2012). Each amplified XR gene was treated with DNA restriction enzymes of *Bam*HI and *Xho*I, and inserted between the *GPD* promoter and *CYC1* terminator in plasmid p426GPD, resulting in the construction of plasmids p426GPD_wXR and p426GPD_mXR. The XR expression cassette of the *GPD* promoter, each XR gene and *CYC1* terminator in a row was PCR-amplified with DNA primers of F2 and R2. After digestion with *Sac*I, the cassette was introduced into chromosomal integration vectors, resulting in the construction of plasmids pRS406_wXR, pRS403_mXR, pITy-3_wXR and pITy-3_mXR. Plasmids pRS406_wXR and pRS403_mXR were linearized by *Xcm*I and *Nhe*I treatment, respectively, transformed and integrated into the chromosome of *S. cerevisiae* D452-2 to construct the DWM strain. Engineered *S. cerevisiae* strains expressing multiple copies of the wXR gene (DWW) and mXR gene (DMM) were constructed by δ-integration of plasmids pITy-3_wXR and pITy-3_mXR in *S. cerevisiae* D452-2, respectively (Parekh et al., 1996). The *ZWF1* and *ACS1* genes were amplified from the *S.cerevisiae* D452-2 genomic DNA, digested with *Xma*I and *Xho*I for *ZWF1*, *EcoR*I and *Xho*I for *ACS*1 and cloned into p425GPD vector to generate plasmids p425GPD_ZWF1 and p425GPD_ACS1. After amplifying the *ZWF1* expression cassette with primers of F2 and R2 and digesting with *Sac*I, the cassette was introduced into plasmid p425GPD_ACS1 to construct

plasmid p425GPD_ZWF1_ACS1. Each resulting plasmid was transformed into the DWM strain, of which transformants were named DWM-ZWF1, DWM-ACS1 and DWM-ZWF1-ACS1. The schemes for plasmid construction are displayed in Fig. 4.2.

A yeast EZ-Transformation kit (BIO 101, Vista, CA, USA) was used for plasmid transformation into *S. cerevisiae*, of which transformants were selected on YNB medium containing 20 g/L glucose, appropriate amino acids (histidine, leucine or uracil). Yeast strains transformed with delta-integration plasmids were propagated on YP medium supplemented with 20 g/L glucose and an appropriate concentration of G418 antibiotic (Calbiochem Co., USA).

4.3.3. Fermentation conditions

S. cerevisiae was grown in 5ml of YP (10 g/L yeast extract and 20 g/L peptone) or YNB leu$^-$medium (6.7 g/L yeast nitrogen base without amino acids and 1.6 g/L yeast synthetic drop-out medium supplement w/o leucine) containing 20 g/L glucose at 30°C and 250 rpm for 20 h. The cells were harvested and inoculated into a 500 mL baffled flask with 100 mL YP medium containing glucose and xylose for batch fermentation at 30°C and 250 rpm. For glucose-limited fed-batch fermentation, the pre-grown cells were transferred into 100 mL of YNB leu- medium with 20 g/L glucose. After 20 h of culture at 30°C and 250

rpm, the cells were harvested and suspended in sterilized water. The suspended cells were inoculated to a 3.7 L fermentor (Bioengineering AG, Wald, Switzerland) with 1 L working volume of YP medium containing 19 g/L glucose and 76-98 g/L xylose at 30°C. Acidity was controlled at pH 5.0 by addition of 2 N HCl and 2 N NaOH. An initial optical density of the cultures was adjusted at about 0.5. An agitation speed and an aeration rate was set at 500 rpm and 1 vvm, respectively. A concentrated glucose solution (600 g/L) was fed constantly at 1.8 g/L-h of feed rate after depletion of glucose initially added. In addition, 600 g/L xylose solution was supplemented intermittently or continuously into the culture broth to control xylose concentration between 35 and 80 g/L or around 80 g/L.

4.3.4. Analytical Methods

Cell concentration was measured using a spectrometer (Ultrospec 2000, Amersham Phamacia Biotech., Uppsala, Sweden) at 600 nm. Dry cell mass was obtained by multiplication of OD with a pre-determined conversion factor, 0.30 g/L/OD. Fermentation products concentrations were determined by high performance liquid chromatography (HPLC, Agilent 1100LC, Santa Clara, CA, USA) equipped with a refractive index detector at 35°C and Rezex ROA-Organic Acid H^+(8%) column (Phenomenex, Torrance, CA, USA). The column was eluted with 0.01N

of H_2SO_4 at a flow rate of 0.6 ml/min at 60°C.

4.3.5. Crude extract preparation and enzyme activity assay

The cells grown at the exponential growth phase were harvested, washed, and treated with Yeast Protein Extraction Reagent (Y-PER, Pierce, Rochford, IL, USA). The treated cells were incubated for 20 min at room temperature. After centrifugation for 10 min at 4°C and 13,200 rpm, the supernatant containing the protein crude extract was used for the enzyme assay. Xylose reductase activity was measured in a reaction mixture with 50 mM potassium phosphate buffer (pH 6.0), 0.2 M xylose and 0.4 mM NADPH or NADH (Verduyn et al., 1985). The reaction solution for glucose-6-phosphate dehydrogenase assay was composed of 50 mM Tris-HCl buffer (pH 7.5), 5 mM $MgCl_2$, 5 mM maleimide, 0.4 mM $NADP^+$ and 10 mM glucose-6-phosphate (Deutsch, 1983) . For the determination of acetyl-CoA synthetase activity, the R-biopharm acetate kit (Cat No. 148261, R-biopharm, Darmstadt, Germany) was used. The reaction mixture contained 10 mM potassium acetate, 2.7 mM ATP, 0.2 mM coenzyme A, 1.1 mM NAD^+, 9.4 mM L-malate, 5.5 U L-malate dehydrogenase and 1.4 U citrate synthase. In all the cases, absorbance of NAD(P)H was monitored by a 96-well microplate reader (Molecular Devices Cel, Menlo Park, Ca, USA) at 340 nm for activity measurement. One unit of enzyme activity is

defined as the amount of an enzyme that oxidizes 1 μmol of NAD(P)H (for XR) or reduces 1 μmol of $NAD(P)^+$ (for Zwf1p and Acs1p) per min at 30°C. Protein concentration was measured by a protein assay kit (Bio-rad Laboratories, Hercules, CA, USA).

4.3.6. Determination of intracellular NAD(P)H and $NAD(P)^+$concentrations

Concentrations of NADPH, $NADP^+$, NADH and NAD^+ were measured using the $NADP^+$/NADPH and NAD^+/NADH assay kits (BioAssay Systems, Hayward, CA, USA). *S. cerevisiae* cells grown in YNB leu- medium with glucose were harvested at the mid-exponential growth phase and suspended in 125μl of the $NAD(P)^+$ extraction buffer. The concentration measurement followed the manufacturer's instruction.

Table 4.1. Lists of *S. cerevisiae* strains and plasmids used in Chapter 4

Strain and plasmid	Description	Reference or source
S. cerevisiae		
D452-2	*MAT α, leu2, his3, ura3, can1*	(Hosaka et al., 1992)
DWW	D452-2 + pITy-3_wXR (δ-integration)	This study
DMM	D452-2 + pITy-3_mXR (δ-integration)	This study
DWM	D452-2 + pRS403_mXR + pRS406_wXR	This study
DWW-C	DWW + p425GPD	This study
DWM-C	DWM + p425GPD	This study
DWM-ZWF1	DWM + p425GPD_*ZWF1*	This study
DWM-ACS1	DWM + p425GPD_*ACS1*	This study
DWW-ZWF1_ACS1	DWW + p425GPD_*ZWF1_ACS1*	This study
DWM-ZWF1_ACS1	DWM + p425GPD_*ZWF1_ACS1*	This study

(be continued)

Strain and plasmid	Description	Reference or source
Plasmids		
pRS406	*URA3*, 2-μ origin	ATCC
pRS403	*HIS3*, 2-μ origin	ATCC
pITy-3	2-μ origin, drug resistance marker ($G418^R$)	(Parekh et al., 1996)
p425GPD	*LEU2*, 2-μ origin, GPD_p-MCS-$CYC1_t$	ATCC
p426GPD	*URA3*, 2-μ origin, GPD_p-MCS-$CYC1_t$	ATCC
p426GPD_wXR	p426GPD with *S. stipitis* wild *XR*	This study
p426GPD_mXR	p426GPD with *S. stipitis* mutant *XR*	This study
pRS406_wXR	pRS406 with wild *XR* under the *GPD* promoter	This study
pRS403_mXR	pRS403 with mutant *XR* under the *GPD* promoter	This study
pITy-3_wXR	pITy-3 with wild *XR* under the *GPD* promoter	This study
pITy-3_mXR	pITy-3 with mutant *XR* under the *GPD* promoter	This study
p425GPD_ZWF1	p425GPD with *S. cerevisiae ZWF1* under the *GPD* promoter	This study
p425GPD_ACS1	p425GPD with *S. cerevisiae ACS1* under the *GPD* promoter	This study
p425GPD_ZWF1_ACS1	p425GPD with *S. cerevisiae ZWF1* and *ACS1* under the *GPD* promoter	This study

Table 4.2. List of DNA oligomers used in Chapter 4. The restriction sites are underlined. [F] and [R] mean the forward and reverse primers, respectively.

Name (restriction site)	**Sequence**	**Target gene**
F1 (*Bam*HI)	CGCGGATCCATGCCTTCTATTAAGTTGAACTCTGG	XR
R1 (*Xho*I)	CCGCTCGAGTTAGACGAAGATAGGAATCTTGTCC	XR
F2 (*Sac*I)	CGAGCTCAGTTTATCATTATCAATACTCGCCA	XR,ZWF expression cassette
R2 (*Sac*I)	CGAGCTCGGCCGCAAATTAAAGCCTTC	XR,ZWF expression cassette
F3 (*Xma*I)	TCCCCCCGGGATGAGTGAAGGCCCCGTCAA	ZWF1
R3 (*Xho*I)	CCGCTCGAGCTAATTATCCTTCGTATCTTCTGG	ZWF1
F4 (*Eco*RI)	CCGGAATTCGGGATGTCGCCCTCTGCCGTACAAT	ACS1
R4 (*Xho*I)	CCGCTCGAGTTACAACTTGACCGAATCAATTAG	ACS1

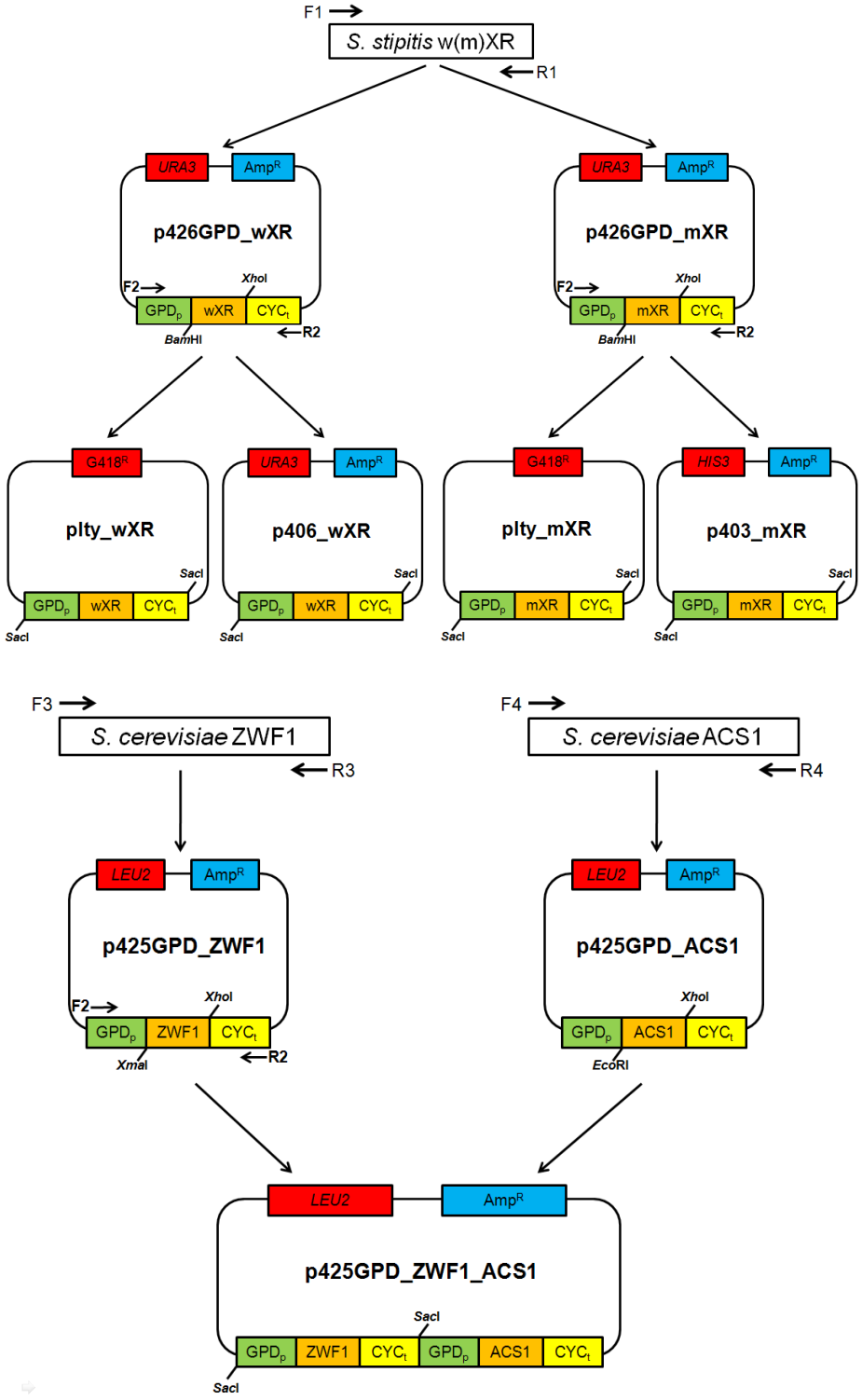

Fig. 4.2. Schemes of plasmid construction used in chapter 4

4.4. Results

4.4.1. Production of xylitol by the strain having wild XR and mutant XR

In order to extend the availability of the two cofactors (NADPH and NADH), and examine the influence of the extended availability of reducing agents on xylitol production, engineered *S. cerevisiae* strains were constructed to express the wild XR (DWW) or mutant XR (DMM) only, and both the XRs (DWM). *In vitro* activity assay of the wild and mutant XRs were carried out to assess their expression and preference of cofactors in the engineered *S. cerevisiae* strains (Table 4.3). The DWW and DMM strains were highly specific for NADPH and NADH, respectively, whereas the DWM strain having dual XRs showed similar activities toward NADPH and NADH as expected. The DWM strain had a similar total XR activity to the DWW strain or 1.4 times higher total activity than the DMM strain.

To analyze the xylitol-producing performance, batch cultures of the DWW, DMM, and DWM strains were performed using YP medium with 21 g/L xylose and 21 g/L glucose (Fig. 4.3). All the engineered *S. cerevisiae* strains consumed glucose at the same consumption rate. After glucose added initially was utilized, the three strains started to

consume xylose with different xylose consumption rates. *S. cerevisiae* is a Crabtree positive strain able to produce ethanol from glucose even in aerobic condition (Piškur et al., 2006). Ethanol produced from glucose was consumed after glucose depletion and used for maintenance of cell viability because xylose cannot flow into the central energy metabolism in all strains. And ethanol and xylose were consumed simultaneously since ethanol was used for the regeneration of the cofactors for xylitol production. Xylitol production was linearly correlated to the consumption of xylose and ethanol (Fig. 4.3). Fermentation parameters of these batch fermentations were summarized in Table 4.3. The DWM strain expressing two types of XR exhibited the highest capability of xylitol production. The batch fermentation of the DWM strain resulted in improved xylitol concentration by 6.6% and 47% than the corresponding values for the DWW and DMM strains expressing each type of XR, respectively. As expected, the xylitol yield in all cases reached the theoretical xylitol yield (1 g-xylitol/1 g-xylose). Interestingly, the DMM and DWM strains showed 1.3 times higher final dry cell mass than the DWW strain, indicating that the partial or complete change of the wild XR to the mutant XR probably reduced a metabolic burden by expression of NADPH-consuming XR and hence elevated final cell mass.

In the batch fermentations, the DWM strain showed the best

performance for xylitol production. To confirm its ability as xylitol producer, glucose-limited fed-batch fermentations of the DWW-C and DWM-C strains were performed in YP medium with 100 g/L xylose and 21 g/L glucose. The DWW-C and DWM-C strains were constructed by introduction of plasmid p425GPD into the DWW and DWM strains, respectively. After depletion of glucose initially added, a concentrated glucose solution was fed continuously to maintain its basal level in the medium, which is called a glucose-limited feeding strategy. To relieve the glucose inhibition on xylose transport (Lee et al., 2002; Lee et al., 2000) and to supply the cofactors and cellular energy, the glucose-limited feeding strategy was chosen in this chapter. By this glucose feeding strategy, xylose was linearly consumed to produce xylitol with different xylitol productivities. The conversion of xylose to xylitol by NADPH-linked XR depleted the intracellular NADPH in the DWW strain, resulting in reduction of xylitol productivity. On the other hand, the DWM strain could use NADPH as well as NADH for conversion of xylose to xylitol. As a results, the glucose-limited fed-batch fermentation of the DWM strain exhibited 72 g/L xylitol concentration and 2.00 g/L-h xylitol productivity which were 13% and 14% higher than those for the DWW strain (Table 4.5) (Fig. 4.4). Based on the XR activity analysis and the xylitol-producing ability in batch and glucose-limited fed-batch fermentations, the balanced expression

of the wild and mutant XRs under high XR expression levels could be a plausible reason for the enhanced production of xylitol by the DWM strain.

Table 4.3. Summarized results of batch cultures of engineered *S. cerevisiae* DWW, DMM and DWM strains using 21 g/L xylose and 21 g/L glucose

Strain	Final dry cell mass[a)] (g/L)	Xylitol concentration[a)] (g/L)	Xylitol productivity[a)] (g/L-h)	Xylitol yield (gxylitol /gxylose)	Specific XR activity[b)] (U/mgprotein)			XRactivity ratio[c)]
					NADPH	NADH	Total	
DWW	5.97	16.5	0.827	~ 1	2.11 ± 0.02	1.53 ± 0.03	3.64	1.39
DMM	7.41	12.0	0.599	~ 1	0.19 ± 0.01	2.47 ± 0.03	2.66	0.08
DWM	8.14	17.6	0.881	~ 1	1.89 ± 0.10	1.77 ± 0.03	3.66	1.07

a) These values are the mean of triplicate experiments.

b) Specific XR activity was measured three times independently.

c) This value was calculated by the division of XR activities on NADPH to NADH.

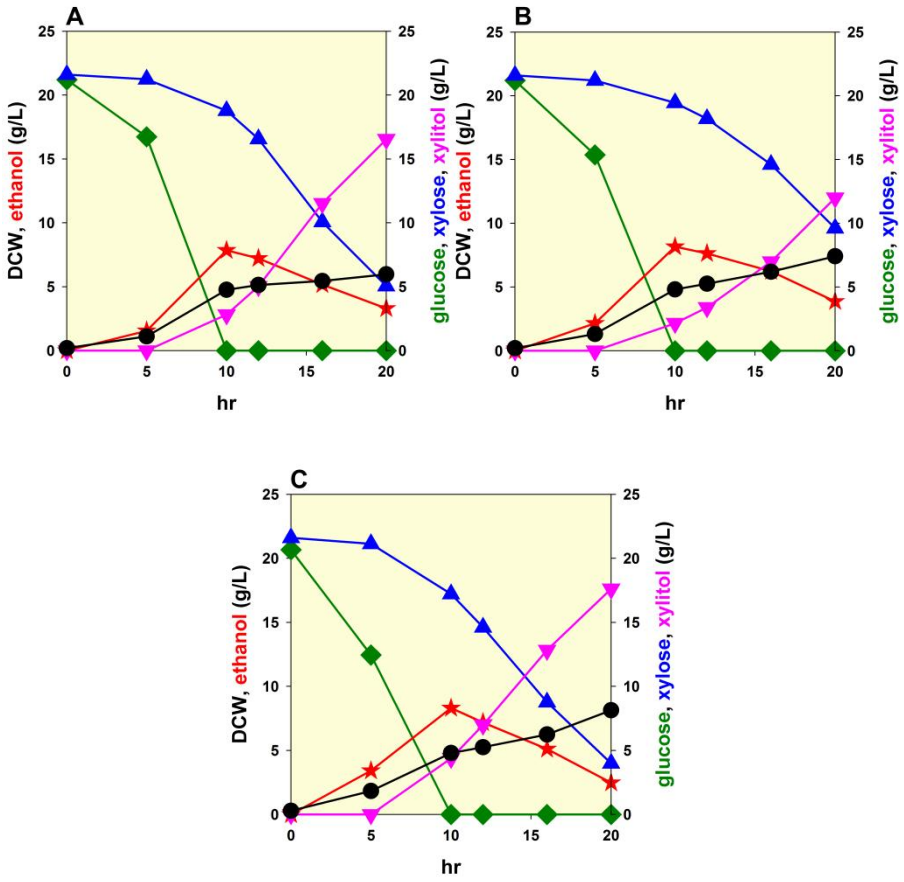

Fig. 4.3. Batch cultures of engineered *S. cerevisiae* DWW (A), DMM (B) and DWM (C) strains in YP medium with 21 g/L xylose and 21 g/L glucose at 30°C and 250 rpm. Results are the means of triplicate experiments. Symbols : glucose (diamond); xylose (triangle up); xylitol (triangle down); ethanol (filled triangle); DCW (filled circle).

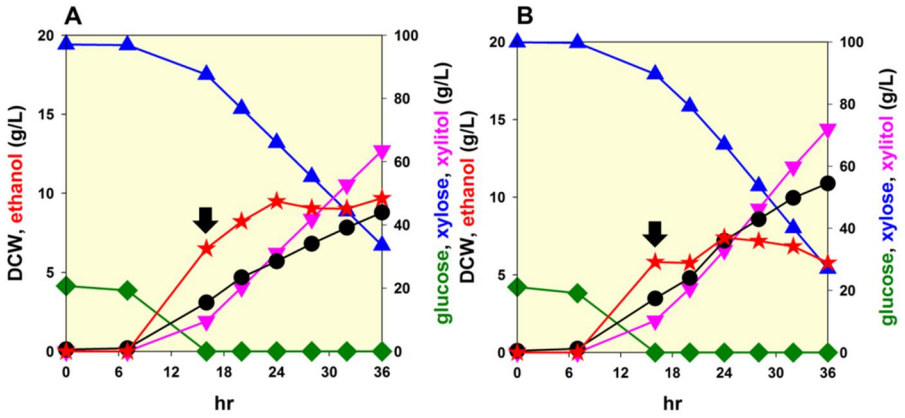

Fig. 4.4. Glucose-limited fed-batch fermentations of engineered *S. cerevisiae* DWW-C (A), DWM-C (B) at 30°C, 500 rpm, 1 vvm and pH 5.0. A mixture of 21 g/L glucose and 100 g/L xylose was added initially. The arrow indicates the start point of the glucose feeding at a rate of 1.8 g/L-h. Symbols : glucose (diamond); xylose (triangle up); xylitol (triangle down); ethanol (filled triangle); DCW (filled circle).

4.4.2. Effects of NADPH and NADH levels on xylitol production

As shown in Fig. 4.1, biological production of xylitol is controlled by the activity and cofactor dependency of XR, and the supply of NADPH and NADH. As harmonized expression of the wild and mutant XRs significantly improved the xylitol-producing performance as presented above, sufficient supply of NADPH and NADH is expected to enhance the xylitol production further. In microbial systems, NADPH and NADH are regenerated by many metabolic enzymes. Among them, glucose-6-phosphate dehydrogenase encoded by the *ZWF1* gene and acetyl-CoA synthetase by the *ACS1* gene were selected as the NADPH and NADH regenerating enzymes, because of their high efficiency.

To investigate the effects of the intracellular levels of NADPH and NADH on xylitol production, Zwf1p and Acs1p were overexpressed in the DWM strain. Plasmids p425GPD_ZWF1 and p425GPD_ACS1 were constructed to harbour each coding gene and transformed into the DWM strain to make the DWM-ZWF1 and DWM-ACS1 strains, respectively. When intracellular concentrations of $NADP^+$, NADPH, NAD^+ and NADH in the DWM-C, DWM-ZWF1 and DWM-ACS1 strains were measured (Table 4.4), overexpression of Zwf1p and Acs1p changed the pools of the hydrogen donors and increased the intracellular concentrations of both NADPH and NADH with different

extents. The *ZWF1* overexpression increased the ratios of NADPH to $NADP^+$ and of NADH to NAD^+ by 19%, compared to the DWM-C control strain. The *ACS1* overexpression led to 2.26- and 1.27-fold improvements in NADPH and NADH concentrations, respectively, relative to those of the DWM-C strain. In addition, the DWM-ACS1 strain showed 4.15 and 1.25 times higher the NADPH/$NADP^+$ and NADH/NAD^+ ratios, respectively, than those of the DWM-C strain. As a result, intracellular pools of NADPH and NADH in the engineered strain were increased by overexpression of the NADPH and NADH-regenerating enzymes in the DWM strain.

To investigate the effects of the overexpression of *ZWF1* or *ACS1* on xylitol production, glucose-limited fed-batch fermentations of DWM-ZWF1 and DWM-ACS1 were performed using 18 g/L glucose and 98 g/L xylose (Fig. 4.5 A, B). The DWM-ZWF1 and DWM-ACS1 strains showed 2.04 and 2.15 g/L-h maximum xylitol productivity, which were 4-15% higher than that of the DWM-C strain. It indicated that either *ZWF1* or *ACS1* overexpression enhanced the xylitol concentration and productivity. As expected, the increments of NADPH and NADH concentrations, and the NADPH/$NADP^+$ and NADH/NAD^+ ratios elevated the xylitol producing performances of the DWM-ZWF1 and DWM-ACS1 strains. Irrespective of the *ZWF1* and *ACS1*

overexpression, xylitol yields in each case were close to the theoretical value.

Individual expression of the *ZWF1* and *ACS1* genes conferred the improved ability of xylitol production to the DWM strains. To maximize the merit of the DWM strain with the broad specificity of the cofactors, plasmid p425GPD_ZWF1_ACS1 was constructed to express both the *ZWF1* and *ACS1* genes, and transformed into the DWM strain. In the analysis of the intracellular cofactor contents (Table 4.4), overexpression of both Zwf1p and Acs1p in the resulting strain of DWM-ZWF1-ACS1 highly elevated the pools of both NADPH and NADH, and the ratios of the reduced cofactors (NADPH and NADH) to the oxidized cofactors ($NADP^+$ and NAD^+) by a 4-fold maximally, relative to those for the DWM-C strain. The coexpression also led to higher ratios of NAD(P)H to $NAD(P)^+$ than the single expression of Zwf1p and Acs1p.

To evaluate the xylitol-producing performance, the DWM-ZWF1-ACS1 strain was cultured using 18 g/L glucose and 98 g/L xylose, and by the same fermentation strategy as the two fed-batch cultivations performed above (Fig. 4.5 C). As the control, the DWW-ZWF1-ACS1 strain was cultured by the same fermentation strategy (Fig. 4.5 D). The patterns of xylose consumption and xylitol production were similar to

other glucose-limited fed-batch fermentations. The DWM-ZWF1-ACS1 strain produced 83.7 g/L xylitol with the final xylitol productivity of 2.33 g/L-h, while the DWW-ZWF1-ACS1 strain did 70.6 g/L xylitol with 1.96 g/L-h productivity (Table 4.5). Especially, the DWM-ZWF1-ACS1 strain showed 17% higher xylitol productivity than that of the DWM-C strain. In comparison to the sole expression of either *ZWF1* or *ACS1*, the DWM-ZWF1-ACS1 strain exhibited 8-14% improvement in xylitol productivity. Considering these fermentation results, it was certain that the balanced expression of the wild and mutant XRs with an aid of the NADPH and NADH regeneration systems exhibited a synergistic effect on xylitol production. To ensure functional expression of Zwf1p and Acs1p in the DWM-ZWF1-ACS1 strain, crude extracts of the yeast cells were collected in the fed-batch culture and their enzyme activities were measured. As shown in Fig. 4.6, the DWM-ZWF1-ACS1 strain had at least 5-fold higher specific activity of glucose-6-phosphate dehydrogenase than the control DWM-C strain at all times. Specific acetyl-CoA synthetase activity of the DWM-ZWF1-ACS1 strain was also 5 times higher than that of the control strain.

Table 4.4. Intracellular concentrations of cofactors (NADPH, $NADP^+$, NADH and NAD^+) in engineered *S. cerevisiae* DWM overexpressing Zwf1p and/or Acs1p

S. cerevisiae strain	Concentration (μmol/g cell)		$NADPH/NADP^+$	Concentration (μmol/g cell)		$NADH/NAD^+$
	NADPH	$NADP^+$	ratio	NADH	NAD^+	ratio
DWM-C	0.96 ± 0.03	1.78 ± 0.03	0.54 ± 0.01	2.44 ± 0.06	7.70 ± 0.47	0.32 ± 0.01
DWM-ZWF1	1.04 ± 0.00	1.61 ± 0.04	0.64 ± 0.01	3.11 ± 0.14	8.09 ± 0.52	0.38 ± 0.01
DWM-ACS1	2.17 ± 0.02	0.97 ± 0.05	2.24 ± 0.10	3.09 ± 0.15	7.72 ± 0.51	0.40 ± 0.01
DWM-ZWF1-ACS1	2.48 ± 0.16	1.09 ± 0.15	2.27 ± 0.16	2.87 ± 0.21	5.49 ± 0.34	0.52 ± 0.01

All concentrations were measured three times independently.

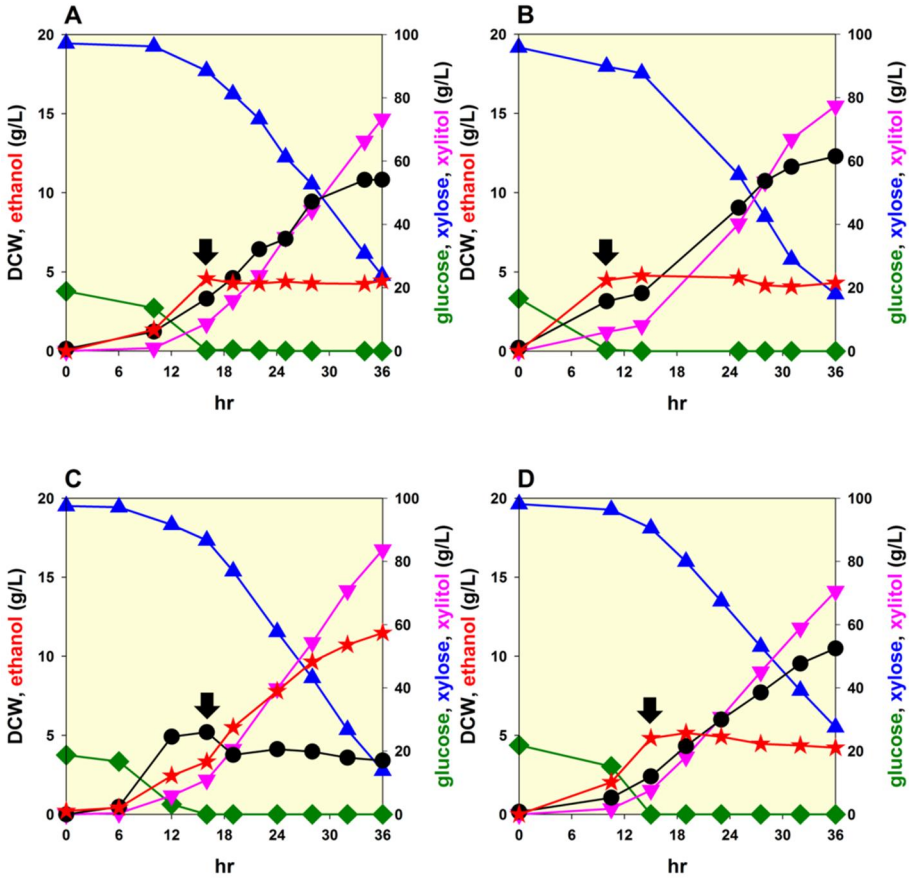

Fig. 4.5. Effect of Zwf1p and Acs1p overexpression on xylitol production in glucose-limited fed-batch fermentations of engineered *S. cerevisiae* DWM-ZWF1 (A), DWM-ACS1 (B), DWM-ZWF1-ACS1 (C) and DWW-ZWF1-ACS1 (D) at 30°C, 500 rpm, 1 vvm and pH 5.0. A mixture of 18 g/L glucose and 98 g/L xylose was added initially. The arrow indicates the start point of the glucose feeding at a rate of 1.8 g/L-h. Symbols : glucose (diamond); xylose (triangle up); xylitol (triangle down); ethanol (filled triangle); DCW (filled circle).

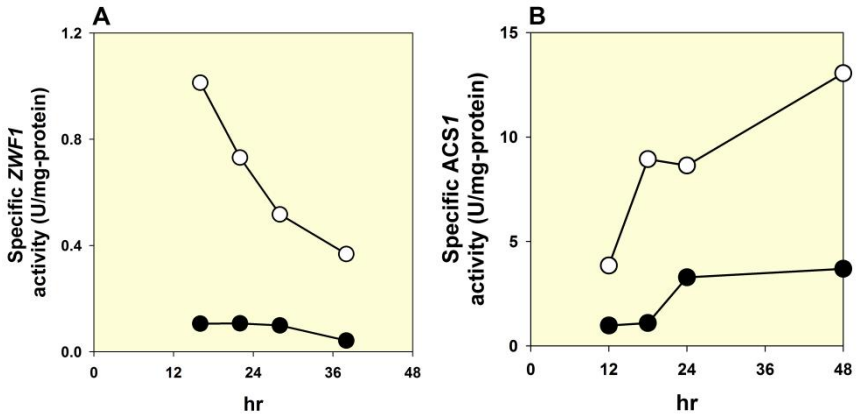

Fig. 4.6. Time-course profile of specific Zwf1p (A) and Acs1p (B) activities in glucose-limited fed-batch fermentations of engineered *S. cerevisiae* DWM-C (●) and DWM-ZWF1-ACS1 (○).

4.4.3. Optimization of fermentation conditions for improving xylitol production

The final strain (DWM-ZWF1-ACS1) showed the highest productivity than other *S. cerevisiae* strains engineered for xylitol production. To extent the period for the highest xylitol productivity and hence elevate final xylitol titre, fed-batch cultivation strategies were designed using intermittent addition or continuous feeding of a concentrated xylose solution to maintain an optimized concentration of xylose in the culture medium (Kim et al., 2002). In the glucose-limited fed-batch fermentation of the DWM-ZWF1-ACS1 strain (Fig. 4.5 C), the highest xylitol productivity was achieved when xylose concentration in the medium ranged from 40 g/L to 80 g/L. So, this range of xylose concentration was adopted to keep the highest xylitol-producing ability. As shown in Fig. 4.7 A and 4.7 B, glucose-limited fed-batch cultures of the DWM-C and DWM-ZWF1-ACS1 strains were carried out by intermittent addition of 600 g/L xylose solution to a bioreactor when xylose concentration in the medium dropped below 40 g/L. The concentrated xylose solution was added four times to control the xylose concentration range between 40 and 80 g/L. Finally, 185.3 g/L xylitol concentration and 3.71 g/L-hr productivity were obtained in 50 h fed-batch culture of the DWM-ZWF1-ACS1 strain (Table 4.5). On the

other hand, the DWM-C strain cultured by the same fermentation strategy produced 150.2 g/L xylitol. Generally, sugar uptake rate depends on extracellular sugar concentration (Shuler & Kargi, 2002). Xylose consumption rate decreased gradually whenever xylose concentration fluctuated. For maximizing xylitol production, glucose-limited fed-batch fermentation was performed by continuous feeding of 600 g/L xylose solution at a constant rate of 10 mL/h. The feed rate was decided from the stage showing the highest xylose consumption rate in Fig. 4.7 B. When initial glucose was depleted, the continuous xylose feeding started at 6 h culture time. During 24 h of the feeding, xylose concentration in the medium was maintained well at 80 g/L as planned and most xylose added was converted into xylitol with the theoretical yield (~1 g/g) (Fig. 4.7 C). As a result, the final xylitol concentration of 196.2 g/L and xylitol productivity of 4.26 g/L-h were obtained in the fed-batch culture by the continuous xylose-feeding strategy (Table 4.5).

Table 4.5. Summarized results of glucose-limited fed-batch fermentations using 76-98 g/L initial xylose in Chapter 4

S. cerevisiae strain	Xylose feeding strategy	Final dry cell mass (g/L)	Final xylitol concentration (g/L)	Final xylitol Productivity (g/L-h)	Xylitol yield (g /g xylose)
DWW-C	No xylose feeding	8.8	63.5	1.76	~1
DWW-ZWF1-ACS1	No xylose feeding	10.5	70.6	1.96	~1
DWM-C	No xylose feeding	10.9	72.0	2.00	~1
DWM-ZWF1-ACS1	No xylose feeding	11.5	83.7	2.33	~1
DWM-C	Intermittent xylose addition[a)]	9.1	150.2	3.00	~1
DWM-ZWF1-ACS1	Intermittent xylose addition[a)]	10.4	185.3	3.71	~1
DWM-ZWF1-ACS1	Continuous xylose feeding[b)]	12.2	196.2	4.27	~1
BJ3505/δXR[c)]	Intermittent xylose addition	22.0	116	2.34	~1
C. tropicalis ATCC 13803[d)]	Continuous xylose feeding	10.4	187	3.90	0.75

a) A concentrated xylose solution of 600 g/L was added four times to control 40-80 g/L xylose concentration in the medium.

b) A concentrated xylose solution of 600 g/L was fed continuously to maintain 80 g/L xylose concentration in the medium.

c) These data were obtained from cell-recycle fermentation (Bae et al., 2004).

d) These data were obtained by optimizing initial xylose concentration and feeding rate (Kim et al., 2002).

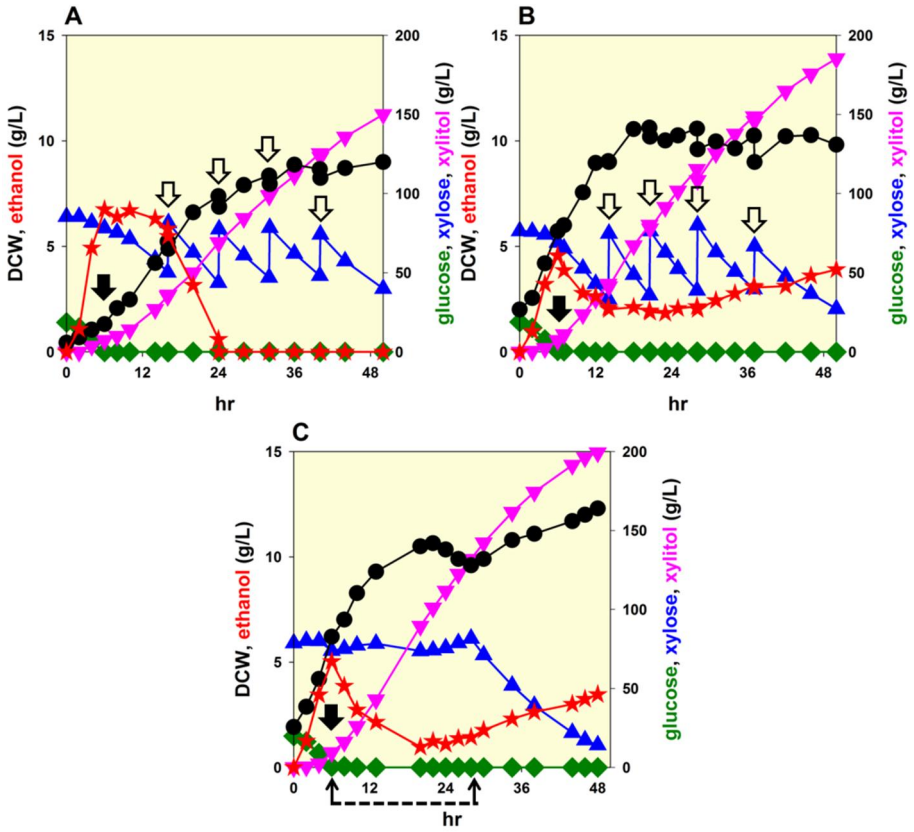

Fig. 4.7. Fed-batch fermentations of engineered *S. cerevisiae* DWM-C (A), DWM-ZWF1-ACS1 (B, C). The closed arrow indicates the initiation of the glucose feeding at a rate of 1.8 g/L-h. In the panels A and B, a concentrated xylose solution of 600 g/L was added intermittently (open arrow). In the panel C, the concentrated xylose solution was fed continuously at a rate of 10 mL/h and the dotted line indicates the period of the continuous feeding. Symbols : glucose (diamond); xylose (triangle up); xylitol (triangle down); ethanol (filled triangle); DCW (filled circle).

4.5. Discussion

Xylose is biologically reduced to xylitol by xylose reductase (XR). The wild XR from *S. stipitis* used in this study is known to be able to utilize both NADPH and NADH as cofactors. But the activity of wild XR on NADPH was 30% higher than that on NADH (Verduyn et al., 1985), so most engineered *S. cerevisiae* strains expressing the wild XR gene as well as conventional xylitol-producing yeasts convert xylose to xylitol using NADPH primarily. Because the intracellular NADH level is much higher than the NADPH level (Vemuri et al., 2007), balanced utilization of both NADPH and NADH is suggested to avoid the depletion of cofactors and hence improve xylitol production in engineered *S. cerevisiae*. Previously, a mutant XR preferring NADH was developed by protein engineering (Watanabe et al., 2007b), and its expression reduced a metabolic disorder of redox-imbalance in the xylose metabolism of engineered *S. cerevisiae*. As shown in the batch and glucose-limited fed-batch cultures (Fig. 4.3, Table 4.5), the DWM strain expressing both the wild and mutant XRs showed higher xylitol producing performances than the DWW and DWM strains, indicating that the harmonized expression of two XRs with different cofactor specificities is a certain reason for the enhanced xylitol production by the DWM strain.

Meanwhile, supply of NADPH or NADH cofactor is a rate-limiting factor for xylitol production as well as the XR expression. Among several metabolic enzymes regenerating NADPH or NADH in the substrate level, glucose-6-phosphate dehydrogenase (Zwf1p) catalyzes the main metabolic pathway for NADPH regeneration in *S. cerevisiae* (Oh et al., 2007). Acetyl-CoA synthetase (Acs1p) converts acetate to acetyl-CoA, which is metabolized further into the tricarboxylic acid cycle with the NADPH and NADH regeneration metabolism. Since acetate is produced from acetaldehyde by NADPH regeneration, overexpression of acetyl-CoA synthetase is expected to modulate both NADPH and NADH levels simultaneously and indirectly (Lee & Kim, 2014; Oh et al., 2012). Overexpression of Zwf1p and Acs1p enhanced the intracellular pools of NADPH and NADH (Table 4.4), resulting in maximum 17% increases in xylitol productivity than the control strain (Fig. 4.5 and Table 4.5). The similar effects of improved production of target molecules by the regeneration of the cofactors could be found in some reports. The overexpression of Zwf1p triggered the production of xylitol, GDP-L-fucose, ε-caprolactone by enhanced NADPH levels (Kwon et al., 2006; Lee et al., 2011; Lee et al., 2007). The Acs1p overexpression influenced the production of many biochemicals such as hydrogen, isopropanol, butanol by increasing the carbon flux into a desired product and decreasing acetate accumulation, which was toxic

to cell growth (Krivoruchko et al., 2013; Wang et al., 2012). When cellobiose and xylose were consumed simultaneously, overexpression of *S. cerevisiae* Idp2p (isocitrate dehydrogenase) increased the NADPH availability and allowed a 63% improvement in xylitol productivity (Oh et al., 2013). As a result, the modulation of the pools and ratios of NADPH and NADH was one of the effective ways to improve xylitol production.

Dual expression of NAD(P)H regenerating enzymes would be an easy way to increase target molecules by changing the pools of NADPH and NADH cofactors. In case of microbial xylitol production, however, this strategy was not always effective. Coexpression of glucose-6-phosphate dehydrogenase and 6-phosphogluconate dehydrogenase, two main NADPH-regenerating enzymes, increased xylitol productivity by engineered *Candida tropicalis* PP (Ahmad et al., 2012). Coexpression of Acs1p and $NADP^+$-dependent aldehyde dehydrogenase 6 (Ald6p) in engineered *S. cerevisiae* BJ3505:δXR exerted a negative effect on xylitol production, compared to their single expression (Oh et al., 2012). As shown in Fig. 4.5, simultaneous expression of Zwf1p and Acs1p in the DWM strain exhibited 19% higher enhancement of xylitol productivity compared to the coexpression of Zwf1p and Acs1p in the DWW strain. It was certain that the coexpression of Zwf1p and

Acs1p with different mechanisms of cofactor regeneration was beneficial for xylitol production mediated by both the wild and mutant XRs in the DWM-ZWF1-ACS1 strain.

The results of the glucose-limited fed-batch fermentations performed in this chapter were summarized in Table 4.5. The control of xylose concentration at an optimized range improved both xylitol concentration and productivity considerably. The continuous xylose-feeding strategy gave the best performances of xylitol production which were 2.3- and 1.8-fold increases in xylitol concentration and xylitol productivity, respectively, relative to the culture of the same strain without controlling xylose concentration. In comparison to the previous results done by other microorganisms, the DWM-ZWF1-ACS1 strain showed 82% and 9% higher xylitol productivity than a engineered *S. cerevisiae* BJ3505 strain expressing the NADPH-dependent XR from *S. stipites* (Bae et al., 2004) and a wild type of *C. tropicalis* ATCC13803(Kim et al., 2002), respectively, which were cultured using a similar fed-batch fermentation strategy. All cultures of the *S. cerevisiae* strains expressing foreign XRs in this chapter resulted in almost the theoretical yield (~1 g/g), whereas a traditional xylitol producer of *C. tropicalis* produced xylitol below the theoretical yield (Bisaria & Kondō, 2014; Kim et al., 2002). Expression of two type of

XRs highly specific for each cofactor along with two metabolic enzymes for increasing the pools of the reduced cofactors could clearly overcome both the process limitation of engineered *S. cerevisiae* (low productivity) and *C. tropicalis* (low yield) reported previously.

In conclusion, insufficient supply of NADPH cofactor and xylose utilization to cellular energy prevents the commercialization of microbial xylitol production. To overcome these hurdles, *S. cerevisiae* unable to metabolize xylose was engineered to express two types of XR using both NADPH and NADH cofactors. Additionally, Zwf1p and Acs1p were coexpressed to facilitate the NADPH and NADH regeneration. Finally, the best engineered *S. cerevisiae* DWM-ZWF1-ACS1 coexpressing NADPH-dependent and NADH-preferring XRs, and Zwf1p and Acs1p produced almost 196.2 g/L xylitol with over 4.27 g/L-h productivity and almost theoretical yield, which might meet the industrial demands for commercialization of microbial xylitol production.

Chapter 5

Conclusions

The main objective of this dissertation is to construct *S. cerevisiae* strain for enhancing xylose metabolism. Xylose is the second most abundant sugar. Therefore, efficient utilization of xylose in hydrolysates is one of the key steps for the economically feasible production of biofuels and chemicals. For decades, *S. cerevisiae* D452-2 has been used in microbial biotechnology research, specially, xylose fermentation.

The background of strain is also important factor for efficient fermentation. To understand the associations between the genetic background and the desired phenotypes, a comparative genomics approach was used. The whole genome of D452-2 was sequenced and compared to that of reference strain S288c. A total of 6,948 SNPs and a 172,733 length of gaps were detected to result in different gene expression pattern. The glycogen synthesis gene, *GPD2* and *GAL2* gene were selected as a candidate gene for enhanced xylose fermentation in this thesis. The mutations of glycogen synthesis genes, *GAL2* and *GPD2* were thought to change the flux of xylose to ethanol, xylose transport capacity and intracellular cofactors, respectively. These alterations could be a plausible reason for the enhanced xylose fermentation of the D452-2 strain. Additionally, the DXS having unexpected higher XR activity was sequenced to identify the mutations responsible. The XR expression cassett was amplified by homologous

recombination. This genome information of D452-2 could be used for searching new target genes not only for xylose fermentation but other desire. Genetic and physiolosical studies with a wide range of *S. cerevisiae* strains are necessary to broaden insight into underlying molecular mechanisms.

The engineered *Saccharomyces cerevisiae* expressing a xylose-assimilating pathway (XR, XDH and XK from *Scheffersomyces stipitis*) has several limitations: 1. Slow uptake rate, 2. Inhibition by glucose, 3. Intermediate secretion, 4. Cofactor imbalance, 5. Slow pentose phosphate pathway, 6. Aerobic meyabolism, 7. byproduct formation/toxicity. Among these limitations, this dissertation focuses on the cofactor imbalance. XR converts xylose to xylitol using NADPH as cofactor and XDH further xylitol to xylulose using NAD^+. This different cofactor requirement between XR and XDH causes to accumulate xylitol and reduce xylose assimilation rate. To alleviate cofactor imbalance, NADPH- or NADH-balanced xylose-fermenting pathway was introduced into the engineered *S. cerevisiae* though protetin engineering of XR and XDH. But these approaches achieved partial successes in that the engineered *S. cerevisiae* with NADPH balanced pathway had a low yield of ethanol and the engineered *S. cerevisiae* with NADH balanced pathway showed slow xylose consumption. Since the NADPH/NADP+ and NADH/NAD+ cofactor

pairs are related in numerous biochemical reactions and regulated tightly in microorganisms, maintaining the cellular redox balance is impartant for efficient xylose fermentation.

In this thesis, a synthetic isozyme system of xylose reductase was used to construct an improved xylose-fermenting strain. The engineered strain having the XR based isozyme was constructed by coexpressing both the NADPH-dependant XR and NADH-dependent XR. This strain (DXS) was able to use NADPH and NADH simultaneously and adjust an intracellular cofactor ratio to produce ethanol efficiently under various fermentation conditions. The DXS strain showed low xylitol accumulation and fast xylose consumption compared to the engineered strains expressing only one type of XRs. This fermentation property was also verified in the silver grass hydrolysates and the engineered strain DXS produced 50.7 g/L ethanol with 0.43 g/g ethanol yield.

In addition, XR-based isozyme system was applied to microbial production of xylitol. *Saccharomyces cerevisiae* D452-2 was engineered to express two types of XRs to implement a isozyme system. The resulting strain (DWM) exhibited improved xylitol concentration and productivity than the corresponding values for the strains expressing only one type of XRs in batch and glucose-limited fed-batch fermentations. Furthermore, coexpression of *S. cerevisiae ZWF1* and

ACS1 involved in cofactor regeneration increased intracellular concentrations of NADPH and NADH, improving xylitol productivity. Since xylose uptake rate was affected by the extracellular xylose concentration, regulation of its concentration was important for maximizing the xylitol productivity. When xylose concentration in the medium was maintained at 80 g/L, the xylitol productivity was the highest to produce 196.2 g/L xylitol with productivity of 4.26 g/L-h. These results were suggested that availability and supply of cofactor play an important role for the enhanced utilization of xylose and the XR-based isozyme system is a promising strategy to meet the industrial demands for production of biofuels and chemicals.

References

Agbor, V.B., Cicek, N., Sparling, R., Berlin, A., Levin, D.B. 2011. Biomass pretreatment: fundamentals toward application. Biotechnol. Adv., 29, 675-685.

Ahmad, I., Shim, W.Y., Jeon, W.Y., Yoon, B.H., Kim, J.-H. 2012. Enhancement of xylitol production in *Candida tropicalis* by co-expression of two genes involved in pentose phosphate pathway. Bioprocess Biosyst. Eng., 35, 199-204.

Akao, T., Yashiro, I., Hosoyama, A., Kitagaki, H., Horikawa, H., Watanabe, D., Akada, R., Ando, Y., Harashima, S., Inoue, T. 2011. Whole-genome sequencing of sake yeast *Saccharomyces cerevisiae* Kyokai no. 7. DNA Res., dsr029.

Almeida, J.R., Runquist, D., Sànchez Nogué, V., Lidén, G., Gorwa-Grauslund, M.F. 2011. Stress-related challenges in pentose fermentation to ethanol by the yeast *Saccharomyces cerevisiae*. Biotechnol. J., 6, 286-299.

Almeida, J.R.M., Modig, T., Petersson, A., Hahn-Hagerdal, B., Liden, G., Gorwa-Grauslund, M.F. 2007. Increased tolerance and conversion of inhibitors in lignocellulosic hydrolysates by *Saccharomyces cerevisiae*. J. Chem. Technol. Biotechnol., 82, 340-349.

Altschul, S.F., Madden, T.L., Schäffer, A.A., Zhang, J., Zhang, Z., Miller, W., Lipman, D.J. 1997. Gapped BLAST and PSI-BLAST: a new generation of protein database search programs. Nucleic Acids Res., 25,

3389-3402.

Ansell, R., Granath, K., Hohmann, S., Thevelein, J.M., Adler, L. 1997. The two isoenzymes for yeast NAD+-dependent glycerol 3-phosphate dehydrogenase encoded by GPD1 and GPD2 have distinct roles in osmoadaptation and redox regulation. EMBO J., 16, 2179-2187.

Argueso, J.L., Carazzolle, M.F., Mieczkowski, P.A., Duarte, F.M., Netto, O.V., Missawa, S.K., Galzerani, F., Costa, G.G., Vidal, R.O., Noronha, M.F. 2009. Genome structure of a *Saccharomyces cerevisiae* strain widely used in bioethanol production. Genome Res., 19, 2258-2270.

Babrzadeh, F., Jalili, R., Wang, C., Shokralla, S., Pierce, S., Robinson-Mosher, A., Nyren, P., Shafer, R.W., Basso, L.C., de Amorim, H.V. 2012. Whole-genome sequencing of the efficient industrial fuel-ethanol fermentative *Saccharomyces cerevisiae strain* CAT-1. Mol. Genet. Genomics, 287, 485-494.

Bae, S.-M., Park, Y.-C., Lee, T.-H., Kweon, D.-H., Choi, J.-H., Kim, S.-K., Ryu, Y.-W., Seo, J.-H. 2004. Production of xylitol by recombinant *Saccharomyces cerevisiae* containing xylose reductase gene in repeated fed-batch and cell-recycle fermentations. Enzyme Microb. Technol., 35, 545-549.

Bengtsson, O., Hahn-Hagerdal, B., Gorwa-Grauslund, M.F. 2009. Xylose reductase from *Pichia stipitis* with altered coenzyme preference improves ethanolic xylose fermentation by recombinant *Saccharomyces cerevisiae*. Biotechnol. Biofuels, 2.

Bera, A.K., Ho, N.W., Khan, A., Sedlak, M. 2011. A genetic overhaul of *Saccharomyces cerevisiae* 424A (LNH-ST) to improve xylose fermentation. J. Ind. Microbiol. Biotechnol., 38, 617-626.

Besemer, J., Borodovsky, M. 2005. GeneMark: web software for gene finding in prokaryotes, eukaryotes and viruses. Nucleic Acids Res., 33, W451-W454.

Bisaria, V.S., Kondō, A. 2014. *Bioprocessing of renewable resources to commodity bioproducts*. Wiley Online Library.

Borneman, A.R., Desany, B.A., Riches, D., Affourtit, J.P., Forgan, A.H., Pretorius, I.S., Egholm, M., Chambers, P.J. 2011. Whole-genome comparison reveals novel genetic elements that characterize the genome of industrial strains of *Saccharomyces cerevisiae*. PLOS Genet., 7, e1001287.

Brachmann, C.B., Davies, A., Cost, G.J., Caputo, E., Li, J., Hieter, P., Boeke, J.D. 1998. Designer deletion strains derived from Saccharomyces cerevisiae S288C: a useful set of strains and plasmids for PCR-mediated gene disruption and other applications. Yeast, 14, 115-132.

Casey, E., Sedlak, M., Ho, N.W., Mosier, N.S. 2010. Effect of acetic acid and pH on the cofermentation of glucose and xylose to ethanol by a genetically engineered strain of *Saccharomyces cerevisiae*. FEMS Yeast Res., 10, 385-393.

Cha, Y.-L., Yang, J., Seo, S.-i., An, G.H., Moon, Y.-H., You, G.-D., Lee, J.-E., Ahn, J.-W., Lee, K.-B. 2016. Alkaline twin-screw extrusion

pretreatment of Miscanthus with recycled black liquor at the pilot scale. Fuel, 164, 322-328.

Chen, X., Li, S., Liu, L. 2014. Engineering redox balance through cofactor systems. Trends Biotechnol., 32, 337-343.

Chin, C.-S., Alexander, D.H., Marks, P., Klammer, A.A., Drake, J., Heiner, C., Clum, A., Copeland, A., Huddleston, J., Eichler, E.E. 2013. Nonhybrid, finished microbial genome assemblies from long-read SMRT sequencing data. Nat. Methods, 10, 563-569.

Chung, Y.-S., Kim, M.-D., Lee, W.-J., Ryu, Y.-W., Kim, J.-H., Seo, J.-H. 2002. Stable expression of xylose reductase gene enhances xylitol production in recombinant *Saccharomyces cerevisiae*. Enzyme Microb. Technol., 30, 809-816.

Clark, J.H., Deswarte, F. 2011. *Introduction to chemicals from biomass*. John Wiley & Sons.

Darling, A.C., Mau, B., Blattner, F.R., Perna, N.T. 2004. Mauve: multiple alignment of conserved genomic sequence with rearrangements. Genome Res., 14, 1394-1403.

de Albuquerque, T.L., da Silva Junior, I.J., Macedo, G.R.d., Rocha, M.V.P. 2014. Biotechnological production of xylitol from lignocellulosic wastes: a review.

De Graef, M.R., Alexeeva, S., Snoep, J.L., de Mattos, M.J.T. 1999. The steady-state internal redox state (NADH/NAD) reflects the external redox state and is correlated with catabolic adaptation in *Escherichia*

coli. J. Bacteriol., 181, 2351-2357.

Demirbas, M.F. 2006. Current technologies for biomass conversion into chemicals and fuels. Energ. Source. PART A, 28, 1181-1188.

Deutsch, J. 1983. Glucose-6-phosphate dehydrogenase. in: *Methods of enzymatic analysis*, Vol. 3, pp. 190-196.

Eichler, E.E., Sankoff, D. 2003. Structural dynamics of eukaryotic chromosome evolution. Science, 301, 793-797.

Farwick, A., Bruder, S., Schadeweg, V., Oreb, M., Boles, E. 2014. Engineering of yeast hexose transporters to transport D-xylose without inhibition by D-glucose. Proc. Natl. Acad. Sci. U.S.A., 111, 5159-5164.

Forsburg, S.L. 2001. The art and design of genetic screens: yeast. Nat. Rev. Genet., 2, 659-668.

Fujitomi, K., Sanda, T., Hasunuma, T., Kondo, A. 2012. Deletion of the *PHO13* gene in *Saccharomyces cerevisiae improves* ethanol production from lignocellulosic hydrolysate in the presence of acetic and formic acids, and furfural. Bioresour. Technol., 111, 161-166.

Garay-Arroyo, A., Covarrubias, A., Clark, I., Nino, I., Gosset, G., Martinez, A. 2004. Response to different environmental stress conditions of industrial and laboratory *Saccharomyces cerevisiae strains*. Appl. Microbiol. Biotechnol., 63, 734-741.

Goffeau, A., Barrell, B.G., Bussey, H., Davis, R. 1996. Life with 6000 genes. Science, 274, 546.

Gorsich, S., Dien, B., Nichols, N., Slininger, P., Liu, Z., Skory, C. 2006. Tolerance to furfural-induced stress is associated with pentose phosphate pathway genes *ZWF1*, *GND1*, *RPE1*, and *TKL1* in *Saccharomyces cerevisiae*. Appl. Microbiol. Biotechnol., 71, 339-349.

Guirimand, G., Sasaki, K., Inokuma, K., Bamba, T., Hasunuma, T., Kondo, A. 2016. Cell surface engineering of *Saccharomyces cerevisiae* combined with membrane separation technology for xylitol production from rice straw hydrolysate. Appl. Microbiol. Biotechnol., 100, 3477-3487.

Guo, Z.-p., Zhang, L., Ding, Z.-y., Wang, Z.-X., Shi, G.-Y. 2009. Interruption of glycerol pathway in industrial alcoholic yeasts to improve the ethanol production. Appl. Microbiol. Biotechnol., 82, 287.

Ha, S.-J., Galazka, J.M., Kim, S.R., Choi, J.-H., Yang, X., Seo, J.-H., Glass, N.L., Cate, J.H., Jin, Y.-S. 2011a. Engineered *Saccharomyces cerevisiae* capable of simultaneous cellobiose and xylose fermentation. Proc. Natl. Acad. Sci. U.S.A., 108, 504-509.

Ha, S.J., Kim, S.R., Choi, J.H., Park, M.S., Jin, Y.S. 2011b. Xylitol does not inhibit xylose fermentation by engineered *Saccharomyces cerevisiae* expressing xylA as severely as it inhibits xylose isomerase reaction in vitro. Appl. Microbiol. Biotechnol., 92, 77-84.

Hahn-Hagerdal, B., Galbe, M., Gorwa-Grauslund, M.F., Liden, G., Zacchi, G. 2006. Bio-ethanol - the fuel of tomorrow from the residues of today. Trends Biotechnol., 24, 549-556.

Hamacher, T., Becker, J., Gárdonyi, M., Hahn-Hägerdal, B., Boles, E.

2002. Characterization of the xylose-transporting properties of yeast hexose transporters and their influence on xylose utilization. Microbiology, 148, 2783-2788.

Hasunuma, T., Sung, K.-m., Sanda, T., Yoshimura, K., Matsuda, F., Kondo, A. 2011. Efficient fermentation of xylose to ethanol at high formic acid concentrations by metabolically engineered *Saccharomyces cerevisiae*. Appl. Microbiol. Biotechnol., 90, 997-1004.

Hector, R.E., Dien, B.S., Cotta, M.A., Qureshi, N. 2011. Engineering industrial *Saccharomyces cerevisiae* strains for xylose fermentation and comparison for switchgrass conversion. J. Ind. Microbiol. Biotechnol., 38, 1193-1202.

Hosaka, K., Nikawa, J.-i., Kodaki, T., Yamashita, S. 1992. A dominant mutation that alters the regulation of INO1 expression in *Saccharomyces cerevisiae*. J. Biochem., 111, 352-358.

Hunter, R.L., Markert, C.L. 1956. Histochemical demonstration of enzymes separated by zone electrophoresis in statch gels. Science, 124, 1294-1295.

Jeffries, T.W., Grigoriev, I.V., Grimwood, J., Laplaza, J.M., Aerts, A., Salamov, A., Schmutz, J., Lindquist, E., Dehal, P., Shapiro, H. 2007. Genome sequence of the lignocellulose-bioconverting and xylose-fermenting yeast *Pichia stipitis*. Nat. Biotechnol., 25, 319-326.

Jeffries, T.W., Jin, Y.S. 2004. Metabolic engineering for improved fermentation of pentoses by yeasts. Appl. Microbiol. Biotechnol., 63, 495-509.

Jeppsson, M., Johansson, B., Hahn-Hägerdal, B., Gorwa-Grauslund, M.F. 2002. Reduced oxidative pentose phosphate pathway flux in recombinant xylose-utilizing *Saccharomyces cerevisiae* strains improves the ethanol yield from xylose. Appl. Environ. Microbiol., 68, 1604-1609.

Jin, Y.S., Alper, H., Yang, Y.T., Stephanopoulos, G. 2005. Improvement of xylose uptake and ethanol production in recombinant *Saccharomyces cerevisiae* through an inverse metabolic engineering approach. Appl. Environ. Microbiol., 71, 8249-8256.

Jin, Y.S., Laplaza, J.M., Jeffries, T.W. 2004. *Saccharomyces cerevisiae* engineered for xylose metabolism exhibits a respiratory response. Appl. Environ. Microbiol., 70, 6816-6825.

Jin, Y.S., Ni, H.Y., Laplaza, J.M., Jeffries, T.W. 2003. Optimal growth and ethanol production from xylose by recombinant *Saccharomyces cerevisiae* require moderate D-xylulokinase activity. Appl. Environ. Microbiol., 69, 495-503.

Jo, J.H., Oh, S.Y., Lee, H.S., Park, Y.C., Seo, J.H. 2015. Dual utilization of NADPH and NADH cofactors enhances xylitol production in engineered *Saccharomyces cerevisiae*. Biotechnol. J., 10, 1935-1943.

Jo, S.-E., Seong, Y.-J., Lee, H.-S., Lee, S.M., Kim, S.-J., Park, K., Park, Y.-C. 2016. Microaerobic conversion of xylose to ethanol in recombinant *Saccharomyces cerevisiae* SX6 MUT expressing cofactor-balanced xylose metabolic enzymes and deficient in *ALD6*. J. Biotechnol., 227, 72-78.

Johansson, B., Christensson, C., Hobley, T., Hahn-Hagerdal, B. 2001. Xylulokinase overexpression in two strains of *Saccharomyces cerevisiae* also expressing xylose reductase and xylitol dehydrogenase and its effect on fermentation of xylose and lignocellulosic hydrolysate. Appl. Environ. Microbiol., 67, 4249-4255.

Johansson, B., Hahn-Hägerdal, B. 2002. The non-oxidative pentose phosphate pathway controls the fermentation rate of xylulose but not of xylose in *Saccharomyces cerevisiae* TMB3001. FEMS Yeast Res., 2, 277-282.

Karhumaa, K., Hahn-Hagerdal, B., Gorwa-Grauslund, M.F. 2005. Investigation of limiting metabolic steps in the utilization of xylose by recombinant *Saccharomyces cerevisiae* using metabolic engineering. Yeast, 22, 359-368.

Karhumaa, K., Sanchez, R.G., Hahn-Hagerdal, B., Gorwa-Grauslund, M.F. 2007. Comparison of the xylose reductase-xylitol dehydrogenase and the xylose isomerase pathways for xylose fermentation by recombinant *Saccharomyces cerevisiae*. Microb. Cell. Fact., 6.

Kim, J., Han, K., Koh, Y., Ryu, Y., Seo, J. 2002. Optimization of fed-batch fermentation for xylitol production by *Candida tropicalis*. J. Ind. Microbiol. Biotechnol., 29, 16-19.

Kim, J.M., Vanguri, S., Boeke, J.D., Gabriel, A., Voytas, D.F. 1998. Transposable elements and genome organization: a comprehensive survey of retrotransposons revealed by the complete *Saccharomyces cerevisiae* genome sequence. Genome Res., 8, 464-478.

Kim, S.-K., Jin, Y.-S., Choi, I.-G., Park, Y.-C., Seo, J.-H. 2015a. Enhanced tolerance of *Saccharomyces cerevisiae* to multiple lignocellulose-derived inhibitors through modulation of spermidine contents. Metab. Eng., 29, 46-55.

Kim, S.R., Ha, S.J., Kong, II, Jin, Y.S. 2012. High expression of XYL2 coding for xylitol dehydrogenase is necessary for efficient xylose fermentation by engineered *Saccharomyces cerevisiae*. Metab. Eng., 14, 336-343.

Kim, S.R., Park, Y.-C., Jin, Y.-S., Seo, J.-H. 2013a. Strain engineering of *Saccharomyces cerevisiae* for enhanced xylose metabolism. Biotechnol. Adv., 31, 851-861.

Kim, S.R., Skerker, J.M., Kang, W., Lesmana, A., Wei, N., Arkin, A.P., Jin, Y.-S. 2013b. Rational and evolutionary engineering approaches uncover a small set of genetic changes efficient for rapid xylose fermentation in *Saccharomyces cerevisiae*. PLoS ONE, 8, e57048.

Kim, S.R., Xu, H., Lesmana, A., Kuzmanovic, U., Au, M., Florencia, C., Oh, E.J., Zhang, G., Kim, K.H., Jin, Y.-S. 2015b. Deletion of *PHO13*, encoding haloacid dehalogenase type IIA phosphatase, results in upregulation of the pentose phosphate pathway in *Saccharomyces cerevisiae*. Appl. Environ. Microbiol., 81, 1601-1609.

Kim, T.-B., Oh, D.-K. 2003. Xylitol production by *Candida tropicalis* in a chemically defined medium. Biotechnol. Lett., 25, 2085-2088.

Ko, J.K., Um, Y., Woo, H.M., Kim, K.H., Lee, S.-M. 2016. Ethanol production from lignocellulosic hydrolysates using engineered

Saccharomyces cerevisiae harboring xylose isomerase-based pathway. Bioresour. Technol., 209, 290-296.

Kogje, A.B., Ghosalkar, A. 2017. Xylitol production by genetically modified industrial strain of *Saccharomyces cerevisiae* using glycerol as co-substrate. J. Ind. Microbiol. Biotechnol., 44, 961-971.

Kotter, P., Ciriacy, M. 1993. XYLOSE FERMENTATION BY *SACCHAROMYCES-CEREVISIAE*. Appl. Microbiol. Biotechnol., 38, 776-783.

Kratzer, S., Schüller, H.-J. 1995. Carbon source-dependent regulation of the acetyl-coenzyme A synthetase-encoding gene *ACSI* from *Saccharomyces cerevisiae*. Gene, 161, 75-79.

Krivoruchko, A., Serrano-Amatriain, C., Chen, Y., Siewers, V., Nielsen, J. 2013. Improving biobutanol production in engineered *Saccharomyces cerevisiae* by manipulation of acetyl-CoA metabolism. J. Ind. Microbiol. Biotechnol., 40, 1051-1056.

Kuyper, M., Toirkens, M.J., Diderich, J.A., Winkler, A.A., van Dijken, J.P., Pronk, J.T. 2005. Evolutionary engineering of mixed-sugar utilization by a xylose-fermenting *Saccharomyces cerevisiae* strain. FEMS Yeast Res., 5, 925-934.

Kwon, D.-H., Kim, M.-D., Lee, T.-H., Oh, Y.-J., Ryu, Y.-W., Seo, J.-H. 2006. Elevation of glucose 6-phosphate dehydrogenase activity increases xylitol production in recombinant *Saccharomyces cerevisiae*. J. Mol. Catal. B: Enzym., 43, 86-89.

Lee, S.-M., Jellison, T., Alper, H.S. 2014. Systematic and evolutionary engineering of a xylose isomerase-based pathway in *Saccharomyces cerevisiae* for efficient conversion yields. Biotechnol. Biofuels, 7, 1.

Lee, S.H., Kodaki, T., Park, Y.C., Seo, J.H. 2012. Effects of NADH-preferring xylose reductase expression on ethanol production from xylose in xylose-metabolizing recombinant *Saccharomyces cerevisiae*. J. Biotechnol., 158, 184-191.

Lee, W.-H., Chin, Y.-W., Han, N.S., Kim, M.-D., Seo, J.-H. 2011. Enhanced production of GDP-L-fucose by overexpression of NADPH regenerator in recombinant *Escherichia coli*. Appl. Microbiol. Biotechnol., 91, 967.

Lee, W.-H., Park, J.-B., Park, K., Kim, M.-D., Seo, J.-H. 2007. Enhanced production of ε-caprolactone by overexpression of NADPH-regenerating glucose 6-phosphate dehydrogenase in recombinant *Escherichia coli* harboring cyclohexanone monooxygenase gene. Appl. Microbiol. Biotechnol., 76, 329-338.

Lee, W.-J., Kim, M.-D., Ryu, Y.-W., Bisson, L., Seo, J.-H. 2002. Kinetic studies on glucose and xylose transport in *Saccharomyces cerevisiae*. Appl. Microbiol. Biotechnol., 60, 186-191.

Lee, W.-J., Ryu, Y.-W., Seo, J.-H. 2000. Characterization of two-substrate fermentation processes for xylitol production using recombinant *Saccharomyces cerevisiae* containing xylose reductase gene. Process Biochem., 35, 1199-1203.

Lee, W.H., Kim, M.D. 2014. Enhanced Production of ε-Caprolactone

by Coexpression of Bacterial Hemoglobin Gene in Recombinant *Escherichia coli* Expressing Cyclohexanone Monooxygenase Gene. J. Microbiol. Biotechnol., 24, 1685-1689.

Lee, Y.-G., Jin, Y.-S., Cha, Y.-L., Seo, J.-H. 2017. Bioethanol production from cellulosic hydrolysates by engineered industrial *Saccharomyces cerevisiae*. Bioresour. Technol. , 228, 355-361.

Li, H., Wu, M., Xu, L., Hou, J., Guo, T., Bao, X., Shen, Y. 2015. Evaluation of industrial *Saccharomyces cerevisiae* strains as the chassis cell for second-generation bioethanol production. Microb. Biotechnol., 8, 266-274.

Madhavan, A., Tamalampudi, S., Ushida, K., Kanai, D., Katahira, S., Srivastava, A., Fukuda, H., Bisaria, V.S., Kondo, A. 2009. Xylose isomerase from polycentric fungus Orpinomyces: gene sequencing, cloning, and expression in *Saccharomyces cerevisiae* for bioconversion of xylose to ethanol. Appl. Microbiol. Biotechnol., 82, 1067-1078.

Mäkinen, K.K. 2011. Sugar alcohol sweeteners as alternatives to sugar with special consideration of xylitol. Med. Princ. Pract., 20, 303-320.

Martin, M.A. 2010. First generation biofuels compete. N. Biotechnol., 27, 596-608.

Matsushika, A., Goshima, T., Fujii, T., Inoue, H., Sawayama, S., Yano, S. 2012. Characterization of non-oxidative transaldolase and transketolase enzymes in the pentose phosphate pathway with regard to xylose utilization by recombinant *Saccharomyces cerevisiae*. Enzyme Microb Tech, 51, 16-25.

Matsushika, A., Inoue, H., Kodaki, T., Sawayama, S. 2009a. Ethanol production from xylose in engineered *Saccharomyces cerevisiae* strains: current state and perspectives. Appl. Microbiol. Biotechnol., 84, 37-53.

Matsushika, A., Inoue, H., Murakami, K., Takimura, O., Sawayama, S. 2009b. Bioethanol production performance of five recombinant strains of laboratory and industrial xylose-fermenting *Saccharomyces cerevisiae*. Bioresour. Technol., 100, 2392-2398.

Matsushika, A., Sawayama, S. 2011. Comparative study on a series of recombinant flocculent *Saccharomyces cerevisiae* strains with different expression levels of xylose reductase and xylulokinase. Enzyme Microb. Technol., 48, 466-471.

Matsushika, A., Sawayama, S. 2010. Effect of initial cell concentration on ethanol production by flocculent *Saccharomyces cerevisiae* with xylose-fermenting ability. Appl. Biochem. Biotechnol., 162, 1952-1960.

Matsushika, A., Watanabe, S., Kodaki, T., Makino, K., Inoue, H., Murakami, K., Takimura, O., Sawayama, S. 2008. Expression of protein engineered NADP+-dependent xylitol dehydrogenase increases ethanol production from xylose in recombinant *Saccharomyces cerevisiae*. Appl. Microbiol. Biotechnol., 81, 243-255.

McIlwain, S.J., Peris, D., Sardi, M., Moskvin, O.V., Zhan, F., Myers, K.S., Riley, N.M., Buzzell, A., Parreiras, L.S., Ong, I.M. 2016. Genome sequence and analysis of a stress-tolerant, wild-derived strain of *Saccharomyces cerevisiae* used in biofuels research. G3: Genes| Genomes| Genetics, 6, 1757-1766.

Minkin, I., Patel, A., Kolmogorov, M., Vyahhi, N., Pham, S. 2013. Sibelia: a scalable and comprehensive synteny block generation tool for closely related microbial genomes. *International Workshop on Algorithms in Bioinformatics*. Springer. pp. 215-229.

Mosier, N., Wyman, C., Dale, B., Elander, R., Lee, Y.Y., Holtzapple, M., Ladisch, M. 2005. Features of promising technologies for pretreatment of lignocellulosic biomass. Bioresour. Technol., 96, 673-686.

Mukhopadhyay, A., Wei, B., Weiner, H. 2013. Mitochondrial NAD dependent aldehyde dehydrogenase either from yeast or human replaces yeast cytoplasmic NADP dependent aldehyde dehydrogenase for the aerobic growth of yeast on ethanol. Biochim. Biophys. Acta, 1830, 3391-3398.

Naik, S.N., Goud, V.V., Rout, P.K., Dalai, A.K. 2010. Production of first and second generation biofuels: a comprehensive review. Renew. Sust. Energ. Rev., 14, 578-597.

Nakamura, N., Yamada, R., Katahira, S., Tanaka, T., Fukuda, H., Kondo, A. 2008. Effective xylose/cellobiose co-fermentation and ethanol production by xylose-assimilating *S. cerevisiae* via expression of β-glucosidase on its cell surface. Enzyme Microb. Technol., 43, 233-236.

Nijkamp, J.F., van den Broek, M., Datema, E., de Kok, S., Bosman, L., Luttik, M.A., Daran-Lapujade, P., Vongsangnak, W., Nielsen, J., Heijne, W.H. 2012. De novo sequencing, assembly and analysis of the genome of the laboratory strain *Saccharomyces cerevisiae* CEN. PK113-7D, a model for modern industrial biotechnology. Microb. Cell Fact., 11, 36.

Nikawa, J., Tsukagoshi, Y., Yamashita, S. 1991. Isolation and characterization of 2 distinct myoinositol transporter genes of *Saccharomyces cerevisiae*. J. Biol. Chem., 266, 11184-11191.

Novo, M., Bigey, F., Beyne, E., Galeote, V., Gavory, F., Mallet, S., Cambon, B., Legras, J.-L., Wincker, P., Casaregola, S. 2009. Eukaryote-to-eukaryote gene transfer events revealed by the genome sequence of the wine yeast *Saccharomyces cerevisiae* EC1118. Proc. Natl. Acad. Sci. U.S.A., 106, 16333-16338.

Oh, E.-J., Bae, Y.-H., Kim, K.-H., Park, Y.-C., Seo, J.-H. 2012. Effects of overexpression of acetaldehyde dehydrogenase 6 and acetyl-CoA synthetase 1 on xylitol production in recombinant *Saccharomyces cerevisiae*. Biocatal. Agric. Biotechnol., 1, 15-19.

Oh, E.J., Ha, S.-J., Rin Kim, S., Lee, W.-H., Galazka, J.M., Cate, J.H., Jin, Y.-S. 2013. Enhanced xylitol production through simultaneous co-utilization of cellobiose and xylose by engineered *Saccharomyces cerevisiae*. Metab. Eng., 15, 226-234.

Oh, E.J., Skerker, J.M., Kim, S.R., Wei, N., Turner, T.L., Maurer, M.J., Arkin, A.P., Jin, Y.-S. 2016. Gene amplification on demand accelerates cellobiose utilization in engineered *Saccharomyces cerevisiae*. Appl. Environ. Microbiol., 82, 3631-3639.

Oh, Y.-J., Lee, T.-H., Lee, S.-H., Oh, E.-J., Ryu, Y.-W., Kim, M.-D., Seo, J.-H. 2007. Dual modulation of glucose 6-phosphate metabolism to increase NADPH-dependent xylitol production in recombinant *Saccharomyces cerevisiae*. J. Mol. Catal. B-Enzym., 47, 37-42.

Ostergaard, S., Olsson, L., Nielsen, J. 2000. Metabolic engineering of *Saccharomyces cerevisiae*. Microbiol. Mol. Biol. Rev., 64, 34-50.

Otero, J.M., Vongsangnak, W., Asadollahi, M.A., Olivares-Hernandes, R., Maury, J., Farinelli, L., Barlocher, L., Østerås, M., Schalk, M., Clark, A. 2010. Whole genome sequencing of *Saccharomyces cerevisiae*: from genotype to phenotype for improved metabolic engineering applications. BMC genomics, 11, 723.

Palmqvist, E., Hahn-Hägerdal, B. 2000. Fermentation of lignocellulosic hydrolysates. I: inhibition and detoxification. Bioresour. Technol., 74, 17-24.

Pampulha, M.E., Loureiro-Dias, M.C. 2000. Energetics of the effect of acetic acid on growth of *Saccharomyces cerevisiae*. FEMS Microbiol. Lett., 184, 69-72.

Parachin, N.S., Bergdahl, B., van Niel, E.W., Gorwa-Grauslund, M.F. 2011. Kinetic modelling reveals current limitations in the production of ethanol from xylose by recombinant *Saccharomyces cerevisiae*. Metab. Eng., 13, 508-517.

Parekh, R.N., Shaw, M.R., Wittrup, K.D. 1996. An integrating vector for tunable, high copy, stable integration into the dispersed Ty δ sites of *Saccharomyces cerevisiae*. Biotechnol. Prog., 12, 16-21.

Park, E.H. 2015. Genome-Wide Screening of *Saccharomyces cerevisiae* Genes Regulated by Vanillin. J. Microbiol. Biotechnol., 25, 50-56.

Park, S.-E., Koo, H.M., Park, Y.K., Park, S.M., Park, J.C., Lee, O.-K.,

Park, Y.-C., Seo, J.-H. 2011. Expression of aldehyde dehydrogenase 6 reduces inhibitory effect of furan derivatives on cell growth and ethanol production in *Saccharomyces cerevisiae*. Bioresour. Technol., 102, 6033-6038.

Pérez-Bibbins, B., Torrado-Agrasar, A., Salgado, J.M., Mussatto, S.I., Domínguez, J.M. 2015. Xylitol production in immobilized cultures: a recent review. Crit. Rev. Biotechnol., 1-14.

Petschacher, B., Nidetzky, B. 2005. Engineering *Candida tenuis* xylose reductase for improved utilization of NADH: antagonistic effects of multiple side chain replacements and performance of site-directed mutants under simulated in vivo conditions. Appl. Environ. Microbiol., 71, 6390-6393.

Piškur, J., Rozpędowska, E., Polakova, S., Merico, A., Compagno, C. 2006. How did *Saccharomyces* evolve to become a good brewer? Trends Genet., 22, 183-186.

Qi, X., Zha, J., Liu, G.-G., Zhang, W., Li, B.-Z., Yuan, Y.-J. 2015. Heterologous xylose isomerase pathway and evolutionary engineering improve xylose utilization in *Saccharomyces cerevisiae*. Front. Microbiol., 6.

Richard, P., Verho, R., Londesborough, J., Penttila, M. 2006. Genetic engineering of *S.cerevisiae* for pentose utilization. in: *Feedstocks for the Future: Renewables for the Production of Chemicals and Materials*, (Eds.) J.J. Bozell, M.K. Patel, Vol. 921, Amer Chemical Soc. Washington, pp. 184-192.

Roca, C., Nielsen, J., Olsson, L. 2003. Metabolic engineering of ammonium assimilation in xylose-fermenting *Saccharomyces cerevisiae* improves ethanol production. Appl. Environ. Microbiol., 69, 4732-4736.

Ruiz, A., Ariño, J. 2007. Function and regulation of the *Saccharomyces cerevisiae ENA* sodium ATPase system. Eukaryotic cell, 6, 2175-2183.

Runquist, D., Hahn-Hagerdal, B., Bettiga, M. 2010. Increased Ethanol Productivity in Xylose-Utilizing *Saccharomyces cerevisiae* via a Randomly Mutagenized Xylose Reductase. Appl. Environ. Microbiol., 76, 7796-7802.

Sakihama, Y., Hasunuma, T., Kondo, A. 2015. Improved ethanol production from xylose in the presence of acetic acid by the overexpression of the *HAA1* gene in *Saccharomyces cerevisiae*. J. Biosci. Bioeng., 119, 297-302.

Sasano, Y., Watanabe, D., Ukibe, K., Inai, T., Ohtsu, I., Shimoi, H., Takagi, H. 2012. Overexpression of the yeast transcription activator Msn2 confers furfural resistance and increases the initial fermentation rate in ethanol production. J. Biosci. Bioeng., 113, 451-455.

Sato, T.K., Tremaine, M., Parreiras, L.S., Hebert, A.S., Myers, K.S., Higbee, A.J., Sardi, M., McIlwain, S.J., Ong, I.M., Breuer, R.J. 2016. Directed Evolution Reveals Unexpected Epistatic Interactions That Alter Metabolic Regulation and Enable Anaerobic Xylose Use by *Saccharomyces cerevisiae*. PLoS Genet., 12, e1006372.

Shen, Y., Chen, X., Peng, B., Chen, L., Hou, J., Bao, X. 2012. An

efficient xylose-fermenting recombinant *Saccharomyces cerevisiae* strain obtained through adaptive evolution and its global transcription profile. Appl. Microbiol. Biotechnol., 96, 1079-1091.

Shuler, M.L., Kargi, F. 2002. *Bioprocess engineering*. Prentice Hall, Englewood Cliffs, NJ.

Silljé, H., Paalman, J., Ter Schure, E., Olsthoorn, S., Verkleij, A., Boonstra, J., Verrips, C. 1999. Function of trehalose and glycogen in cell cycle progression and cell viability in *Saccharomyces cerevisiae*. J. Bacteriol., 181, 396-400.

Stovicek, V., Borodina, I., Forster, J. 2015. CRISPR–Cas system enables fast and simple genome editing of industrial *Saccharomyces cerevisiae* strains. Metab. Eng. Commun., 2, 13-22.

Suga, H., Matsuda, F., Hasunuma, T., Ishii, J., Kondo, A. 2013. Implementation of a transhydrogenase-like shunt to counter redox imbalance during xylose fermentation in *Saccharomyces cerevisiae*. Appl. Microbiol. Biotechnol., 97, 1669-1678.

Tanino, T., Hotta, A., Ito, T., Ishii, J., Yamada, R., Hasunuma, T., Ogino, C., Ohmura, N., Ohshima, T., Kondo, A. 2010. Construction of a xylose-metabolizing yeast by genome integration of xylose isomerase gene and investigation of the effect of xylitol on fermentation. Appl. Microbiol. Biotechnol., 88, 1215-1221.

Tatusov, R.L., Fedorova, N.D., Jackson, J.D., Jacobs, A.R., Kiryutin, B., Koonin, E.V., Krylov, D.M., Mazumder, R., Mekhedov, S.L., Nikolskaya, A.N. 2003. The COG database: an updated version

includes eukaryotes. BMC Bioinform., 4, 41.

Tatusov, R.L., Galperin, M.Y., Natale, D.A., Koonin, E.V. 2000. The COG database: a tool for genome-scale analysis of protein functions and evolution. Nucleic Acids Res., 28, 33-36.

Teusink, B., Walsh, M.C., van Dam, K., Westerhoff, H.V. 1998. The danger of metabolic pathways with turbo design. Trends Biochem. Sci., 23, 162-169.

Toivari, M.H., Aristidou, A., Ruohonen, L., Penttila, M. 2001. Conversion of xylose to ethanol by recombinant *Saccharomyces cerevisiae*: Importance of xylulokinase (XKS1) and oxygen availability. Metab. Eng., 3, 236-249.

Ullah, A., Orij, R., Brul, S., Smits, G.J. 2012. Quantitative analysis of the modes of growth inhibition by weak organic acids in *Saccharomyces cerevisiae*. Appl. Environ. Microbiol., 78, 8377-8387.

van Maris, A.J.A., Winkler, A.A., Kuyper, M., de Laat, W., van Dijken, J.P., Pronk, J.T. 2007. Development of efficient xylose fermentation in *Saccharomyces cereviside*: Xylose lsomerase as a key component. in: *Biofuels*, (Ed.) L. Olsson, Vol. 108, Springer-Verlag Berlin. Berlin, pp. 179-204.

Vemuri, G., Eiteman, M., McEwen, J., Olsson, L., Nielsen, J. 2007. Increasing NADH oxidation reduces overflow metabolism in *Saccharomyces cerevisiae*. Proc. Natl. Acad. Sci. USA, 104, 2402-2407.

Verduyn, C., Van Kleef, R., Frank, J., Schreuder, H., Van Dijken, J.,

Scheffers, W. 1985. Properties of the NAD(P)H-dependent xylose reductase from the xylose-fermenting yeast *Pichia stipitis*. Biochem. J., 226, 669-677.

Verho, R., Londesborough, J., Penttila, M., Richard, P. 2003. Engineering redox cofactor regeneration for improved pentose fermentation in *Saccharomyces cerevisiae*. Appl. Environ. Microbiol., 69, 5892-5897.

Wahlbom, C.F., Otero, R.R.C., van Zyl, W.H., Hahn-Hägerdal, B., Jönsson, L.J. 2003. Molecular analysis of a *Saccharomyces cerevisiae* mutant with improved ability to utilize xylose shows enhanced expression of proteins involved in transport, initial xylose metabolism, and the pentose phosphate pathway. Appl. Environ. Microbiol., 69, 740-746.

Wang, R.-Y., Shi, Z.-Y., Chen, J.-C., Wu, Q., Chen, G.-Q. 2012. Enhanced co-production of hydrogen and poly-(*R*)-3-hydroxybutyrate by recombinant PHB producing *E. coli* over-expressing hydrogenase 3 and acetyl-CoA synthetase. Metab. Eng., 14, 496-503.

Wang, Y., San, K.-Y., Bennett, G.N. 2013. Cofactor engineering for advancing chemical biotechnology. Curr. Opin. Biotechnol., 24, 994-999.

Warner, J.R., Patnaik, R., Gill, R.T. 2009. Genomics enabled approaches in strain engineering. Curr. Opin. Microbiol., 12, 223-230.

Watanabe, S., Abu Saleh, A., Pack, S.P., Annaluru, N., Kodaki, T., Makino, K. 2007a. Ethanol production from xylose by recombinant

Saccharomyces cerevisiae expressing protein engineered NADP(+)-dependent xylitol dehydrogenase. J. Biotechnol., 130, 316-319.

Watanabe, S., Kodaki, T., Makino, K. 2005. Complete reversal of coenzyme specificity of xylitol dehydrogenase and increase of thermostability by the introduction of structural zinc. J. Biol. Chem., 280, 10340-10349.

Watanabe, S., Saleh, A.A., Pack, S.P., Annaluru, N., Kodaki, T., Makino, K. 2007b. Ethanol production from xylose by recombinant *Saccharomyces cerevisiae* expressing protein-engineered NADH-preferring xylose reductase from *Pichia stipitis*. Microbiology, 153, 3044-3054.

Weber, C., Farwick, A., Benisch, F., Brat, D., Dietz, H., Subtil, T., Boles, E. 2010. Trends and challenges in the microbial production of lignocellulosic bioalcohol fuels. Appl. Microbiol. Biotechnol., 87, 1303-1315.

Wei, N., Quarterman, J., Kim, S.R., Cate, J.H., Jin, Y.-S. 2013. Enhanced biofuel production through coupled acetic acid and xylose consumption by engineered yeast. Nat. Commun., 4, 2580.

Wei, W., McCusker, J.H., Hyman, R.W., Jones, T., Ning, Y., Cao, Z., Gu, Z., Bruno, D., Miranda, M., Nguyen, M. 2007. Genome sequencing and comparative analysis of *Saccharomyces cerevisiae* strain YJM789. Proc. Natl. Acad. Sci. U.S.A., 104, 12825-12830.

Wohlbach, D.J., Kuo, A., Sato, T.K., Potts, K.M., Salamov, A.A., LaButti, K.M., Sun, H., Clum, A., Pangilinan, J.L., Lindquist, E.A.

2011. Comparative genomics of xylose-fermenting fungi for enhanced biofuel production. Proc. Natl. Acad. Sci. U.S.A., 108, 13212-13217.

Yadav, M., Mishra, D.K., Hwang, J.-S. 2012. Catalytic hydrogenation of xylose to xylitol using ruthenium catalyst on NiO modified TiO_2 support. Appl. Catal. A-Gen., 425, 110-116.

Young, E.M., Tong, A., Bui, H., Spofford, C., Alper, H.S. 2014. Rewiring yeast sugar transporter preference through modifying a conserved protein motif. Proc. Natl. Acad. Sci. U.S.A., 111, 131-136.

Yue, H., Zhao, Y., Ma, X., Gong, J. 2012. Ethylene glycol: properties, synthesis, and applications. Chem. Soc. Rev., 41, 4218-4244.

Zeng, W.-Y., Tang, Y.-Q., Gou, M., Sun, Z.-Y., Xia, Z.-Y., Kida, K. 2017. Comparative transcriptomes reveal novel evolutionary strategies adopted by *Saccharomyces cerevisiae* with improved xylose utilization capability. Appl. Microviol. Biotechnol., 101, 1753-1767.

Zhang, G.-C., Kong, I.I., Kim, H., Liu, J.-J., Cate, J.H., Jin, Y.-S. 2014. Construction of a quadruple auxotrophic mutant of an industrial polyploid *Saccharomyces cerevisiae* strain by using RNA-guided Cas9 nuclease. Appl. Environ. Microbiol, 80, 7694-7701.

Zhang, G.C., Liu, J.J., Ding, W.T. 2012. Decreased Xylitol Formation during Xylose Fermentation in *Saccharomyces cerevisiae* Due to Overexpression of Water-Forming NADH Oxidase. Appl. Environ. Microbiol., 78, 1081-1086.

Appendix 1

The list of COG categorized genes presented in Fig. 2.6

D452-2 gene	COG category			description
ChrI__ACS1	COG0365	Acs	I	Acyl-coenzyme A synthetase/AMP-(fatty) acid ligase
ChrI__FLO1	COG5048	COG5048	R	FOG: Zn-finger
ChrII__ARO4	COG0722	AroG1	E	3-deoxy-D-arabino-heptulosonate 7-phosphate (DAHP) synthase
ChrII__CDC27	COG0457	TPR	R	Tetratricopeptide (TPR) repeat
ChrII__CHS3	COG1215	BcsA	N	Glycosyltransferase, catalytic subunit of cellulose synthase and poly-beta-1,6-N-acetylglucosamine synthase
ChrII__CYC8	COG0457	TPR	R	Tetratricopeptide (TPR) repeat
ChrII__DSF2	COG3595	YvlB	S	Uncharacterized conserved protein YvlB, contains DUF4097 and DUF4098 domains
ChrII__DUT1	COG0756	Dut	FV	dUTPase
ChrII__ENP1	COG5384	Mpp10	J	U3 small nucleolar ribonucleoprotein component
ChrII__FMT1	COG0223	Fmt	J	Methionyl-tRNA formyltransferase
ChrII__FUS3	COG0515	SPS1	T	Serine/threonine protein kinase
ChrII__GAL1	COG0153	GalK	G	Galactokinase
ChrII__GAL10	COG1087	GalE	M	UDP-glucose 4-epimerase
ChrII__ISW1	COG0553	HepA	KL	Superfamily II DNA or RNA helicase, SNF2 family
ChrII__MNN2	COG0515	SPS1	T	Serine/threonine protein kinase
ChrII__NTH2	COG1626	TreA	G	Neutral trehalase
ChrII__PDR3	COG5665	COG5665	K	CCR4-NOT transcriptional regulation complex, NOT5 subunit
ChrII__PKC1	COG0515	SPS1	T	Serine/threonine protein kinase
ChrII__POP4	COG1588	POP4	J	RNase P/RNase MRP subunit p29
ChrII__SCO2	COG1999	Sco1	O	Cytochrome oxidase Cu insertion factor, SCO1/SenC/PrrC family
ChrII__SCT1	COG5271	MDN1	J	Midasin, AAA ATPase with vWA domain, involved in ribosome maturation
ChrIII__LEU2	COG0473	LeuB	CE	Isocitrate/isopropylmalate dehydrogenase
ChrIV__BSC1	COG3889	COG3889	S	Predicted periplasmic protein
ChrIV__ENA2	COG0474	MgtA	P	Magnesium-transporting ATPase (P-type)
ChrIV__NUM1	COG1196	Smc	D	Chromosome segregation ATPase
ChrIV__PKH1	COG0515	SPS1	T	Serine/threonine protein kinase

ChrIV__RPL27B	COG2163	RPL14A	J	Ribosomal protein L14E/L6E/L27E
ChrIX__EFM4	COG2890	HemK	J	Methylase of polypeptide chain release factors
ChrIX__FAF1	COG5271	MDN1	J	Midasin, AAA ATPase with vWA domain, involved in ribosome maturation
ChrIX__HIS6	COG0106	HisA	E	Phosphoribosylformimino-5-aminoimidazole carboxamide ribonucleotide (ProFAR) isomerase
ChrIX__IMA3	COG0366	AmyA	G	Glycosidase
ChrIX__MLP2	COG1196	Smc	D	Chromosome segregation ATPase
ChrIX__NDC80	COG5185	HEC1	D	Protein involved in chromosome segregation, interacts with SMC proteins
ChrIX__PRK1	COG0515	SPS1	T	Serine/threonine protein kinase
ChrIX__SGA1	COG5301	COG5301	X	Phage-related tail fibre protein
ChrIX__SLN1	COG0784	CheY	T	CheY chemotaxis protein or a CheY-like REC (receiver) domain
ChrIX__SSL2	COG1061	SSL2	KL	Superfamily II DNA or RNA helicase
ChrIX__TMA108	COG0308	PepN	E	Aminopeptidase N
ChrIX__YKE4	COG0428	ZupT	P	Zinc transporter ZupT
ChrV__CAN1	COG0833	LysP	E	Amino acid permease
ChrV__COX15	COG1612	CtaA	H	Heme A synthase
ChrV__GDI1	COG5044	MRS6	O	RAB proteins geranylgeranyltransferase component A (RAB escort protein)
ChrV__MAG1	COG0122	AlkA	L	3-methyladenine DNA glycosylase/8-oxoguanine DNA glycosylase
ChrV__UBC6	COG5078	COG5078	O	Ubiquitin-protein ligase
ChrV__UBP5	COG5533	COG5533	O	Ubiquitin C-terminal hydrolase
ChrVI__FET5	COG2132	SufI	DPM	Multicopper oxidase with three cupredoxin domains
ChrVII__GSC2	COG0033	Pgm	G	Phosphoglucomutase
ChrVII__PYC1	COG1038	PycA	C	Pyruvate carboxylase
ChrVII__SPT6	COG2183	Tex	K	Transcriptional accessory protein Tex/SPT6
ChrVII__XRN1	COG5049	XRN1	L	5'-3' exonuclease
ChrVIII__AAP1	COG0308	PepN	E	Aminopeptidase N
ChrVIII__ARO9	COG1167	ARO8	KE	DNA-binding transcriptional regulator, MocR family, contains an aminotransferase domain
ChrVIII__ATG7	COG0476	ThiF	H	Molybdopterin or thiamine biosynthesis adenylyltransferase

ChrVIII__CDC23	COG5010	TadD	UW	Flp pilus assembly protein TadD, contains TPR repeats
ChrVIII__CRP1	COG3115	ZipA	D	Cell division protein ZipA, interacts with FtsZ
ChrVIII__DOG1	COG0637	YcjU	GR	Beta-phosphoglucomutase or related phosphatase, HAD superfamily
ChrVIII__ERC1	COG0534	NorM	V	Na+-driven multidrug efflux pump
ChrVIII__ERG9	COG1562	ERG9	I	Phytoene/squalene synthetase
ChrVIII__HTD2	COG3777	HTD2	I	Hydroxyacyl-ACP dehydratase HTD2, hotdog domain
ChrVIII__INM1	COG0483	SuhB	G	Archaeal fructose-1,6-bisphosphatase or related enzyme of inositol monophosphatase family
ChrVIII__KOG1	COG2319	WD40	R	WD40 repeat
ChrVIII__MRPL6	COG0097	RplF	J	Ribosomal protein L6P/L9E
ChrVIII__MTG2	COG0536	Obg	DL	GTPase involved in cell partioning and DNA repair
ChrVIII__NAM8	COG0724	RRM	J	RNA recognition motif (RRM) domain
ChrVIII__NCP1	COG0369	CysJ	P	Sulfite reductase, alpha subunit (flavoprotein)
ChrVIII__NMD3	COG1499	NMD3	J	NMD protein affecting ribosome stability and mRNA decay
ChrVIII__PUT2	COG4230	PutA2	E	Delta 1-pyrroline-5-carboxylate dehydrogenase
ChrVIII__RPP1	COG1603	RPP1	J	RNase P/RNase MRP subunit p30
ChrVIII__RRF1	COG0233	Frr	J	Ribosome recycling factor
ChrVIII__RRM3	COG0507	RecD	L	ATP-dependent exoDNAse (exonuclease V), alpha subunit, helicase superfamily I
ChrVIII__RRP3	COG0513	SrmB	L	Superfamily II DNA and RNA helicase
ChrVIII__SKG6	COG5271	MDN1	J	Midasin, AAA ATPase with vWA domain, involved in ribosome maturation
ChrVIII__SLT2	COG0515	SPS1	T	Serine/threonine protein kinase
ChrVIII__SMF2	COG1914	MntH	P	Mn2+ and Fe2+ transporters of the NRAMP family
ChrVIII__SSF1	COG5019	CDC3	DZ	Septin family protein
ChrVIII__SSZ1	COG0443	DnaK	O	Molecular chaperone DnaK (HSP70)
ChrVIII__THP2	COG4694	RloC	J	Wobble nucleotide-excising tRNase
ChrVIII__YCK1	COG0515	SPS1	T	Serine/threonine protein kinase
ChrVIII__YHI9	COG0384	YHI9	R	Predicted epimerase YddE/YHI9, PhzF superfamily
ChrX__DAN4	COG5048	COG5048	R	FOG: Zn-finger

ChrX__GEA1	COG5307	COG5307	R	Guanine-nucleotide exchange factor, contains Sec7 domain
ChrX__GEF1	COG0038	ClcA	P	H+/Cl- antiporter ClcA
ChrX__HXT16	COG0477	ProP	GEPR	MFS family permease
ChrX__MDE1	COG0235	AraD	G	Ribulose-5-phosphate 4-epimerase/Fuculose-1-phosphate aldolase
ChrX__TES1	COG1946	TesB	I	Acyl-CoA thioesterase
ChrX__TOR1	COG5032	TEL1	T	Phosphatidylinositol kinase or protein kinase, PI-3 family
ChrXI__GAP1	COG0833	LysP	E	Amino acid permease
ChrXI__HSL1	COG0515	SPS1	T	Serine/threonine protein kinase
ChrXI__MEH1	COG5271	MDN1	J	Midasin, AAA ATPase with vWA domain, involved in ribosome maturation
ChrXI__PTK1	COG0515	SPS1	T	Serine/threonine protein kinase
ChrXII__BNA5	COG3844	Bna5	E	Kynureninase
ChrXII__CCC1	COG1814	Ccc1	P	Predicted Fe2+/Mn2+ transporter, VIT1/CCC1 family
ChrXII__CDA1	COG0726	CDA1	GM	Peptidoglycan/xylan/chitin deacetylase, PgdA/CDA1 family
ChrXII__CDA2	COG0726	CDA1	GM	Peptidoglycan/xylan/chitin deacetylase, PgdA/CDA1 family
ChrXII__CDC25	COG5048	COG5048	R	FOG: Zn-finger
ChrXII__CTS1	COG3469	Chi1	G	Chitinase
ChrXII__DBP9	COG0513	SrmB	L	Superfamily II DNA and RNA helicase
ChrXII__ECM38	COG0405	Ggt	E	Gamma-glutamyltranspeptidase
ChrXII__GAL2	COG0477	ProP	GEPR	MFS family permease
ChrXII__GCD7	COG1184	GCD2	J	Translation initiation factor 2B subunit, eIF-2B alpha/beta/delta family
ChrXII__GPI13	COG1524	Npp1	R	Predicted pyrophosphatase or phosphodiesterase, AlkP superfamily
ChrXII__GSY2	COG0438	RfaB	M	Glycosyltransferase involved in cell wall bisynthesis
ChrXII__GUF1	COG0481	LepA	J	Translation elongation factor EF-4, membrane-bound GTPase
ChrXII__HSP104	COG0542	ClpA	O	ATP-dependent Clp protease ATP-binding subunit ClpA
ChrXII__HSP60	COG0459	GroEL	O	Chaperonin GroEL (HSP60 family)
ChrXII__IFH1	COG5271	MDN1	J	Midasin, AAA ATPase with vWA domain, involved in ribosome maturation
ChrXII__IMH1	COG1196	Smc	D	Chromosome segregation ATPase

ChrXII__IRC20	COG0553	HepA	KL	Superfamily II DNA or RNA helicase, SNF2 family
ChrXII__ISA1	COG0316	IscA	O	Fe-S cluster assembly iron-binding protein IscA
ChrXII__KNS1	COG0515	SPS1	T	Serine/threonine protein kinase
ChrXII__LCB5	COG1597	LCB5	IR	Diacylglycerol kinase family enzyme
ChrXII__MDL1	COG1132	MdlB	V	ABC-type multidrug transport system, ATPase and permease component
ChrXII__MLH2	COG0323	MutL	L	DNA mismatch repair ATPase MutL
ChrXII__NNT1	COG3897	Nnt1	R	Predicted nicotinamide N-methyase
ChrXII__PIG1	COG3672	COG3672	O	Predicted transglutaminase-like cysteine proteinase
ChrXII__RCK2	COG0515	SPS1	T	Serine/threonine protein kinase
ChrXII__RKM5	COG3583	YabE	S	Uncharacterized conserved protein YabE, contains G5 and tandem DUF348 domains
ChrXII__RSA3	COG1340	COG1340	S	Uncharacterized coiled-coil protein, contains DUF342 domain
ChrXII__SPA2	COG1196	Smc	D	Chromosome segregation ATPase
ChrXII__SSA2	COG0443	DnaK	O	Molecular chaperone DnaK (HSP70)
ChrXII__STT4	COG5032	TEL1	T	Phosphatidylinositol kinase or protein kinase, PI-3 family
ChrXII__TOP3	COG0550	TopA	L	DNA topoisomerase IA
ChrXII__UTP13	COG2319	WD40	R	WD40 repeat
ChrXII__YEF3	COG0488	Uup	R	ATPase components of ABC transporters with duplicated ATPase domains
ChrXII__YRF1-4	COG0513	SrmB	L	Superfamily II DNA and RNA helicase
ChrXIV__ADE12	COG0104	PurA	F	Adenylosuccinate synthase
ChrXIV__BXI1	COG0670	YbhL	R	Integral membrane protein, interacts with FtsH
ChrXIV__CLA4	COG0515	SPS1	T	Serine/threonine protein kinase
ChrXIV__CNM67	COG1196	Smc	D	Chromosome segregation ATPase
ChrXIV__JJJ1	COG0484	DnaJ	O	DnaJ-class molecular chaperone with C-terminal Zn finger domain
ChrXIV__KRE33	COG1444	TmcA	J	tRNA(Met) C34 N-acetyltransferase TmcA
ChrXIV__KRI1	COG1196	Smc	D	Chromosome segregation ATPase
ChrXIV__MCK1	COG0515	SPS1	T	Serine/threonine protein kinase
ChrXIV__MGS1	COG2256	RarA	L	Replication-associated recombination protein RarA (DNA-dependent ATPase)

ChrXIV__MRPS18	COG0100	RpsK	J	Ribosomal protein S11
ChrXIV__NPR1	COG0515	SPS1	T	Serine/threonine protein kinase
ChrXIV__RAP1	COG5492	YjdB	R	Uncharacterized conserved protein YjdB, contains Ig-like domain
ChrXIV__RHO5	COG1100	Gem1	R	GTPase SAR1 family domain
ChrXIV__SQS1	COG5271	MDN1	J	Midasin, AAA ATPase with vWA domain, involved in ribosome maturation
ChrXIV__STB1	COG5048	COG5048	R	FOG: Zn-finger
ChrXIV__TRF5	COG5260	TRF4	L	DNA polymerase sigma
ChrXIV__UBP10	COG5533	COG5533	O	Ubiquitin C-terminal hydrolase
ChrXIV__YPT11	COG1100	Gem1	R	GTPase SAR1 family domain
ChrXV__ADH1	COG1064	AdhP	G	D-arabinose 1-dehydrogenase, Zn-dependent alcohol dehydrogenase family
ChrXV__ALD4	COG1012	AdhE	C	Acyl-CoA reductase or other NAD-dependent aldehyde dehydrogenase
ChrXV__ARG1	COG0137	ArgG	E	Argininosuccinate synthase
ChrXV__AVO1	COG5644	COG5644	S	U3 small nucleolar RNA-associated protein 14
ChrXV__BSC6	COG0738	FucP	G	Fucose permease
ChrXV__CMK2	COG0515	SPS1	T	Serine/threonine protein kinase
ChrXV__CTR9	COG1196	Smc	D	Chromosome segregation ATPase
ChrXV__DDR2	COG4380	COG4380	S	Uncharacterized protein
ChrXV__DIS3	COG0557	VacB	K	Exoribonuclease R
ChrXV__DUF1	COG5048	COG5048	R	FOG: Zn-finger
ChrXV__ENV9	COG1028	FabG	IQR	NAD(P)-dependent dehydrogenase, short-chain alcohol dehydrogenase family
ChrXV__GAL11	COG4372	COG4372	S	Uncharacterized conserved protein, contains DUF3084 domain
ChrXV__GAS5	COG5048	COG5048	R	FOG: Zn-finger
ChrXV__GPD2	COG0240	GpsA	C	Glycerol-3-phosphate dehydrogenase
ChrXV__GPM3	COG0588	GpmA	G	Phosphoglycerate mutase (BPG-dependent)
ChrXV__HAL9	COG5048	COG5048	R	FOG: Zn-finger
ChrXV__HST1	COG0846	SIR2	O	NAD-dependent protein deacetylase, SIR2 family
ChrXV__LAG2	COG3853	TelA	V	Uncharacterized conserved protein YaaN involved in tellurite resistance

ChrXV__MAM3	COG1253	TlyC	R	Hemolysin or related protein, contains CBS domains
ChrXV__MDM38	COG3064	TolA	M	Membrane protein involved in colicin uptake
ChrXV__MET22	COG1218	CysQ	P	3'-Phosphoadenosine 5'-phosphosulfate (PAPS) 3'-phosphatase
ChrXV__MPD2	COG1196	Smc	D	Chromosome segregation ATPase
ChrXV__MSE1	COG0008	GlnS	J	Glutamyl- or glutaminyl-tRNA synthetase
ChrXV__MSH2	COG0249	MutS	L	DNA mismatch repair ATPase MutS
ChrXV__NGL1	COG5239	CCR4	A	mRNA deadenylase, 3'-5' endonuclease subunit Ccr4
ChrXV__NUF2	COG1196	Smc	D	Chromosome segregation ATPase
ChrXV__PSH1	COG3343	RpoE	K	DNA-directed RNA polymerase, delta subunit
ChrXV__PSK2	COG0515	SPS1	T	Serine/threonine protein kinase
ChrXV__PUT4	COG0833	LysP	E	Amino acid permease
ChrXV__REX4	COG2176	PolC	L	DNA polymerase III, alpha subunit (gram-positive type)
ChrXV__RIB2	COG0564	RluA	J	Pseudouridylate synthase, 23S rRNA- or tRNA-specific
ChrXV__SMC5	COG1196	Smc	D	Chromosome segregation ATPase
ChrXV__SPO21	COG1196	Smc	D	Chromosome segregation ATPase
ChrXV__SRL1	COG3889	COG3889	S	Predicted periplasmic protein
ChrXV__TAT2	COG0833	LysP	E	Amino acid permease
ChrXV__THI20	COG0351	ThiD	H	Hydroxymethylpyrimidine/phosphomethylpyrimidine kinase
ChrXV__TSR4	COG1572	COG1572	O	Serine protease, subtilase family
ChrXV__YAP7	COG5527	COG5527	X	Protein involved in initiation of plasmid replication
ChrXV__YGK3	COG0515	SPS1	T	Serine/threonine protein kinase
ChrXVI__ALG5	COG0463	WcaA	M	Glycosyltransferase involved in cell wall bisynthesis
ChrXVI__ARR3	COG0798	ACR3	P	Arsenite efflux pump ArsB, ACR3 family
ChrXVI__HDA3	COG1196	Smc	D	Chromosome segregation ATPase
ChrXVI__HUT1	COG2510	COG2510	S	Uncharacterized membrane protein
ChrXVI__MMT2	COG0053	FieF	P	Divalent metal cation (Fe/Co/Zn/Cd) transporter
ChrXVI__NAB3	COG5271	MDN1	J	Midasin, AAA ATPase with vWA domain, involved in ribosome maturation

ChrXVI__NEW1	COG0488	Uup	R	ATPase components of ABC transporters with duplicated ATPase domains
ChrXVI__POS5	COG0061	NadF	F	NAD kinase
ChrXVI__SGE1	COG2814	AraJ	G	Predicted arabinose efflux permease, MFS family
ChrXVI__SRP68	COG5055	RAD52	L	Recombination DNA repair protein (RAD52 pathway)
ChrXVI__USV1	COG5048	COG5048	R	FOG: Zn-finger

국문 초록

미생물을 이용한 목질계 바이오매스로부터의 바이오 연료 및 바이오 화학소재 생산은 지속가능하며 친환경적인 생산공정이다. 목질계 바이오매스는 주로 포도당과 자일로스로 이루어져 있으며 이 두 당을 효율적으로 이용하는 것이 중요하다. 대사공학을 이용하여 자일로스를 대사할 수 있는 *Saccharomyces cerevisiae* (이하 효모로 지칭)를 구축하였지만 포도당 발효능보다 자일로스 발효능은 현저히 떨어졌다. 따라서 자일로스를 효과적으로 이용할 수 있는 효모의 구축이 바이오연료 및 화학소재 생산에 필수적이라 할 수 있다. 본 연구의 목적은 대사공학기술을 이용하여 자일로스를 효과적으로 전환할 수 있는 재조합 효모를 구축하는 것이다.

본 연구에서 사용한 *S. cerevisiae* D452-2 효모는 자일로스로부터 고부가가치 물질 생산에 널리 사용 되었다. 다른 실험용 효모들은 유전체 분석을 통해 다양한 정보를 얻었지만 D452-2는 유전체 분석이 진행되지 않았고 유전적 정보가 부족하다. Pacbio 유전체 분석 기술을 이용하여 D452-2 전체 유전자 서열을 분석하였고 기준 효모인 S288c와 거의 유사한 서열을

얻을 수 있었다. 비교 분석을 통해 D452-2에 존재하는 유전자 변이들을 확인하였고 자일로스 대사에 중요할 것으로 예상되는 유전자 후보군을 제시하였다.

목질계 바이오매스로부터 에탄올을 생산하기 위하여 자일로스를 이용할 수 있는 *Scherffersomyces stipitis* 의 자일로스 대사 관련 유전자 (XR, XDH, XK)를 효모에 도입하였다. 하지만 도입한 유전자는 보조인자 요구성이 달라 자일리톨이 축적되는 문제가 있었다. 단백질 공학을 통해 XR, XDH의 보조인자 요구성을 바꾸었고 그 결과 자일리톨이 쌓이지 않았지만 자일로스 대사 속도가 감소하였다. 균형잡힌 보조인자 요구성과 이용능은 자일로스를 효과적으로 전환하기 위한 속도 결정 단계라 할 수 있다. 본 연구에서는 이런문제를 해결하기 위해 동질효소(isozyme) 시스템을 이용하였다. NADH 의존적인 XR을 NADPH 의존적인 XR과 XDH, XK를 가진 재조합 효모에 도입하였다. 기존의 재조합 효모들은 어느 한쪽의 보조인자에 의존적이지만 동질효소 시스템을 가진 재조합 효모는 NADPH, NADH 둘 다 비슷한 활성을 나타내었다. 동질효소 시스템을 가진 재조합 효모는 대조군들에 비해 자일로스를 빠르게 소비하였고 자일리톨도 적게 축적하였다. 발효능을 다양한 조건에

서 검증하였고 억새가수분해물을 이용한 발효에서 50.7 g/L의 에탄올을 0.43 g/g의 수율로 생산하였다.

동질효소 시스템을 에탄올 생산뿐만 아니라 고부가가치 물질인 자일리톨 생산에도 적용해 보았다. 이 시스템을 가진 재조합 효모는 회분식 발효에서 높은 자일리톨 생산성을 보였고 보조인자의 공급을 원활하게 하기 위해 재생유전자를 과발현하였다. *ZWF1* (glucose-6-phosphate dehydrogenase), *ACS1*(acetyl-coA synthetase) 유전자의 과발현을 통해 세포 내 보조인자의 농도가 증가하였고 이에 자일리톨 생산성도 증가하였다. 자일리톨 생산성을 극대화하기 위해 발효조건을 최적화하였고 196.2 g/L의 자일리톨을 4.27 g/L-h의 생산성으로 생산하였다. 동질효소 시스템은 미생물을 이용하여 자일로스로부터 고부가가치 물질 생산에 사용 할 수 있는 강력한 전략이다.

주요어: 효모, 목질계 바이오매스, 자일로스, 바이오연료, 자일리톨, 동질효소, NADH 의존적인 XR, 보인자 재생, 혼합당 발효, 비교 유전체 분석

학번: 2010-21262